STUDIES ON THE FUNCTION OF THE GLAUCOMA-ASSOCIATED PROTEIN OPTINEURIN AND ITS MUTANTS

Thesis submitted for the degree of

DOCTOR OF PHILOSOPHY

TO

DEPARTMENT OF BIOCHEMISTRY
SCHOOL OF LIFE SCIENCES
UNIVERSITY OF HYDERABAD
HYDERABAD - 500 046
INDIA

By

Madhavi Latha Chalasani

Hyderabad Eye Research Foundation
L.V. Prasad Eye Institute,
Hyderabad - 500 034

September 2008

Enrollment No: 03LBPH13

UNIVERSITY OF HYDERABAD

School of Life Sciences

Department of Biochemistry

Hyderabad - 500 046 (India)

DECLARATION

The research work embodied in this thesis entitled, **"Studies on the Function of the Glaucoma-Associated Protein Optineurin and its Mutants"**, has been carried out by me under the guidance of Prof. D. Balasubramanian at L. V. Prasad Eye Institute, Dr. Ghanshyam Swarup at Centre for Cellular and Molecular Biology and Prof. T. Suryanarayana. I hereby declare that this work is original and has not been submitted in part or full for any other degree or diploma of any other university.

Madhavi Latha Chalasani

Prof. D. Balasubramanian
Supervisor
Director, Research
L.V. Prasad Eye Institute
Hyderabad

Dr. Ghanshyam Swarup
Co-Supervisor
CCMB
Hyderabad

Prof. T. Suryanarayana
Co-supervisor
Department of Biochemistry
School of Life Sciences
University of Hyderabad

UNIVERSITY OF HYDERABAD

School of Life Sciences

Department of Biochemistry

Hyderabad - 500 046 (India)

CERTIFICATE

This is to certify that this thesis entitled, "**Studies on the Function of the Glaucoma-Associated Protein Optineurin and its Mutants**", submitted by **Madhavi Latha Chalasani** for the degree of **Doctor of Philosophy** to the University of Hyderabad is based on the work carried out by her at the L. V. Prasad Eye Institute and CCMB, Hyderabad, under our supervision. This work has not been submitted for any diploma or degree of any other University or Institution.

Prof. D. Balasubramanian
Supervisor
Director, Research
L. V. Prasad Eye Institute
Hyderabad

Dr. Ghanshyam Swarup
Co-supervisor
CCMB
Hyderabad

Prof. T. Suryanarayana
Co-supervisor
Department of Biochemistry
School of Life Sciences
University of Hyderabad

Head
Department of Biochemistry
School of Life Sciences
University of Hyderabad

Dean
School of Life Sciences
University of Hyderabad

Dedicated to the Millions of Glaucoma Patients....

ACKNOWLEDGEMENTS

It is my pleasure to thank all the people who made this thesis possible and hence I would like to pay my acknowledgements to each one of them who made my Ph. D a memorable and successful journey.

First of all, I would like to express my deep and sincere gratitude to Prof. D. Balasubramanian, Director of Research, LVPEI, for giving me an opportunity to initiate my Ph. D work at LVPEI and supervising my work in LVPEI and for being a constant support during my transition to CCMB for the collaborative research work.

I am deeply grateful to my project collaborator and co-supervisor, Dr. Ghanshyam Swarup for his detailed and constructive comments, and for his immense support throughout this work. His wide knowledge and logical way of thinking have been of great value for me. He gave me untiring help during my difficult moments. His encouragement and guidance right from inception has provided a good basis for the present thesis.

I wish to express my warm and sincere thanks to Dr. Radha who has helped me in apoptosis counting and in other areas I required help.

I also thank Dr. Vijay Gupta, who trained me initially in molecular biology and tissue culture techniques and also for his help in yeast two-hybrid screening.

I would like to thank Prof. T. Suryanarayana, University of Hyderabad, for having agreed to be my co-supervisor.

I owe my thanks to Dr.Neeraj Agarwal, UNT Health Science Centre, Texas, for gifting me the RGC-5 cell line for my research work. Thanks to Nandini Rangarajan for her help in confocal microscopy.

I specially thank Dr. G.N. Rao, chairman, and Dr. Chandrasekhar, the current director of L.V.Prasad Eye Institute, for providing the necessary infrastructure at LVPEI.

I also thank Dr. Lalji Singh for providing such high end facilities at CCMB and allowing me to use the same for my research work.

I thank all the research faculty at LVPEI who have constantly encouraged me through out my Ph. D. I warmly thank my friends at LVPEI, Venu, a wonderful friend, Rajeshwari, Purushottham, Kalyan, Srilatha and Guru for their prompt help whenever needed and for the memorable time we spent together. I will always cherish the time I spent with Venu, the long scientific discussions we used to have on phone and I would like to thank him for being a pillar of moral strength. Thanks to my friends Anees, Surya, Afia, Kiran, Hardeep and my juniors for their friendly help. I have thoroughly enjoyed my time with the group during my stay at LVPEI. I am grateful to my seniors at LVPEI, Geetha and BM Reddy who have given initial guidance in my scientific career.

I wish to thank my friends at CCMB, Madhavi- my sis, Yatin and Andy for making me feel comfortable in the lab and also for their continued support and creating a fun filled environment while working in CCMB. Madhavi and Yatin for their complete help in late night work and confocal microscopy. We had spent wonderful tea-times and

joyfilled gatherings during week-ends. Thanks to my lab friends Nag, Vipul, Kunal, Kapil, Megha and Rajesh Kumar Gupta (RKG) who have helped me in various ways and who have shared common reagents with me. Thanks to RKG for making me comfortable in dealing with live cell microscopy work. Priyanka and Nitin have been good friends at CCMB and I would like to thank them for their helpful and friendly nature. Special thanks to Madhavi, Yatin and Priyanka for critical proof-reading of my thesis. Also, thanks to opposite lab members Ritika, Pankaj and Indu.

I also thank my seniors Preeti, Subhashani, Nishant and Subhash for their guidance in my research work. I am grateful to Dr. Sudhakar, Scientist, for trouble shooting my experiments and add his experience to resolve some of my problem areas.

I owe my thanks to Ganeshan for keeping the labware in a ready-to-use mode and Lakshmi for maintaining clean glassware. I also wish to thank the staff of tissue culture facility Mubarak, Parthasarthy, Johnson, Dayakar, Late Chandramohan, Izra and others for maintaining good tissue culture facilities. Thanks also to the staff of digital imaging, photography section, sequencing and fine biochemicals facility.

My family has been a constant source of strength and support to me. I express my sincere gratitude to my mom and dad who have given me quality education and also for their unconditional support and encouragement. I owe my loving thanks to my dear brother ‘chinni’, who is my best buddy, for his constant support in this journey and also to his wife ‘Bhavana’.

I am deeply thankful to my husband and my daughter “Sowmya” for their understanding and tremendous support especially during my late working hours. My husband has been very understanding and I am truly indebted for all the love and care he showered on me. I am also greatly indebted to my sister-in-law “Kalyani” and my in-laws for their constant prayers for my success and my dear grandparents for their continuous support during my Ph.D. Apart from my husband, my mom and Kalyani have been the best support and are a major contributory factor for success of my research project and without their encouragement and understanding it would have been impossible for me to finish this work. I will also remember the weekends I spent with my dear sis ‘Phani’.

The financial support of CSIR-UGC and LVPEI is gratefully acknowledged.

-Madhavi

Table of Contents

CHAPTER 4 IDENTIFICATION OF OPTINEURIN INTERACTING PROTEINS BY YEAST TWO-HYBRID SCREENING

LIST OF FIGURES

LIST OF TABLES

LIST OF ABBREVIATIONS

%	percent
μ	micron
°C	degrees Celsius
μg	microgram
μl	microliter
ATP	adenosine triphosphate
BCIP	2-bromo, 3-chloro indolyl phosphate
bp	base pair
BSA	bovine serum albumin
CCD	cooled camera device
CMV	cytomegalovirus
Cy3	indocarbocyanine
Cyc	cycloheximide
DAPI	4', 6-Diamidino-2-phenylindole dihydrochloride
DEPC	diethylpyrocarbonate
DMEM	Dulbecco's modified Eagle medium
DTT	dithiothreitol
ECL	enhanced chemiluminiscence
EDTA	ethylene diamine tetra acetic acid
EGFP	enhanced green fluorescent protein
FCS	fetal calf serum
FITC	fluorescein isothiocyanate
g	unit gravitational force
GFP	green fluorescent protein
gm	gram
H_2O_2	hydrogen peroxide
HA	hemagglutin tag
HEPES	(N-[2-Hydroxy ethyl] piperazine-N'-[2-ethane sulphonic acid])
HRP	horseradish peroxidase
IP	immunoprecipitation
IPTG	isopropyl-beta-D-thiogalactoside
kDa	kilodalton
LiAc	lithium acetate
M	molar
mA	milliampere
MAb	mouse monoclonal antibody
mg	milligram
min	minute
ml	milliliter
mm	millimeter
mM	millimolar

MOPS	3-[N-morpholino] sulphonic acid
NBT	nitro blue tetrazolium
nm	nanometer
OD_{260}	optical density at 260 nm
PAGE	polyacrylamide gel electrophoresis
PBS	phosphate buffered saline
PCR	polymerase chain reaction
PEG	polyethylene glycol
PMSF	phenyl methyl sulphonyl fluoride
RNA	ribonucleic acid
rpm	revolutions per minute
RT	reverse transcription
SDS	sodium dodecyl sulphate
TBST	Tris buffered saline containing tween-20
TEMED	N,N,N',N'-tetramethylene diamine
UV	ultra-violet
VSVG	vesicular stomatitis virus G protein
X-gal	5-bromo-4-chloro-3-indolyl-β-D-galactoside
YC	yeast complete (minimal defined) medium
YPAD	yeast peptone dextrose adenine (complex) medium
GAL4	transcription factor required for the activation of the GAL(galactose) genes (genes required for galactose metabolism)

Table of Amino Acids with Three Letter Codes and Single Letter Codes

AMINO ACID	THREE LETTER CODE	SINGLE LETTER CODE
Alanine	Ala	A
Arginine	Arg	R
Asparagine	Asn	N
Aspartate	Asp	D
Cysteine	Cys	C
Glutamate	Glu	E
Glutamine	Gln	Q
Glycine	Gly	G
Histidine	His	H
Isoleucine	Ile	I
Leucine	Leu	L
Lysine	Lys	K
Methionine	Met	M
Phenylalanine	Phe	F
Proline	Pro	P
Serine	Ser	S
Threonine	Thr	T
Tryptophan	Trp	W
Tyrosine	Tyr	Y
Valine	Val	V

ABSTRACT

Glaucoma is the second major leading cause of bilateral blindness in the world which affects approximately 67 million people world wide. According to the WHO statistics released in 2004, 12.3% of blindness in the world accounts for glaucoma. It is a genetically heterogeneous group of optic neuropathies characterized by optic nerve head cupping and progressive loss of vision due to retinal ganglion cell death. Although raise in intraocular pressure is a major risk factor, there is no set threshold for intraocular pressure that causes glaucoma. If left untreated, it leads to permanent damage of optic nerve head and loss of visual field and permanent blindness. A number of genetic susceptibility factors have been suggested to contribute to glaucoma.

One of the genes associated with normal tension glaucoma (NTG), as well as primary open angle glaucoma (POAG), is *OPTN*, which codes for the protein optineurin. Certain missense mutations in the coding region of *OPTN* are associated with adult onset as well as juvenile NTG and E50K is the most common disease-causing mutation of optineurin reported so far. However little is known about the molecular mechanisms responsible for the pathogenesis of glaucoma caused by such mutations. Several functions for optineurin have been proposed, however, none of these experiments explore the role of wild type optineurin or the pathogenicity of mutants in the eye particularly retinal ganglion cells, cell type relevant for glaucoma. All the experiments have been done in non-ocular cell lines which do not hold physiological relevance. It has been speculated that optineurin has a neuroprotective role in the eye and optic nerve, but it has not been demonstrated experimentally. Hence, we chose to investigate the function of optineurin and its mutants in the ocular environment. Since the

primary defect in glaucoma is the death of retinal ganglion cells, we analyzed the effect of expression of optineurin and its mutants on the survival of retinal ganglion cells.

So, the main objectives of this work have been:

A) To understand the function of wild type optineurin
B) To elucidate the mechanism by which optineurin mutations, like E50K, H26D, H486R and R545Q cause glaucoma.

Chapter 1 provides information on the disease glaucoma, the genes involved and on optineurin, the main gene of interest in the current study.

Chapter 2 provides information on the reagents and materials, as well as a detailed description of methodologies used in the study.

Chapter 3 describes results, where we show that E50K, the severe mutant of optineurin, induces death of retinal ganglion cells on overexpression and that this death is cell type specific as it does not cause death of other cell lines tested, viz., Cos-1, HeLa, IMR-32 (non-ocular cell lines) and D407 (ocular cell line). Other mutants of optineurin tested (H26D, H486R and R545Q) did not induce death of RGC. E50K induced cell death shows features of apoptosis and involves caspases-1 & 9. Antioxidant treatment rescued the retinal ganglion cells from E50K induced cell death and there was increased ROS production on E50K overexpression. Also, both wild type and E50K mutant potentiate TNF-α induced cell death in RGC-5 cells. Optineurin does not seem to have a generalized cytoprotective function as speculated because under certain conditions of stress, (e.g., TNF-α here), even wild type optineurin kills retinal ganglion cells.

Chapter 4 describes the identification of novel optineurin interacting proteins using the yeast two-hybrid approach. In addition the interaction of these optineurin interacting proteins with mutants of optineurin was also analyzed. We obtained three NF-κB regulators as optineurin-interacting partners, which suggest that optineurin has a role in the regulation of NF-κB pathway. Apart from the above mentioned proteins, proteins involved in vesicular transport, immune response and transcriptional repression were also identified as interacting partners. Hence, it is seen that optineurin interacts with diverse cellular proteins. E50K and H486R showed altered interaction with some of the optineurin-interacting proteins whereas H26D and R545Q behaved like the wild type. Finally, we observed that two of the interacting partners of optineurin lie in the region of known glaucoma loci.

Chapter 5 describes results of experiments designed to explore the possible mechanisms involved in cell death caused by E50K in RGC-5 cells. Since the mutant shows death only of retinal ganglion cells, we chose to see if there is defect in RGC-5 in responding to oxidative stress. We observed that the cell line does not show a generalized defect in responding to oxidative stress and antioxidant treatment; however there might be a selective defect in the inducibility of MnSOD. On E50K expression, one of the genes, PGC1α, which normally gets induced upon oxidative stress showed a decrease in mRNA levels. Hence, a defect in the mRNA levels of this gene might be one possible reason for not eliciting protective response by this cell line on E50K overexpression. Also, we observed that E50K shows subtle alteration in interaction with Rab8 (a protein involved in membrane recycling) compared to wild type optineurin. While, optineurin interacts with Rab8, it does not interact with Rab11 suggesting therefore that E50K might affect Rab8 mediated membrane recycling specifically.

Chapter 1

Introduction

1. Introduction

1.1 Glaucoma

Glaucoma is a complex eye disease leading to irreversible blindness worldwide. It is a heterogeneous group of optic neuropathies characterized by retinal ganglion cell death, visual field defects and degeneration of the optic nerve head (Shields *et al*., 2005). According to the WHO statistics on global burden of visual impairment (Resnikoff *et al*., 2004), glaucoma is the second major cause of blindness (12.3%) after cataract (47.8%). Since the peripheral vision is lost first and the disease is typically pain free, it goes unrecognized until substantial degree of vision loss occurs. Hence, glaucoma is called 'the sneak thief of sight'. Although raise in intraocular pressure is a major risk factor, there is no set threshold for intraocular pressure that causes glaucoma. If left untreated, it leads to permanent damage of optic nerve head and loss of visual field and permanent blindness.

1.1.1 Aqueous humor outflow pathway

The anterior chamber (the space between the cornea and the iris) of the eye is filled with a liquid called aqueous humor (AH). After being produced by the ciliary body, the aqueous humor enters the anterior chamber and finally enters the venous cavity through a sieve like region called the trabecular meshwork (TM) and Schlemm's canal. The fine balance between its production and drainage maintains the intraocular pressure of the eye within its physiological range (10-22mm Hg). In certain pathological states, the aqueous humor gets accumulated in the eye, leading to a raise in intraocular pressure (IOP). This

causes damage to the optic nerve and visual impairment. The loss of vision is because of degenerative changes in the retina, particularly retinal ganglion cells- the sensory cues of the eye. The aqueous humor outflow is depicted in Figure 1.1A.

1.1.2 Optic nerve head cupping and glaucomatous neurodegeneration

The optic nerve head (optic disc) consists of axons from approximately one million ganglion cells that have their cell bodies in the retina (Weinreb *et al*., 2004). The axons converge on the optic disc to form the optic nerve (Figure 1.2A). The fibers exit the eye through lamina cribrosa and synapse in the lateral geniculate nucleus of the brain. The convergence of the axons in the optic disc form a central depression called the optic cup. The neuroretinal rim of the optic nerve head is pink in colour and surrounds the cup.

Glaucomatous progression is characterized by a decrease in the width of the neuroretinal rim with a concomitant enlargement of the cup (Weinreb *et al*., 2004). As axons within the nerve die (largely through apoptosis) and the plates of the lamina cribrosa sclerae (a specialized area of sclera) collapse due to IOP or ischemia, loss of optic nerve tissue produces a characteristic excavation or “cupping” of the optic nerve head (Figure 1.2A&B). Thinning or notching of the disk rim, or disk hemorrhages might also be seen. When a vertical cup-to-disk ratio of 0.6 or greater is seen, glaucoma should be suspected. The cupping of the optic nerve head is directly related to the loss of one's peripheral visual field leading to tunnel vision. With peripheral vision loss, a person can see in front of him- or herself but has lost the vision to the side (Figure 1.2C).

A

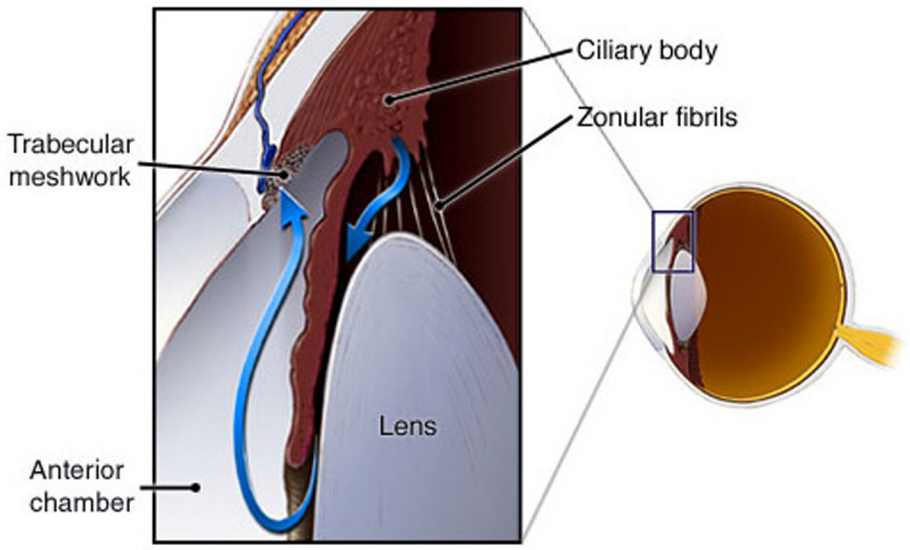

B

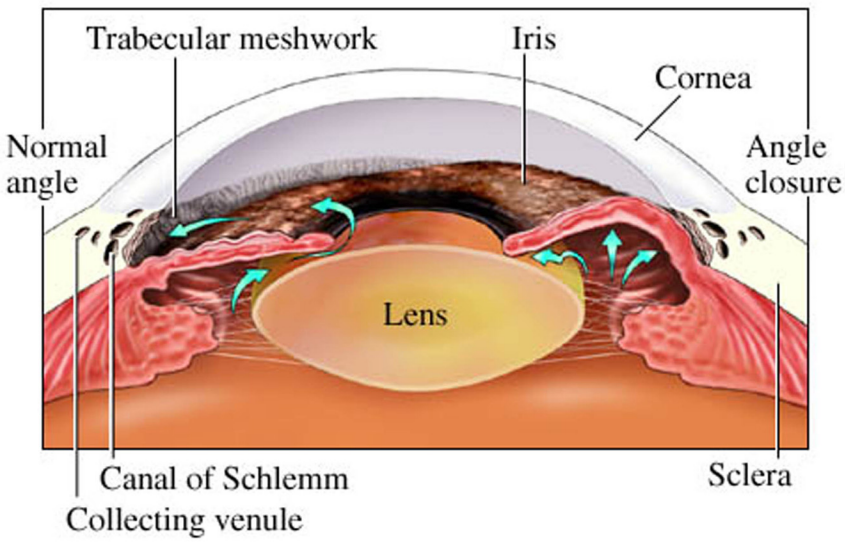

Figure 1.1: Diagram showing aqueous humor outflow pathway.
(A) Normal aqueous humor outflow pathway.
http://www.ahaf.org/glaucoma/about/aqueousflowBorder.jpg
(B) Illustration showing normal angle glaucoma and angle closure glaucoma.
http://catalog.nucleusinc.com/generateexhibit.php?ID=8908&ExhibitKeywordsRaw=&TL=&A=2

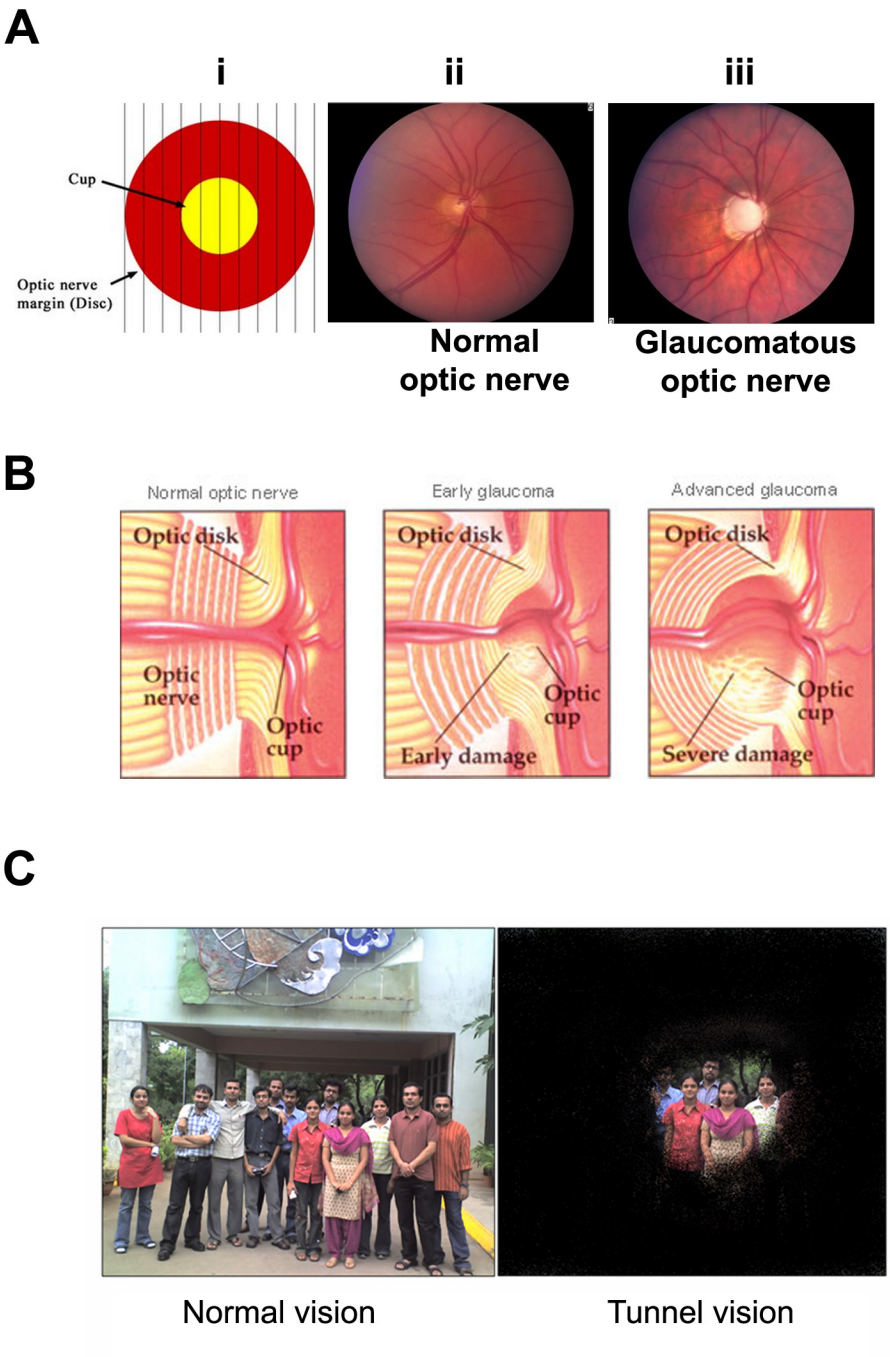

Figure 1.2: Normal and abnormal optic nerve head in glaucoma.
(A) (i) The optic nerve is divided into tenths and the cup is compared to the entire optic nerve (optic disc) to obtain the cup-to-disc ratio. This C/D ratio here is 0.4. (ii) Normal optic nerve (iii) abnormal optic nerve. http://www.medrounds.org/glaucoma-guide/2006/02/section-1-b-meaning-of-cupping.html
(B) Picture showing progressive loss of vision in glaucoma. http://www.eyesoftexas.us/cataracts/fig_02.jpg
(C) Vision of a normal person and an advanced glaucoma patient, who has "tunnel" vision.

1.1.3 Types of glaucoma

Glaucoma can be classified based on different criteria and one of the classifications based on the mechanism is mentioned below (Shields *et al*., 2005).

a. Primary open-angle glaucoma (POAG)

POAG is classified based on the visibility of the anterior chamber angle structures, TM, scleral spur and ciliary body upon gonioscopy (Shields *et al*., 2005). POAG is the most common clinically defined subset of glaucoma. As the term open angle suggests the angle between the cornea and iris is unimpeded, yet there is obstruction in the outflow of aqueous humor. Based on the age of onset, POAG is divided into juvenile onset POAG (JOAG) and adult onset POAG. JOAG occurs during the ages of 5-35 and adult onset POAG occurs at an older age. POAG patients have IOP consistently above 22mm Hg, which is hence also called high tension glaucoma (HTG). Approximately, one-third (33%) of POAG patients have IOP within normal range (<22mm Hg), or normal tension glaucoma (NTG) or low- pressure glaucoma (LPG) (Kamal & Hitchings, 1998). But the ultimate theme in both HTG and NTG is retinal ganglion cell death and visual field loss whose mechanism is still unclear.

b. Primary angle closure glaucoma (PACG)

In PACG, the iridocorneal angle (angle between iris and cornea) is closed, and hence a blockage for the aqueous humor to flow through the trabecular meshwork in to the venal system. As a result IOP rises and causes optic nerve head cupping and blindness. ACG is more common in people who have

shallower anterior chambers and narrower angles, like patients with hypermetropia (far sightedness). It is more common in people with Asian racial background. ACG can be either chronic or acute. Unlike POAG, patients with ACG may have intermittent symptoms like eye ache with cloudy vision, nausea, headache or vomiting. Patients with ACG can be provided relief by performing a surgery called laser iridotomy, in which a hole is made in the iris to allow normal outflow of AH through the exit channels. The defect is depicted in Figure 1.1B.

c. Developmental glaucoma

This is mainly classified based on the developmental abnormalities in the structures of conventional aqueous outflow pathway such as trabecular meshwork and Schlemm's canal. Congenital glaucoma is a type of developmental glaucoma and, as the name suggests, occurs at birth, and is due to an improper development of the eye's drainage channel (trabecular meshwork). Although individual clinical manifestations exist for the various types of glaucoma mentioned, the ultimate pathology in all of these involves the degeneration of retinal ganglion cell axons and soma, which is manifested as progressive visual field defects.

1.1.4 Risk factors for glaucoma

Awareness and early detection is very important in treating glaucoma because the disease can be well managed if diagnosed early. While everyone is at risk for developing glaucoma, some are at a higher risk and need regular eye check-ups to take care. High IOP is the strongest known risk factor for glaucoma (Sommer *et al*., 1991). Apart from IOP, other risk factors include increasing age

(Mitchell *et al*., 1996), family history of glaucoma (Tielsch *et al.,* 1994; Wolfs *et al*., 1998), and high myopia (Xu *et al.,* 2007). Other risk factors, particularly for NTG, include race (Suzuki *et al*., 2006), primary vascular dysregulation (Flammer *et al*., 1999), and low blood pressure (Kaiser and Flammer, 1991).

1.1.5 Molecular genetics of glaucoma

Glaucoma is a genetically heterogeneous disease and involves multiple factors. While a smaller proportion follows monogenic inheritance, majority of the cases involve multiple factors. Although autosomal dominant and recessive glaucomas exist, the disease is much more complex in many individuals, thus making it difficult to understand the molecular genetics. The most common forms of glaucoma do not exhibit Mendelian inheritance but the immediate relatives of the proband are at higher risk than general population. Multiple genetic and environmental factors play a major role in its etiology. Molecular geneticists have identified 17 chromosomal loci till date, which have been shown to be linked with various forms of glaucoma (Fan *et al.,* 2006) (Table: 1.1), but only 4 genes are identified. The 3 known POAG genes include *Myocilin/ TIGR* (Stone *et al*., 1997)*, Optineurin (OPTN)* (Rezaie *et al*., 2002) and *WDR36 (Monemi* et al., 2005). *CYP1B1* is the candidate gene for congenital glaucoma (Stoilov *et al.,* 1997).

Myocilin, also called *TIGR* (Trabecular meshwork induced glucocorticoid response) was the first gene discovered as a POAG gene (Stone *et al*., 1997), and is located as *GLC1A* locus at the position 1q23-25. Mutations in MYOC are responsible for approximately 3% of adult onset POAG and a major proportion of JOAG (Libby *et al*., 2005). The protein's structure includes an amino terminal signal sequence, a myosin-like domain, a leucine zipper domain and an

olfactomedin domain (Tamm, 2002). Most of the mutations reported till date lie in the olfactomedin domain. MYOC is expressed in both ocular and non-ocular tissues and the wild type protein is said to be secreted (Tamm, 2002). It was reported that the mutant proteins of MYOC form aggregates in the cytoplasm, lose the capacity to get secreted and hence its accumulation in the cell causes cellular stress (Caballero *et al*., 2000; Joe *et al*., 2003). Though the importance of MYOC in glaucoma is known, the function of normal MYOC protein in aqueous humor physiology remains an enigma.

OPTN was idenitified as a candidate gene for POAG, particularly NTG. Since the main focus of the project is on optineurin, a detailed introduction will be given about the same later.

The third candidate gene in POAG, *WDR36*, mapped onto chromosome 5q22.1 (*GLC1G*) (Monemi *et al*., 2005), comprises 23 exons and codes for a 951 amino acid residue protein containing a domain of the dipeptide WD repeated 36 times with several conserved residues. These domains are involved in protein-protein interactions. Mutations in *WDR36* were initially reported in 17% of POAG cases (Hauser *et al*., 2006) but some studies could not replicate its association to POAG (Fingert *et al*., 2007).

CYP1B1 (Cytochrome P4501B1) was the first gene of the CYP450 superfamily whose mutations are accounted for autosomal recessive primary congenital glaucoma (Stoilov *et al*., 1997; Bejjani *et al.,* 1998; Martin *et al*., 2000). This protein is expressed in the tissues of the anterior chamber angle of the eye and in several other cell types. It is an autosomal recessive trait with incomplete penetrance. Mutations in this gene have been observed in different populations,

accounting for 20-100% of all primary congenital glaucoma (PCG) patients (Mashima *et al*., 2001, Reddy *et al.,* 2004). Molecular modeling experiments suggest that mutations in CYP1B1 lead to loss of integrity of the protein and inherent instability; this is because substantial portion of the mutations reported are either deletions or insertions.

Only a small proportion of the genetics of glaucoma is accounted for. Even the cell biology aspects remain poorly understood. Much more research has to be focused on the genetic and linkage studies of the disease in order to have a better understanding. These efforts must be combined with genomic and proteomic approaches to speed up the rate at which glaucoma genes can be identified. Also there appears to be genetic alteration by genetic modifiers, and some mutations may cause the disease only when present in a susceptible genetic context. So this complexity in phenotype-to-genotype associations makes it difficult to clearly understand the specific allele responsible for the disease. Moreover, since multiple factors are involved, using animal models would be useful, whereby the effect of specific alleles in a defined genetic background and controlled environment can be studied. There are a few glaucoma models in mice, eg., C57BL/6J (Danias *et al*., 2003) and GLAST$^{-/-}$ and EAAC1$^{-/-}$ mice (Harada *et al*., 2007). C57BL/6J is an inbred mouse model and is reported to lose almost 50% of its retinal ganglion cells during aging. The *OPTN* ortholog of this strain has a glutamine at residue 552 and a lysine at residue 98 (respectively orthologous to the POAG-associated variants R545Q and M98K) (Rezaie *et al*., 2002). It is intriguing that this mouse has an extensive RGC loss despite a normal IOP, and hence represents an experimental mouse model for NTG (Libby *et al*., 2005).

GLAST (glutamate/aspartate transporter) and EAAC1 (excitatory aminoacid carrier1) are the glutamate transporters in Muller cells and retinal ganglion cells, respectively. In mice knocked out for either of these transporters, RGC and optic nerve degeneration are observed in the absence of high IOP. Hence, these mice represent NTG models, which offer a powerful system for determining mechanisms and evaluating new treatments for NTG (Harada *et al*., 2007)

1.1.6 Understanding the mechanism of glaucoma pathogenesis

Although apoptosis of retinal ganglion cells is known to be the main event occurring in glaucoma, the events leading to the cell death are not known. Elevation of intraocular pressure was earlier considered to be indispensable for glaucoma to occur. But later observations show that there is a subset of glaucoma, where IOP is in normal limits, and yet the disease progression occurs, namely in normal-tension glaucoma (NTG). Thus, understanding the etiology of the optic neuropathy in such cases remains complicated. Several pathophysiological mechanisms have been hypothesized to play a role in causing RGC death in glaucoma. Cellular and molecular biological studies are now focused on understanding the changes in patients in the trabecular meshwork, optic nerve head and retinal ganglion cells. The pathogenesis of glaucoma has been heavily debated since mid-nineteenth century and the changing concepts over the years led to the proposal of three theories (Flammer *et al*., 2002), which attempt to explain both IOP-dependent and independent mechanisms of RGC death.

In 1858 Muller proposed the **Mechanical theory** where abnormally elevated intraocular pressure relative to normal pressure of an eye causes mechanical deformation of the cribriform plates of the lamina cribrosa, which includes posterior bulging and deformation of the pores (Flammer *et al*., 2002); the deformation of the lamina cribrosa causes compression of the optic nerve bundle which in turn leads to glaucomatous changes in the optic nerve. Alteration of axoplasmic flow may therefore be associated with the disease progress. Such changes are observed in eye with high IOP and the degree of damage depends on the severity of the IOP elevation (Yamamoto & Kitazawa, 1998).

The second theory is **vascular theory/ ischemic theory;** here elevation of IOP causes compression of optic nerve fibers and the optic arteries at the lamina cribrosa which results in alterations in the blood supply to the optic nerve head, leading to ischemic damage of optic nerve head and progressive death of retinal ganglion cells. The main evidence for this theory comes from (i) blood flow incompetence at ONH in glaucoma patients (Chung *et al.,* 1999), and (ii) presence of retinal blood flow abnormalities in glaucoma patients (Arend *et al.,* 2004).

Excitotoxicity theory suggests that like any other neurodegenerative disease, glaucoma too is characterized by excitotoxicity. It occurs when the glutamate receptor gets overstimulated, leading to excessive glutamate intake leading to an abnormal calcium ion influx. This leads to free radical formation, as well as the activation of enzymes causing cellular damage. If neurons are injured or unable to properly control glutamate levels, secondary damage can result, even if the primary cause is not related to glutamate. Injured neurons are more vulnerable to even normal levels of glutamate, become overstimulated and die.

Glutamate is the major excitatory neurotransmitter in the retina and its levels have been shown to be increased in glaucomatous eyes. An interesting observation is that persistent levels of glutamate cause death of RGC, independent of elevated IOP (Casson *et al*., 2006). Excitotoxic damage is suggested to be one of the mechanisms of RGC damage during glaucoma, and hyperactivity of NMDA receptors has been described in glaucoma. A partial NMDA receptor antagonist is being tested as a potential therapeutic agent in glaucoma (Lipton, 2003).

1.1.7 Factors contributing to glaucomatous neurodegeneration

Apart from rise in IOP, some other factors play a major role in glaucomatous neurodegeneration. These include ischemia, glutamate excitotoxicity, aberrant immunity and alteration in glial cells (Weinreb and Khaw, 2004) (Figure 1.3). The relative significance of each specific factor varies between patients depending on the magnitude of IOP elevation, oxidative stress and individual life style (John, 2005).

a) Ischemia: Elevated IOP induces ischemia, which results in blockage of axoplasmic flow and obstruction in normal flow of growth factors leading to RGC death. Optic nerve blood flow is compromised in glaucomatous patients (Flammer *et al.,* 1994). Ischemia enhances the levels of reactive oxygen species (ROS), glutamate release, and nitric oxide production, which increase the levels of Ca^{2+} that show detrimental effect on RGC cells (Cioffi, 2005).

b) Excitotoxicity: Glutamate is an essential excitatory amino acid in the central nervous system and in the retina as well. In several neurological diseases,

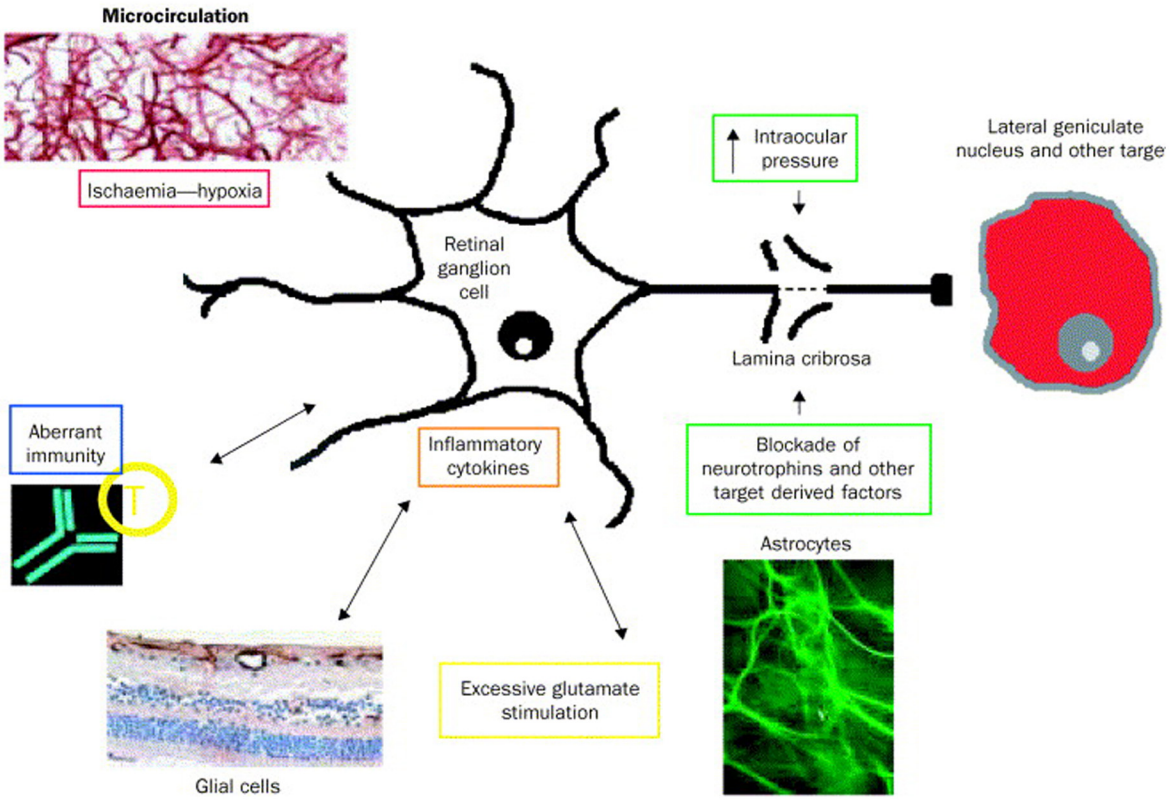

Figure 1.3: Factors contributing to the pathophysiology of glaucomatous neurodegeneration.
Apart from IOP, other contributing factors for glaucoma include ischemia-hypoxia, excitotoxicity, alterations in glial cells and aberrant immunity (Weinreb *et al.*, 2004).

excessive glutamate induces over-excitation of neurons, which ultimately leads to the death of neuronal cells. It has recently been shown that glutamate excitotoxicity plays an important role in the pathogenesis of glaucoma (Vorwerk *et al.,* 1999). The evidence comes from the fact that (i) vitreal glutamate levels are elevated in experimental and clinical glaucoma (Dreyer *et al.,* 1996), (ii) ischaemia plays a role in glaucoma (Lam *et al.,* 1997), (iii) neuroprotection based animal studies and (iv) secondary degeneration of RGCs after optic nerve injury.

c) Autoimmunity: Franz *et al.* (2004) showed circulating autoantibodies against several ocular antigens in glaucoma patients, and suggested the role of auto-immunity in glaucoma. The auto-antibodies observed include heat shock proteins (HSPs), rhodopsin, γ-enolase, glutathione-S-transferase (GST), tumor necrosis factor-α, and γ-synuclein. These antibodies may play role in the formation of inflammation that can induce apoptosis of RGCs.

d) Glial cell activation: Glial cells are important structural and functional components of the optic nerve head or ONH. The glial cells present in ONH and retina include astrocytes, oligodendrocytes and microglia. These glial cells support neuronal tissue by supplying metabolites and growth factors, and by scavenging toxic metabolites. Therefore, glial activation in glaucomatous eyes may initially represent a cellular attempt to limit the extent of neuronal injury and to promote tissue repair. However, activated glial cells may also have toxic effects on neuronal tissue by creating mechanical injury and/or changing the microenvironment of neurons. The activated glial cells in glaucomatous eyes produce neurotoxic substances such as nitric oxide synthase and TNF-α. In addition, *in vitro* experiments have provided direct evidence that glial cells are

activated in response to glaucomatous stressors such as elevated pressure and ischemia, and are directly involved in facilitating the apoptosis of retinal ganglion cells due to increased production of apoptosis-promoting substances, including nitric oxide and TNF-α (Tezel *et al.,* 2000).

1.1.8 Diagnosis and treatment strategies for glaucoma

Early diagnosis is the key to successful management of glaucoma. Since glaucoma occurs without any signs or symptoms, regular eye-check ups are a must particularly for people above the age of 40. The diagnosis of glaucoma no longer relies simply on the presence of pressure within the eye; it requires that there be optic nerve damage or a strong suggestion of damage, which can be clearly seen during a dilated eye examination of the optic nerve. In general, the hallmark sign of this condition is a loss of peripheral vision. Glaucoma evaluation has several components. Apart from measuring the IOP by tonometry, the health of the optic nerve is also examined by ophthalmoscopy and visual field test. In order to determine early damage in the optic nerve, a number of diagnostic instruments have been developed to assess the nerve fiber layers at the back of the eye (the fundus) and to check for optic disk cupping. The cup of the optic disc is the center portion, which enlarges as nerve damage progresses. A cup-to-disc ratio is critical when evaluating glaucoma. The cup-to-disc ratio is the amount of the entire nerve head that has been cupped out or where glaucoma has caused damage. Readings range from 0 meaning no cupping at all to 1.0 where the entire optic nerve is cupped out. Many people have some cupping- which is normal. Gonioscopy helps in examining the intactness of the anterior part of the eye using a specific lens.

The treatment strategies for glaucoma usually include medicated eye drops which lower the IOP by either decreasing aqueous humor production or increasing its outflow. In extreme cases when the medications do not improve the condition, surgeries are performed such as **trabeculoplasty,** where high energy laser beam is used to shrink one part of the trabecular meshwork so that the other half stretches and allows drainage of aqueous humor, or a conventional surgery like **trabeculectomy**. In this surgery the trabecular meshwork is excised from the patient completely so that the aqueous humor can easily leave the eye through the hole. In a few cases like secondary glaucoma or for children with glaucoma, **drainage implants** are inserted for effective drainage of aqueous humor. While the above surgical techniques are applied for open angle glaucoma, angle closure glaucoma needs a different surgery called laser iridotomy.

The primary goal of glaucoma treatment is to preserve vision. However, current knowledge of the factors causing optic nerve damage and visual loss is limited. Proven existing therapies focus mainly on IOP reduction although elevated IOP is not always a diagnostic feature for glaucoma. So, a multidrug approach will be of use which includes agents targeted towards lowering IOP as well as an agent directed at preserving and protecting the optic nerve from glaucoma.

1.1.9 Complete therapy

Glaucoma is a neurodegenerative disease. Current therapeutic agents under investigation include neuroprotectants, which target the disease progress manifested by death of retinal ganglion cells, axonal loss and irreversible loss of

vision. Neuroprotectants, when used in conjunction with IOP-reducing therapy, form a complete therapy for glaucoma management. Till date, no such medications have been approved. Drugs which protect RGC degeneration belong to different groups, which include NMDA antagonists such as memantine and dexanabinol, inhibitors of inducible nitric oxide synthase (NOS-2), neurotrophic factors such as nerve growth factor (NGF), brain derived neurotrophic factor (BDNF), and neurotropin 3 (Rudziniski *et al*., 2005). One interesting drug which has reached phase 3 (final stage) clinical trial is memantine, which is a N-methyl-D-aspartate receptor blocker. Similarly, trophic factors are used to protect degenerating RGC neurons. Trophic factors such as BDNF or NGF act on the tyrosine kinase (Trk) receptor signaling, but this kind of cell signaling is not specific to only RGCs. They might affect others as well, which might lead to unwanted side effects.

Thus, there is a need to search for compounds which show maximum advantage, with minimum or no side effects. One such possibility is the search for natural anti-oxidants, which can also work through different and multiple mechanisms, such as oxidative stress induced or excitotoxicity induced mechanisms of RGC degeneration in glaucoma.

1.2 Oxidative stress in glaucoma

Oxidative stress is caused by an imbalance between the production of reactive oxygen species (ROS) and a biological system's ability to readily detoxify the reactive intermediates or easily repair the resulting damage (Mozaffarieh *et al*., 2008). All forms of life maintain a reducing environment within their cells. This reducing environment is preserved by enzymes that maintain the

reduced state through a constant input of metabolic energy. Disturbances in this normal redox state can cause toxic effects through the production of peroxides and free radicals that damage all components of the cell, including proteins, lipids, and DNA. DNA damage is involved in the pathogenesis of various chronic-degenerative diseases like cancer, atherosclerosis and neurodegenerative diseases (De Flora *et al*., 1996). Increasing experimental evidence indicates that oxidative stress plays a major role in the pathogenesis of glaucoma (Izzotti *et al*., 2003).

Since the major risk factor for the disease is rise in IOP, initial therapeutic management was focused on drugs that help in lowering the IOP. However, although IOP lowering treatment can provide neuroprotection and retard the disease progression in many glaucoma patients, it is not always sufficient to fully prevent disease progression. This is just one reason why recent efforts have focused on the development of alternative treatment strategies for neuroprotection. In addition, IOP is not always elevated in the eyes exhibiting glaucomatous degeneration. Clinical (Tezel *et al*., 1996) and histopathological (Wax *et al*., 1998) findings in the glaucomatous eyes with either elevated or normal IOP indicate that there is also an IOP-independent component of neuronal damage in glaucoma. It becomes more important in the cases of normal tension glaucoma, where patients suffer from the disease in spite of normal IOP. In such cases, increased glutamate levels (Shen *et al.,* 2004), oxidative stress (Moreno *et al*., 2004), vascular alterations (Chung *et al*., 1999) can be considered as other concomitant factors associated with the disease.

The ability of oxidative damage to alter several structures of the eye has been recognized as an etiopathogenetic factor in various ocular diseases like

cataract, age-related macular degeneration (AMD) (Ohia *et al*., 2005) and only recently in POAG (Izzotti *et al.,* 2003). Increasing evidence supports that the glaucomatous tissue stress initiated by elevated IOP or tissue hypoxia also involves an oxidative component (Bonne *et* al., 1998; Tezel, 2006). Multiple pathogenic mechanisms have been proposed for glaucomatous neurodegeneration which include axonal injury, which may result in neurotrophin deprivation, mechanical injury, glutamate excitotoxicity, and vascular ischemia. Most of these mechanisms appear to be associated with a common pathway of oxidative injury. Alvarado *et al*. have suggested that the progressive loss of trabecular meshwork cells in patients with glaucoma may be attributable to the long term effect of free radical damage (Alvarado *et al*., 1984). This hypothesis has been supported indirectly by experimental studies. Experimental elevation of IOP induces oxidative stress in the retina of experimental rat models with glaucoma (Ko *et al.*, 2005). The inner retinal layers, particularly retinal ganglion cells show, high carbonyl reactivity indicating that the RGCs are prominently exposed to oxidative stress in the ocular hypertensive eyes (Tezel *et al.,* 2005). Additional supportive evidence for the role of oxidative stress in glaucomatous degeneration comes from studies on glaucoma patients. It is shown that the ROS production is more in the trabecular meshwork of POAG patients than in the age matched controls (Izzotti *et al*., 2003). Yang *et al*. have detected autoantibodies against GST in the glaucomatous patients' sera; GST which belongs to a major group of detoxifying enzymes gets regulated *in vivo* by the levels of ROS (Yang *et al*., 2001). Moreover, a recent study reports increased mRNA and protein levels of the iron-regulating proteins transferrin, ceruloplasmin, and ferritin in an experimental monkey model of glaucoma (and in human glaucoma) suggesting

the involvement of iron and copper metabolism and associated antioxidant systems in the pathogenesis of glaucoma (Farkas *et al*., 2004).

One of the harmful consequences of ROS generation in glaucoma is the oxidative modification of many important retinal proteins like HSP72 and glutamine synthetase (Tezel *et al*., 2005). Adult GLAST$^{-/-}$ and EAAC1$^{-/-}$ mice show increased lipid hydroperoxides in retina suggesting the involvement of oxidative stress in RGC loss (Harada *et al*., 2007). EAAC1 and GLAST are glutamate transporters located in different regions of the retina. Glutamate transporters play an important role in the removal of excess glutamate from the extracellular fluid of the retina (Harada *et al*., 2007). Indeed, these mice models were the first NTG animal models developed to investigate IOP-independent mechanisms of RGC loss. However, whatever the effect is seen, it largely reflects the balance between a variety of intracellular signaling pathways linked to cell survival or death that are activated in response to the oxidative insult (Kamata and Hirata, 1999). The major signaling pathways known to be involved in regulating the cellular response to oxidative stress include MAPKs, PI3-kinase/Akt pathway, heat shock protein expression, p53 signaling, and NF-*κ*B signaling (Martindale and Holbrook, 2002). All the studies mentioned above focus on oxidative stress to be a key component in both IOP-dependent and independent cases of glaucomatous neurodegeneration.

1.3 Optineurin

1.3.1 Identification as a candidate gene for glaucoma

The gene *OPTN* (accession numbers: NM_001008211.1, protein NP_001008212.1) was identified as a candidate gene for glaucoma where mutations in the coding region are responsible for NTG and POAG (Rezaie *et al*., 2002). In fact, *OPTN* remains the only candidate gene reported for NTG till date. In humans the gene is located within the GLC1E locus at chromosome *10p14-p15* (Sarfarazi *et al*., 1998). The initial study was conducted in 54 families and sequence alterations in *OPTN* were identified in 16.7% of the families with hereditary POAG, including a proportion with normal IOP (Rezaie *et al*., 2002).

1.3.2 History of optineurin before identification as a glaucoma candidate gene

Optineurin was initially discovered as FIP-2 because of its interaction with adenoviral 14.7kDa protein (Li *et al.,* 1998). Later FIP-2 was shown to interact with diverse cellular proteins like huntingtin (HYPL) (Faber *et al*., 1998), Rab8 (Hattula & Peranen, 2000) and TFIIIA (Moreland *et al*., 2000) and the protein sequence shows 56% similarity to NEMO which is a central molecule for NF-κB activation (Schwamborn *et al*., 2000). Hence optineurin is also called NEMO related protein (NRP).

1.3.3 Structural features, alternative splicing and sub-cellular localization

Optineurin has a total of 16 exons; the first 3 are non-coding at the 5'-UTR and the rest 13 exons code for a 577- amino acid protein. Sequence analysis

suggests that the protein has several putative domains, including one bZIP motif, two leucine zippers, coiled-coil motifs and a c-terminal C_2H_2-type zinc finger domain (Figure 1.4). Alternative splicing at the 5'-UTR generates three mRNA forms all coding for the same protein (Genbank accessions AF420371 to AF420373). The OPTN homologs from monkey, mouse and rat share substantial degree of similarity to human OPTN. The localization of endogenous protein remains a controversy still as there are opposing reports on its cellular distribution. Optineurin was initially shown to be a Golgi localizing protein (Schwamborn *et al*., 2000; Rezaie *et al*., 2002) but later report shows that the protein shows diffused cytoplasmic distribution and is by and large not associated with Golgi (Park *et al*., 2006).

1.3.4 Expression of optineurin in various ocular and non-ocular tissues

Various teams have studied optineurin expression in human, mouse, monkey and chicken species at the mRNA and protein levels. In humans, optineurin exists as three different transcripts. The levels of optineurin vary among various tissues, e.g., heart, brain, placenta, lung, skeletal muscle, liver, kidney and pancreas, with maximum levels in skeletal muscle (Li *et al*., 1998). The difference in the sizes of the three message forms is most likely because of alternative spicing at the 5'- end of the gene. Further studies showed that optineurin shows expression in human trabecular meshwork, non-pigmented ciliary epithelium, retina, adrenal cortex, lymphocyte and fibroblast (Rezaie *et al*., 2002).

In mouse, the highest expression of optineurin mRNA is in liver, heart and testis, although expression is seen in the eye and muscle. Similar to the human

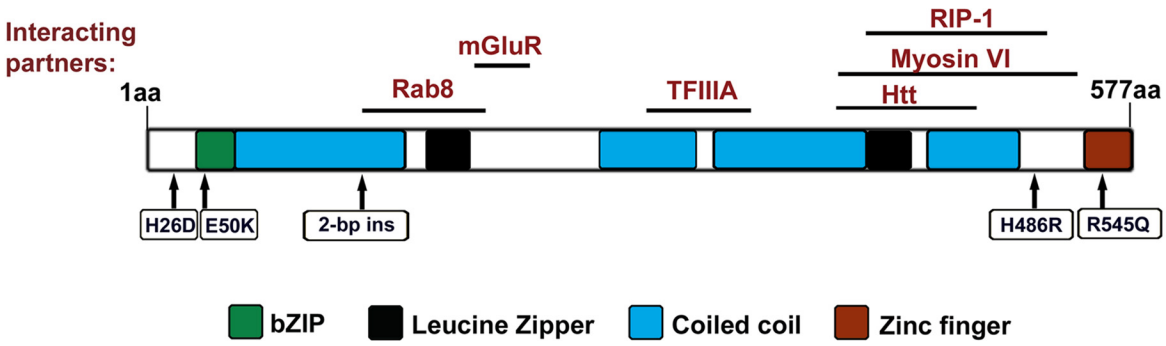

Figure 1.4: Schematic representation of the protein optineurin, showing predicted structural motifs and known binding sites for cellular proteins.

The locations of some of the mutations found in NTG or POAG are also shown. The binding sites (amino acids) for cellular proteins are: Rab 8 (141-209), metabotropic glutamate receptor (mGluR1a, 202-246), transcription factor IIIA, huntingtin (Htt, 411-461), myosin VI (412-520), Rip1 (424-509). In addition adenoviral E3-14.7 kDa protein binds in the region of residues 395-577.

counterpart, optineurin here exists as at least three major transcripts. Within the eye, optineurin shows most intense expression in the pigmented epithelium and also in the retinal ganglion cells of the retina. In the anterior eye, expression is seen in cornea, trabecular meshwork and iris (Rezaie and Sarfarazi, 2005; Kroeber *et al*., 200; De Marco *et al*., 2006). *In situ* hybridization studies revealed optineurin expression in the developing mouse eye at E10.5, but not at the late developmental stage till adult phase (De Marco *et al*., 2006; Rezaie *et al*., 2007). Optineurin transcripts were also detected in the forelimb buds of the mouse embryo (Rezaie *et al*., 2007). The relative abundance of optineurin in the RGCs emphasizes the importance of the protein in the context of glaucoma where apoptosis of RGC is observed.

In monkey, optineurin is present as two different transcripts and the highest level of mRNA expression is in skeletal muscle, similar to its human counterpart. Expression in heart, brain, kidney, lung is comparable to human and mouse (Rezaie *et al*., 2005). Immunohistochemistry revealed maximum expression in retinal pigmented epithelium and retinal ganglion cells of the retina apart from neighbouring surrounding cell types similar to the mouse counterpart. In the anterior segment optineurin expression is seen in the iris, trabecular meshwork and non-pigmented ciliary epithelium (Rezaie *et al*., 2005).

In chicken, in contrast to other species, there is a single optineurin transcript and it is expressed in muscle, spleen, kidney, brain, liver and lung (Stroissnigg *et al*., 2002).

1.3.5 Optineurin mutations

Mutations in OPTN were initially reported in 16.7% of families with hereditary POAG, with most of them having NTG (Rezaie *et al*., 2002). Also, 13.6% of risk-associated alterations were observed in both familial and sporadic individuals. Out of 16.7% of mutations, the major proportion of patients, i.e. 13.5% of them carried a missense mutation [$Glu^{50} \rightarrow$ Lys (E50K)] where glutamic acid at position 50 was mutated to lysine. Here, 81.5% of the E50K patients had normal intraocular pressure (IOP) suggesting that this mutation was majorly responsible for NTG. The recurrent E50K mutation is located in the putative bZIP motif of optineurin which is conserved in mouse, macaque and bovine genomes. This motif is a transcription factor domain and is involved in DNA binding and protein dimerization, so the E50K mutation located in the bZIP motif may have a dominant negative effect (Rezaie *et al*., 2002). Later, this mutation was observed in a patient with positive family history of NTG in a larger study comprising of 1048 mixed glaucoma patients (Alward *et al*., 2003). Moreover, patients with the most common mutation E50K appear to have a more severe form of NTG than those glaucoma patients without this mutation (Aung *et al*., 2005).

Another mutation which accounts for 2.2% of the disease was a 2-bp AG insertion (c691-692insAG) leading to premature truncation. All the patients carrying this mutation had normal IOP. This mutation truncates the protein by 76% and hence the disease in this case may be attributed to haploinsufficiency or loss of function. R545Q was reported initially as a disease causing mutation (Rezaie *et al*., 2002), but was later observed in normal controls in the Chinese (Leung *et al*., 2003) and Japanese populations (Toda *et al.,* 2004; Funayama *et al.*, 2004). Later screening studies have revealed one interesting mutation H486R [$His^{486} \rightarrow$ Arg] which represents the first reported OPTN mutation responsible for

juvenile open angle glaucoma (JOAG), although this mutation is also seen in NTG cases (Willoughby *et al*., 2004).

In the Indian scenario, an earlier study did not implicate OPTN as a candidate gene in POAG (Mukhopadhyay *et al*., 2005); however a possible role of SNPs rather than mutations in OPTN is suggested to be implicative in glaucoma pathology (Sripriya *et al*., 2006). Table 1.2 represents the disease-causing mutations of optineurin reported till date.

1.3.6 Functional studies on optineurin

1.3.6.1 Optineurin - component of TNF-α and NF-κB signaling pathway

TNF-α is a multifunctional proinflammatory cytokine that belongs to the tumor necrosis factor (TNF) superfamily. It signals through two distinct cell surface receptors, TNFR1 and TNFR2. NF-κB is a transcription regulator that is activated by various intra and extra cellular stimuli including cytokines like TNF-α. The TNF-α induced NF-κB activity involves the five mammalian NF-kappaB/Rel proteins: c-Rel, NF-kappaB1 (p50/p105), NF-kappaB2 (p52/p100), RelA/p65, RelB. In the absence of TNF-α stimulation, NF-κB is associated with the inhibitor IkappaB in the cytoplasm. TNF-α induced activation of NF-kB largely relies on phosphorylation dependent ubiquitination and degradation of inhibitor of kappa B (IkB) proteins. The inhibitor of kappa B kinase (IKK) complex, a multiprotein kinase complex is responsible for the TNF alpha induced phosphorylation of IkB. The free NF-κB translocates to the nucleus and induces expression of certain genes. TRADD adaptor molecule interacts with TNFR1 and recruits the additional adaptor proteins like RIP, TRAF2, and FADD, which in turn recruit

additional key components to TNFR1 responsible for initiating downstream events and mediating programmed cell death signaling and NF-κB activation. This pathway is involved in the regulation of a wide spectrum of biological processes including cell proliferation, differentiation, apoptosis, lipid metabolism, and coagulation.

Optineurin was initially identified as FIP-2 (E3-14.7K interacting protein) while screening for interacting partners of E3-14.7K adenoviral protein. Upon overexpression of TNFR1 (TNF-α receptor 1; TR55) intracellular domain which is a potent inducer of apoptosis and E3-14.7K, the latter showed a protective effect on TR55 induced cytolysis. But in the presence of optineurin, the protective effect was reversed. On the basis of this observation it was suggested that optineurin is a component of TNF-α signaling pathway, although no effect of optineurin on TNF-α-induced or TR55-induced apoptosis was reported (Li *et al.,* 1998). Interaction between TNF-α and optineurin is further supported by findings that show an increase in the expression of optineurin in trabecular meshwork cells (Vittitow and Borras, 2002) and HeLa cells (Schwamborn *et al*., 2000) following TNF-α treatment (Vittitow and Borras, 2002) and a possible interaction between polymorphisms in the *OPTN* and *TNF-α* genes that appear to increase the risk for glaucoma (Funayama *et al*., 2004)

As mentioned earlier, a multi-subunit complex called IKK complex (comprising of IKKα/β/γ) plays the major role in Iκ-B phosphorylation and degradation. IKKγ, also called NEMO (NF-κB Essential Modulator), forms the structural and regulatory subunit of this high molecular kinase complex. Optineurin (called as NRP or NEMO-related protein) shares 53% aminoacid

similarity to NEMO and is structurally homologous to it (Schwamborn *et al*., 2000). Though there is significant similarity between these two proteins, it appears that NRP cannot substitute for NEMO nor can associate with IKKβ or NEMO (Schwamborn *et al*., 2000). But a later study showed that optineurin has a ubiquitin binding domain (Wagner *et al*., 2008) just like NEMO and competitively antagonizes NEMO's binding to poly ubiquitinated RIP and inhibits TNF-α induced NF-κB activation (Zhu *et a*l., 2007). Moreover, a recent study reports that optineurin mRNA levels get induced by S100A4, metastasis promoting protein, in a NF-κB dependant manner (Boye *et al*., 2008). This was also supported by earlier evidence which shows that optineurin is a direct NF-κB target; a deletion of putative NF-κB binding site in the promoter region of optineurin completely abolishes the enhancing action and modulatory effect of NF-κB on optineurin (Mrowka *et al*., 2008). Together, all the investigations discussed above indicate that optineurin is a part of the negative feed back system that is important in regulating NF-κB activity.

1.3.6.2 Regulation of transcription and gene expression by optineurin

Optineurin interacts with transcription factor IIIA (TFIIIA) at its C-terminus and in turn facilitates TFIIIA-dependent 5S gene transcription (Moreland *et al*., 2000). Moreover, optineurin knock down by siRNA leads to the identification of genome wide- expression changes (Weisschuh *et al*., 2007). A wide variety of differentially expressed genes belonging to categories, like genes involved in cell morphology, organelle movement and organization of the actin cytoskeleton were obtained on optineurin knockdown. Hence, this study further emphasizes the role of optineurin in gene expression directly or indirectly.

1.3.6.3 Role of optineurin in Golgi organization and vesicular transport

Rab8 is a small GTPase molecule of around 203 amino acids and is involved in vesicular trafficking. It is a unique Rab member which promotes radical changes in cell shape by actin and microtubule reorganization. It controls polarized membrane transport by modulating cellular morphogenesis (Peranen *et al*., 1996). Studies on FIP-2 (an earlier name of optineurin) shows that it mediates the interaction of huntingtin (huntington's disease protein) with Rab8 forming a complex that regulates membrane trafficking and cellular morphogenesis (Hattula and Peranen, 2000). In this process, the amino-terminal region of optineurin (position 141-209) is essential for binding to Rab8 and the carboxy terminal region 411-461 binds to huntingtin. Coexpression of FIP-2 and huntingtin relocates huntingtin to Rab8-positive vesicular structures. Optineurin is shown to protect NIH3T3 cells from H_2O_2 induced cell death and during this process it translocates to the nucleus which is mediated by the GTPase activity of Rab8 (De Marco *et al.,* 2006). While wild type optineurin shows protection, the disease associated mutant, E50K, does not show any protection on apoptotic stimulus and no translocation to the nucleus. Therefore, Rab8 may have a role in mediating response to stress which needs further investigation.

Optineurin also interacts with myosin VI, a Golgi protein involved in the steady-state organization of Golgi complex and post-Golgi membrane traffic. When optineurin is knocked down by siRNA in HeLa cells, Golgi gets fragmented and exocytosis is hampered. Also optineurin targets myosin VI to the Golgi complex and is responsible for colocalization of myosin VI and Rab8 in the perinuclear region around the Golgi and vesicles underneath the plasma membrane, both of which are important regulators of membrane trafficking

(Sahlender *et al.,* 2005). The authors suggest that optineurin plays two major linker functions: (a) optineurin together with huntingtin links via the minus end directed motor dynein to the microtubule network and by directly interacting with myosin VI, is linked to the actin cytoskeleton, thus playing a co-ordinated microtubule and actin based motor activity around the Golgi complex, (b) optineurin might link myosin VI to the Rab8 involved in sorting molecules to the exocytic pathway at the trans-Golgi network and in membrane fusion at the plasma membrane (Sahlender *et al*., 2005).

1.3.6.4 Optineurin and metabotropic glutamate receptor signaling

Glutamate is the major excitatory neurotransmitter in the retina (Kuehn *et al*., 2005). Glutamate is thought to mediate excitatory synaptic transmission at the photoreceptor/bipolar cell synapses and at the bipolar/ ganglion cell synapses, acting through activation of glutamate receptors (Nakanishi, 1992). These receptors have been divided according to their primary signal transduction mechanism into ionotropic glutamate receptors and G-protein coupled metabotropic receptors. Glutamate is released by the presynaptic cells and acts through various postsynaptic receptors including N-methyl-D-aspartate (NMDA) receptors. If excessive amount of glutamate is released or glutamate clearance is insufficient, neuronal cell death occurs though a process known as excitotoxicity. Group I metabotropic glutamate receptors (mGLuRs) play an important role in regulating neurotoxicity and neuroprotection. These G-protein coupled receptors (GPCRs) are coupled to inositol 1,4,5-triphosphate formation and the release of Ca^{2+} stores, play an important role in regulating neuronal function. G-protein coupled receptor kinase-2 (GRK2) is an essential GPCR protein that protects cells from receptor overactivation and is present at low levels in striatal tissue.

Optineurin is shown to interact with mGLuR and inhibits the latter's signaling to form inositol triphosphate (Anborgh *et al*., 2005). An optineurin interacting partner, huntingtin also interacts with mGLuR and a mutant form of huntingtin enhances optineurin mediated inhibition of mGLuR signaling. A mutant form of optineurin, H486R, does not interact with mutant huntingtin and inturn fails to attenuate mGLuR mediated inositol triphosphate formation. The study shows a novel mechanism for mGLuR desensitization by optineurin in striatal tissue where GRK2 is at low levels and an additional biochemical link between glutamate receptor signaling and huntington's disease- a neurodegenerative disease.

1.3.6.5 Optineurin in the context of glaucoma

Various risk factors are associated with glaucoma, and a few unrelated risk factors are shown to induce optineurin gene expression levels (Vittitow and Borras, 2002). One risk factor, namely, elevation of IOP is associated with elevation in optineurin mRNA level (Vittitow and Borras, 2002), although a later report contradicts the increase in optineurin mRNA levels after an increase in IOP (Kamphuis and Schneemann, 2003). The role of TNF-α in the eye and its potential contribution to eye disease has been well studied. In the human glaucomatous optic nerve head, expression of TNF-α and its receptor, TNFR1 are significantly upregulated (Yuan and Neufeld, 2000). Increase in TNF-α levels has been associated with elevated hydrostatic pressure (Tezel and Wax, 2000) and retinal degeneration (Cotinet *et al*., 1997). Moreover evidence exists for the possible interaction between polymorphisms in the optineurin and TNF-α genes that would increase the risk for glaucoma (Funayama *et al*., 2004). Patients

treated with glucocorticoids develop steroid-induced glaucoma and dexamethasone is the most commonly used steroid which is shown to induce optineurin levels (Vittitow and Borras, 2002). The induction in mRNA levels of optineurin by TNF-α (and by interferon-γ) has been reported earlier (Li *et al*., 1998; Schwamborn *et al*., 2000).

Incidentally, a recent report shows that optineurin, on overexpression, dramatically induced the mRNA levels of myocilin (MYOC, first candidate gene for glaucoma) (Park *et al*., 2007). This suggests a possible molecular interaction between these two glaucoma genes, which may have pathological consequences.

The functional studies discussed above do not explain the possible role of optineurin and its mutants in the eye, particularly in the retinal ganglion cells. It has been speculated that optineurin has a neuroprotective function, but it is not experimentally demonstrated in the eye or cells that are relavant for glaucoma. Hence, the main aim of my research was to study the role of optineurin in the eye and to elucidate the functional association between optineurin mutations and glaucoma phenotype.

1.4 Background and objectives of the current study

One of the genes associated with normal tension glaucoma (NTG), as well as primary open angle glaucoma (POAG), is *OPTN*, which codes for the protein optineurin. Certain missense mutations in the coding region of *OPTN* are associated with adult onset as well as juvenile NTG and E50K is the most common disease-causing mutation of optineurin reported so far. Though there

are a few reports on the functional aspects of optineurin, the role of the protein in the eye has not been explored.

Hence, we chose to investigate the function of optineurin and its mutants in the ocular environment. Since the primary defect in glaucoma is the death of retinal ganglion cells, we analyzed the effect of expression of optineurin and its mutants on the survival of retinal ganglion cells.

The main objectives of this work have been:

A) To understand the function of wild type optineurin, and

B) To elucidate the mechanism by which optineurin mutations such as E50K, H26D, H486R and R545Q cause glaucoma.

Chapter 1 provides information on the disease glaucoma, the genes involved and on optineurin, the main gene of interest in the current study.

Chapter 2 provides information on the reagents and materials, as well as a detailed description of methodologies used in the study.

Chapter 3 describes results, where we show that E50K, the severe mutant of optineurin, induces death of retinal ganglion cells on overexpression and that this death is cell type specific as it does not cause death of other cell lines tested, viz., Cos-1, HeLa, IMR-32 (non-ocular cell lines) and D407 (ocular cell line). Other mutants of optineurin tested (H26D, H486R and R545Q) did not induce death of RGC. E50K induced cell death shows features of apoptosis and involves caspases-1 & 9. Antioxidant treatment rescued the retinal ganglion cells from E50K induced cell death and there was increased ROS production on E50K

overexpression. Also, both wild type and E50K mutant potentiate TNF-α induced cell death in RGC-5 cells. Optineurin does not seem to have a generalized cytoprotective function as speculated because under certain conditions of stress, (e.g., TNF-α here), even wild type optineurin kills retinal ganglion cells.

Chapter 4 describes the identification of novel optineurin interacting proteins using the yeast two-hybrid approach. In addition the interaction of these optineurin interacting proteins with mutants of optineurin was also analyzed. We obtained three NF-κB regulators as optineurin-interacting partners, which suggests that optineurin has a role in the regulation of NF-κB pathway. Apart from the above mentioned proteins, proteins involved in vesicular transport, immune response and transcriptional repression were also identified as interacting partners. Hence, it is seen that optineurin interacts with diverse cellular proteins. E50K and H486R showed altered interaction with some of the optineurin-interacting proteins whereas H26D and R545Q behaved like the wild type. Finally, we observed that two of the interacting partners of optineurin lie in the region of known glaucoma loci.

Chapter 5 describes results of experiments designed to explore the possible mechanisms involved in cell death caused by E50K in RGC-5 cells. Since the mutant shows death only of retinal ganglion cells, we chose to see if there is defect in RGC-5 in responding to oxidative stress. We observed that the cell line does not show a generalized defect in responding to oxidative stress and antioxidant treatment; however there might be a selective defect in the inducibility

of MnSOD. On E50K expression, one of the genes, PGC1α, which normally gets induced upon oxidative stress showed a decrease in mRNA levels. Hence, a defect in the mRNA levels of this gene might be one possible reason for not eliciting protective response by this cell line on E50K overexpression. Also, we observed that E50K shows subtle alteration in interaction with Rab8 (a protein involved in membrane recycling) compared to wild type optineurin. While, optineurin interacts with Rab8, it does not interact with Rab11 suggesting therefore that E50K might affect Rab8 mediated membrane recycling specifically.

Table 1.1 Candidate genes/ loci involved in glaucoma

Candidate Loci	Gene	Phenotype	Reference
GLC1A (1q24.3-q25.2)	Myocilin (MYOC)	JOAG	Stone *et al.,* 1997
GLC1B (2cen-q13)	-	POAG	Stoilova *et al.,* 1996
GLC1C (3q21-q24)	-	POAG	Wirtz *et al.,* 1997
GLC1D (8q23)	-	POAG	Trifan *et al.,* 1998
GLC1E (10p15-p14)	Optic neuropathy inducing protein (*OPTN*)	NTG	Rezaie *et al.,* 2002
GLC 1F (7q35-q36)	-	POAG	Wirtz *et al.,* 1999
GLC 1G (5q22.1)	WD repeat-containing protein 36 (*WDR 36*)	POAG	Monemi *et al.,* 2005
GLC 1H (2p16.3-p15)	-	POAG	Suriyapperuma *et al.,* 2007
GLC 1I (15q11-q13)	-	POAG	Allingham *et al.,* 2005
GLC 1J (9q22)	-	JOAG	Wiggs *et al.,* 2004
GLC 1K (20p12)	-	JOAG	Wiggs *et al.,* 2004
GLC 1L (3p21-22)	-	POAG	Baird *et al.,* 2005
GLC 1M (5q22.1-q32)	-	JOAG	Fan *et al.,* 2007
GLC 1N (15q22-q24)	-	POAG	Wang *et al.,* 2006
19q12-14	-	POAG	Wiggs *et al*., 2000
GLC3A (2p21)	Cytochrome P450 1B1 (*CYP1B1*)	PCG	Stoilov *et al.,* 1997
GLC3B (1p36.2-p36.1)	-	PCG	Akarsu *et al.,* 1996
GLC3C (14q24.3-q31.1)	-	PCG	Stoilov, 2002

Table 1.2 Reported optineurin mutations and their percent occurrence

Mutation	cDNA change	Percent of mutations	Type of glaucoma	Reference
Disease causing alterations				
E50K	c.458G>A	13.5%	NTG & POAG	Rezaie *et al*., 2002
		3.5%	NTG subset	Alward *et al*., 2003
		1.5%	NTG subset	Aung *et al*., 2003
		1.5%	NTG subset	Hauser *et al*., 2006
		3%	NTG subset	Ayala-Lugo *et al*., 2007
Premature stop	c.691-692insAG	2.2%	NTG subset	Rezaie *et al*., 2002
		0.46%	POAG	Ayala-Lugo *et al*., 2007
H26D	c.386C>G	1.12%	POAG	Fuse *et al*., 2004
		0.5%	POAG	Funayama *et al*., 2004
H486R	c.1767A>G	1.5%	JOAG	Willoughby *et al.,* 2004
A336G	c.1317C>G	0.9%	NTG	Weisschuh *et al.,* 2005
A377T	c.1439G>A	0.9%	NTG	Weisschuh *et al*., 2005
Risk-associated alterations				
M98K	c.603T>A	13.6% in patients and 2.2% in controls	NTG & POAG	Rezaie *et al.,* 2002
		16.9% in POAG, 15.4% in NTG and 5% in controls	NTG & POAG	Fuse *et al*., 2004
		17% in POAG, 22.1% in NTG and 16.5% in controls	NTG & POAG	Funayama *et al*., 2004
		28.6% in POAG and 24.6% in controls	POAG	Leung *et al.,* 2003
		9.1% in NTG, 16.3% in POAG and 2.9% in controls	NTG & POAG	Willoughby *et al*., 2004
		14.5% in POAG, 14.2% in NTG and 1.7% in controls	NTG &POAG	Umeda *et al*., 2004

Polymorphisms				
R545Q	c.1944G>A	2.2%	NTG	Rezaie *et al.,* 2002
		5.7% in POAG, 6.9% in NTG and 5% in controls	POAG & NTG	Funayama *et al*., 2004
		1.5% in NTG	NTG	Fuse *et al*., 2004
		1.5% in NTG and 1.6% in controls	NTG	Willoughby *et al*., 2004

Chapter 2

Materials and Methods

2.1. Materials

2.1.1. Sources of Chemicals

Acrylamide, bis-acrylamide, agarose, β-mercaptoethanol, BSA fraction V, BCIP, calcium chloride, cycloheximide, DEPC, DMSO, DTT, EDTA, ethidium bromide, HEPES, IPTG, kanamycin, leupeptin, lithium acetate, lysozyme, NBT, penicillin, PEG-3350, PIPES, PMSF, Ponceau S, sodium salt of deoxyribonucleic acid from salmon sperm DNA, sodium dodecyl sulphate (SDS), sorbitol, streptomycin, succinic acid, TEMED, Tris base, Triton X-100, trypsin, Tween-20 and X-gal were all obtained from Sigma. Medium molecular weight marker proteins for SDS-PAGE, DNA markers and PCR reagents were from Bangalore Genei & New England Biolabs. Lipofectamine 2000, Lipofectamine-PLUS reagent, Trizol Reagent, Superscript II first strand cDNA synthesis kit, FBS and DMEM were obtained from Invitrogen. RNase A and glycerol were from Calbiochem. Hybond C, Hybond-ECL membranes were purchased from Amersham Life Science. Western lighting chemiluminescence reagent was from Perkin Elmer Life Science. Columns for preparing transfection grade DNA were from Qiagen or Life Technologies. Restriction enzymes, T4 DNA ligase were from New England Biolabs and Bangalore Genei. All amino acids and adenine hemisulphate were from Himedia. Zymolyase (100T) for yeast cell wall digestion was from Seikagaku Corporation. Tryptone, agar and yeast extract were from Difco Laboratory and Blotto was from Santacruz. Whatman filter papers were from Whatman International Ltd; X-ray films were from Konica Corporation or Kodak. Other reagents were from local suppliers like Himedia, Qualigens, SRL, SD fine-chemicals Ltd., and Merck India Ltd. and were of analytical grade.

2.1.2. Antibodies

The antibodies used to carry out the experiments are listed below:

a) Anti-optineurin antibody (rabbit polyclonal) was from Abcam.

b) Anti-HA (rabbit polyclonal), anti-calnexin (rabbit polyclonal), anti-cdk2 (rabbit polyclonal) were from SantaCruz Biotechnology.

c) Anti-HA (mouse monoclonal) and anti-Myc were from Roche.

d) Giantin (mouse monoclonal) antibody was a kind gift from Dr.Hans Peter Hauri, Biocentre, Basel, Switzerland.

e) secondary antibodies- Cy-3 conjugated anti-mouse and anti-rabbit IgG were from Amersham. Texas red or Fluorescein Isothiocynate or FITC conjugated anti-mouse and rabbit IgG were from Vector Labs. Secondary antibodies for western blotting were from Amersham LifeScience.

2.1.3. Bacterial Strains

E. coli **DH5α :** F' end A1 hsd R17 (r_{k-} , M_{k-}) sup E44 thi-1 rec A1 gyr A96 (Nal^r) rel A1 Δ (lac ZYA-arg F) $_{u169}$ (ϕ80 lac Zδ M15).

The above-described strain of *Escherichia coli* was used for all transformations, plasmid isolations and for selection of recombinant clones.

2.1.4. Cell Lines

The cell lines used in this study and their tissue types are listed below.

a) RGC-5 - cell line derived from rat retinal ganglion cells (Krishnamoorthy *et al*., 2001)

b) D407 - human adult retinal pigment epithelial cell line (Davis *et al*., 1995)

c) Cos-1 - African green monkey (*Cercopithecus aethiops*) kidney cell line transformed by SV 40, established from CV-1 Simian cells

d) HeLa - human cervical adenocarcinoma

e) IMR-32 - human neuroblastoma cell line

2.1.5. Plasmids

a) pcDNA3.1-HA-wild type optineurin, pcDNA3.1-HA-E50K, pcDNA3.1-HA-R545Q, pcDNA3.1-HA-H26D and pcDNA3.1-HA-H486R plasmids have cDNAs for the in-frame with a hemagglutinin (HA) tag into pcDNA 3.1 vector.

b) pcDNA3-MnSOD vector was the kind gift from Joseph J. Cullen, University of Iowa College of Medicine.

c) Mutant caspase-1, Caspase-9S and Bcl-2

d) pEGFP-C3-Rab8 and pcDNA3.1-HA-Rab8

e) pEGFP-C3-IK cytokine and pcDNA3.1-HA-IK cytokine

f) pEGFP-C3 vector contains enhanced GFP to which proteins of interest can be tagged as a fusion to the GFP C-terminus. This plasmid was from Clontech.

2.1.6. Bacterial Media, Antibiotics and Chemical Stocks

1X PBS or Phosphate buffered saline: 137 mM NaCl, 2.7 mM KCl, 4.3 mM Na_2HPO_4 and 1.4 mM KH_2PO_4. A 10X stock solution was prepared in double distilled water, pH adjusted to 7.4 with HCl and autoclaved.

1X TBE or Tris/Boric acid/EDTA: 89 mM Tris base, 89 mM boric acid and 1 mM EDTA in double distilled water. 10X stock solution prepared was filtered, autoclaved and stored at room temperature.

1X TBS or Tris buffered saline: 10mM Tris base, 150mM NaCl was in double distilled water and pH was adjusted to 8.0 by HCl. 10X stock solution prepared was filtered, autoclaved and stored at room temperature.

30% acrylamide solution: 29.2 g of acrylamide and 0.8 g of N, N'-Methylene bis-acrylamide was dissolved in double distilled water, made up to 100 ml and stored at 4°C in an amber-coloured bottle.

6X agarose gel loading buffer: 0.25% bromophenol blue and 0.25% xylene cyanol in 30% glycerol.

Amido-black staining solution: 0.1% amidoblack 10B, 25% isopropanol and 10% acetic acid in water.

Ampicillin: 1000X stock solution (100mg/ml) was made by dissolving ampicillin in sterile double distilled water.

BCIP or 5-bromo-4-chloro-3-indolyl phosphate: 50 mg/ml stock solution was made using di-sodium salt of BCIP in double-distilled water and stored at -20°C.

Buffer saturated phenol: Melted phenol was mixed with equal volume of 0.5M Tris-HCl pH 8.0 and 0.1% 8-hydroxyquinoline and mixed well. The upper aqueous phase was removed and the process repeated with 0.1M Tris-HCl pH 8.0. This step was repeated till the pH of the aqueous solution was equilibrated to 8.0. It was mixed with 0.1 volume of 0.1M Tris-HCl (pH 8.0) and stored in an amber-colored bottle at 4°C.

Chloroform:Isoamyl alcohol: 24:1 (v/v) chloroform:isoamyl alcohol mixture was prepared.

CM-H_2DCFDA or Chloromethyl-2'-7'-dichlorofluorescein diacetate:50µM stock was prepared in DMSO and stored in a dark vial at -70°C.

Cycloheximide: 100X stock solution was made by dissolving 10mg/ml of cycloheximide in double distilled water and stored at -20^0C.

DEPC or Diethylpyrocarbonate water: Milli-Q water for RNA isolation was treated with 1% DEPC, left overnight and subsequently autoclaved to remove excess DEPC.

Developing Solution for Alkaline phosphatase reaction: 100mM Tris pH 9.0, 100mM NaCl, 5mM $MgCl_2$ solution.

DMEM or Dulbecco's Modified Eagle's Medium (1X): 13.4 g of DMEM and 3.7 g of $NaHCO_3$ was dissolved in milli-Q water to make 1 litre of the medium. The pH was adjusted to 7.4 using HCl and subsequently filter sterilized.

Ethidium Bromide: 10 mg/ml solution in water.

HBSS or Hank's balanced salt solution: 0.14 g $CaCl_2$, 0.4 g KCl, 0.06 g KH_2PO_4, 0.1 g $MgCl_2.6H_2O$, 0.1 g $MgSO_4.7H_2O$, 8 g NaCl, 0.35 g $NaHCO_3$, 0.048 g Na_2HPO_4 and 1 g glucose were dissolved in 1 litre of water. pH should be ~7.4

LB or Luria Bertani agar: LB media reconstituted with 1.5% Bactoagar was used for pouring LB plates.

Luria-Bertani or LB broth: 1% Bactotryptone, 1% NaCl and 0.5% Bacto-yeast extract were dissolved in double distilled water. pH was adjusted to 7.4 using 10N NaOH and then autoclaved.

Mountant: 90% glycerol, 10% antifade solution (10 mg/ml para-phenylene diamine hydrochloride in 10X PBS) and 0.01mg/ml DAPI (from 5 mg/ml stock) in 1X PBS.

NBT or 4-nitroblue tetrazolium chloride: 50 mg/ml stock solution was made in 70% Dimethyl formamide and stored at -20°C.

Penicillin, streptomycin, kanamycin: 600 mg penicillin, 1000 mg kanamycin and 500 mg streptomycin were dissolved in 100 ml 1X PBS and filter sterilized to make a 100X stock which was stored frozen at -20°C. 1X antibiotic solution was included in all tissue culture media used for cell maintenance.

Ponceau S: A 10X stock of Ponceau S was made containing 2% Ponceau S, 30% trichloroacetic acid and 30% sulfosalisylic acid in water.

RNase A: 20 mg/ml stock solution was made in 15 mM NaCl and 10mM Tris (pH 7.5). It was then boiled for 15 minutes and cooled slowly to room temperature. The stock was then aliquoted and stored at -20°C.

SDS-PAGE sample buffer (3X): 180mM Tris-Cl pH 6.8, 6% SDS, 15% glycerol, 7.5% β-mercaptoethanol and 0.01% bromophenol blue in double-distilled water and stored at -20°C.

Tris EDTA pH 8.0 (TE): 10 mM Tris HCl (pH 8.0) and 1 mM EDTA (pH 8.0).

Trypsin EDTA: 0.125% trypsin (cell culture grade) and 0.1% EDTA were dissolved in 1X PBS, filter sterilized and stored at -20°C.

2.2. Methods

2.2.1. Sterilization

All glassware and plasticware were sterilized by autoclaving at a steam pressure of 15 psi at 121°C for 20 min. Sterile, disposable material was used for cell culture techniques. Solutions were prepared in double-distilled water and generally sterilized by autoclaving or filter sterilized through a sterile 0.45 μm nitrocellulose filter (Millipore). Bacterial growth media were autoclaved for 40 min at 15 psi at 121°C. Cell culture media, antibiotics and trypsin were sterilized by filtration through 0.2 μm filters. Glassware for RNA work was baked at 180°C overnight in addition to autoclaving.

2.2.2. Plasmid Isolation

Plasmid DNA miniprep was carried out by boiling lysis method as described by Sambrook *et al.,* 1989, with certain modifications. Restriction digestion of plasmids for screening purposes was carried out after the RNase treatment. In order to prepare plasmids for sequencing purposes, an alternate method of plasmid purification from the technical manual of the ABI prism

3700 sequencer was used. In this method, 3 ml of overnight grown bacterial culture was pelleted and re-suspended in 100 μl of double-distilled water. 100 μl of lysis buffer (100 μl of 10% SDS, 20μl of 0.5M EDTA and 10 μl 10N NaOH made up to 1ml with water) was added and the tube was kept in boiling water for 2 minutes. 50 μl of 1M $MgCl_2$ was added to these, mixed by tapping and kept on ice for 2 minutes. The mixture was spun at maximum speed (≥10,000g) in a microcentrifuge for 2 minutes. To the supernatant, 50 μl of 5M potassium acetate was added and kept on ice for 2 minutes. The tube was then spun at maximum speed for 2 minutes and the supernatant transferred to a separate tube. DNA was precipitated by adding 600 μl of isopropanol followed by 2 minutes incubation on ice. The tube was then spun at maximum speed for 2 minutes to pellet the plasmid DNA. The pellet was washed with 1 ml of 70% ethanol and air-dried. The pellet was subsequently re-suspended in 100μl TE pH 8.0 containing RNase A (20μg/ml).

Plasmids for transfections were prepared using QIAGEN-tip20 (miniprep) and QIAGEN-tip 100 (midiprep) columns according to manufacturer's instructions. The protocol involves alkaline lysis of cells followed by column purification of DNA that yields high purity plasmids with relatively low levels of impurities.

2.2.3 Quantitation of Nucleic Acids

The nucleic acid concentration was determined by measuring the absorbance at 260 nm (Maniatis *et al.,* 1982). Empirical relationship of 50 μg of double stranded DNA, 33 μg of single stranded DNA or 40 μg of single stranded RNA was taken to be equal to 1.0 OD_{260}. Purity of the preparation was estimated using ratio of absorbance at 260 nm to 280 nm.

2.2.4 Agarose Gel Electrophoresis

After adding appropriate amounts of 6X loading dye, DNA and RNA samples were resolved, depending on size, in 0.8-1.5% agarose gels made in 1X TBE buffer. 0.25 μg/ml ethidium bromide was added to gels during preparation for visualizing nucleic acids.

2.2.5 Restriction Endonuclease Digestion

Plasmid DNA (1-2.5μg) was digested with 1-2.5 units of restriction enzyme in a compatible buffer in a 20 μl final volume, as per manufacturers instructions. Digested products were visualized by resolving in an agarose gel along with appropriate DNA markers.

2.2.6 Gel Elution of DNA Fragments

The DNA fragments to be purified for subsequent processes like ligation were resolved in an agarose gel and excised out. The GeneClean purification kit from eppendorf was used for obtaining purified gel-eluted DNA and the protocol as mentioned in their technical bulletin was followed.

2.2.7 Ligation

DNA fragments obtained after gel purification of PCR products or restriction digests were ligated using T4 DNA ligase at 16°C for 8 hours to overnight. A molar ratio of vector to insert of 1:3 was generally used.

2.2.8 Preparation of Ultracompetent Cells

The method (Inoue *et al.*, 1990) was used for high efficiency ultracompetent cells. Pre-inoculum of *E.coli* DH-5α strain from a single colony was grown overnight in 10 ml of LB at 37°C. 0.1% inoculum of this culture was added to 250 ml LB medium in a 2-litre flask and kept under vigorous shaking (250rpm) at 18°C till absorbance at 600 nm reached about 0.6. The culture

was kept on ice for 10 min and the cells harvested by centrifuging at 2500 g for 10 min at 4°C. The cell pellet was resuspended in 80 ml of ice-cold filter sterilized PIPES buffer (10 mM PIPES, 15 mM $CaCl_2$, 250 mM KCl, 55 mM $MnCl_2$ pH 6.7) and placed on ice for 10 min. Cells were re-centrifuged at 2500g and gently resuspended in 20 ml of PIPES buffer with 7% DMSO. The cells were kept on ice for about 10 min, aliquoted and snap frozen using liquid nitrogen for storage at -80°C.

2.2.9 Transformation of *E.Coli*

Ultracompetent cells (50μl) were thawed on ice, 5μl of the ligated mixture or 5-10ng of pure plasmid was gently mixed with the cells and incubated on ice for 30 minutes. Heat shock was given at 42^0C for 90 seconds and immediately kept on ice for 1-2 minutes. 200μl of LB was added for recovery and the tube was incubated at 37^0C for 45 minutes. Cells were then spread on LB plates containing the required antibiotic and plates were incubated overnight at 37°C for colonies to grow.

2.2.10 DNA Sequencing

ABI Prism Model 3700 DNA Analyzer or Model 3730 DNA Analyzer was used for all DNA sequencing reactions. 50-100 ng of plasmid DNA and 2.5-5 pmoles of primer was constituted in a volume of 3.2 μl and mixed with 1.8 μl of the reagent from big-dye-terminator sequencing kit (Taq polymerase and fluorescent-tagged dNTPs) from Perkin-Elmer. PCR was carried out in the Gene Amp PCR System 9600 Thermal Cycler at the following conditions: Denaturation at 96°C for 10 sec, annealing at 50°C for 5 sec and extension at 60°C for 4 min, for a total of 35 cycles and a final extension was done for 5 minutes. The reactions were then ethanol precipitated for 10 minutes on ice

and washed twice with 70% ethanol. The samples were then resuspended in 10 μl High-dye-formamide from Perkin-Elmer and 5 μl was loaded in the capillaries.

2.2.11 RNA Isolation

RNA was prepared using TRIZOL reagent, monophasic mixture of phenol and guanidium isothiocyanate (GITC), according to the manufacturer's instructions. Isolated RNA was dissolved in appropriate amounts of DEPC water, quantitated and visualized on gel.

2.2.12 Polymerase Chain Reaction (PCR)

For routine PCR reactions 10-20ng of DNA template was used in a 50μl reaction. PCR was done in a reaction mix containing 1X PCR buffer (10 mM Tris-HCl pH 9.0, 50 mM KCl, 1.5 mM $MgCl_2$, 0.01% gelatin-Taq buffer 10A from Bangalore Genei), 150μM of dNTPs (2.5 mM stock), 100 ng primers and 1.5 units of Taq DNA polymerase. After an initial denaturation at 94°C for 2 min required number of cycles was carried out. Each cycle consisted of denaturation at 94°C for 30 sec, annealing [at 4°C below melting temperature of the primer T_m which was calculated by the empirical formula T_m= 2(A/T) + 4(G/C)] for 30 seconds and extension at 72°C for 1 minute. A final extension for 7 minutes was given at 72°C for completion of elongation products.

2.2.13 Reverse Transcription and Polymerase Chain Reaction (RT-PCR)

RNA was isolated by TRIZOL reagent and RT reaction was carried out using the Superscript II first strand cDNA synthesis kit (Invitrogen) according to the manufacturers recommended protocol. 2 μg of total RNA was used as the template and oligo-dT or random hexamers was used as primers for reverse transcription in 20 μl reaction volume.

Table 2.1: List of primers used for RT-PCRs

Gene	Primer Name	Sequence	Amplicon size	Annealing temp. & no. of cycles
PGC1α (Rat)	PF1	5'-GCA GAA AGC AAT TGA AGA GCG-3'	393 bp	58°C, 35 cycles
	PR2	5'-CGT TAC CTG CGC AAG CTT CTC-3'		
HO-1 (Rat)	HF	5'-GCT CTA TCG TGC TCG CAT GAA-3'	323 bp	60°C, 35 cycles
	HR	5'-CAT AAA TTC CCA CTG CCA CGG-3'		
MnSOD (Rat)	SDF1	5'-CTG GAC AAA CCT GAG CCC TAA G-3'	371 bp	58°C, 40 cycles
	SDR1	5'-GGC TTC ACT TCT TGC AAA CTA TG-3'		
OPTN (Human)	RT-PCR	5'-GCT GCA AAT GGA TGA AAT GAA GCA-3'	412 bp	65°C, 26 cycles
	REV	5'-CCG CTC GAG ACA TCA ACA CTT AAA TGA TGC AAT CC-3'		
Actin (Rat)	AF	5'-GAG GGA AAT CGT GCG TGA CAT-3'	527 bp	60°C, 20 cycles
	AR	5'-CTC AGT AAC AGT CCG CCT AGA-3'		

The RNA was annealed with 500 ng of oligo-$dT_{(12-18)}$ at 65°C for 5 min in a 10 μl reaction volume. This was incubated at 42°C for 2 min in a reaction mix containing 1X RT buffer (20 mM Tris-HCl pH 8.4, 50 mM KCl), 5 mM $MgCl_2$, 10 mM DTT, 500 μM of each dNTP and 40 units of RNase inhibitor. The reverse transcription was carried out at 42°C for 50 min using 50 units of Superscript II RT enzyme. The reaction was stopped by incubation at 70°C for 15 mins. The reverse transcription product (1μl which corresponds to 200ng of total RNA) was used as template for semi-quantitative PCR reactions of 50μl in which the mRNAs of genes of interest were amplified using specific primer. The list of primers used for RT-PCRs in the study is given in Table 2.1.

2.2.14 Plasmid Vectors

2.2.14.1 Cloning vectors

(a) pMOS Blue: This vector is a part of the PCR-blunt-cloning kit obtained from Amersham Biosciences. This is a high copy plasmid and enables easy cloning of blunt-ended PCR products. It carries an ampicillin resistance (*bla*) gene and *lacZ* gene, which enables antibiotic and blue-white colony selection, respectively.

2.2.14.2 Mammalian expression vectors

(a) pEGFP (C1/C3): These mammalian expression vectors are of 4.7 kb size and were obtained from CLONTECH Laboratories Inc. They have a cytomegalovirus (CMV) promoter, kanamycin resistance gene for bacterial selection and neomycin resistance gene which allows for the selection of stably transfected eukaryotic cells using the G418 antibiotic. This vector is used for making fusion proteins with GFP at the N-terminus of the protein of interest.

(b) pcDNA3.1(+): This mammalian expression vector is of 5.4 kb size and was obtained from Invitrogen Life Technologies. It has a CMV promoter, MCS, ampicillin resistance gene for bacterial selection and neomycin resistance gene, which allows for the selection of stably transfected eukaryotic cells using G418.

2.2.15 Yeast Two Hybrid Expression Vectors

(a) pGBKT7

The pGBKT7 vector from CLONTECH Laboratories Inc expresses proteins fused to amino acids 1-147 of the GAL4 DNA binding domain (DNA-BD). In yeast, fusion proteins are expressed at high levels from the constitutive ADH1 promoter, transcription is terminated by the T7 and ADh1 transcription termination signals. pGBKT7 also contains the T7 promoter, a c-

MYC epitope tag and a MCS. pGBKT7 replicates autonomously in both *E.coli* and *S.cerevisiae* from the pUC and 2 μ ori, respectively. The vector carries the Kan^r for selection in E.coli and the TRP1 nutritional marker for selection in yeast. Yeast strains containing pGBKT7 exhibit higher transformation efficiency than strains carrying other DNA-BD domain vectors.

(b) pACT2

pACT2 from CLONTECH Laboratories Inc generates a fusion of the GAL4 –AD (amino acids 768-881), HA epitope tag and a protein of interest (or protein encoded by a cDNA in a fusion library) cloned into the MCS in the correct orientation and reading frame. The hybrid protein is expressed at high levels in yeast host cells from the constitutive ADH1 promoter, transcription is terminated at the ADH1 transcription termination signal. The protein is targeted to the yeast nucleus by the nuclear localization signal from SV40 T-antigen which has been cloned into the 5' end of the Gal4 AD sequence. pACT2 is a shuttle vector that replicates autonomously in both *E.coli* and *S.cerevisiae* and carries the *bla* gene, which confers ampicillin resistance in *E.coli*. pACT2 also contains the *LEU2* nutritional gene that allows yeast auxotrophs to grow on limiting synthetic media. Transformants with AD/library plasmids can be selected by complementation by the *LEU2* gene by using an *E.coli* strain that carries a leuB mutation (e.g., HB101).

2.2.16 Optineurin Expression Vectors

All cloning experiments were performed according to standard procedures. Full length optineurin was amplified from human placental cDNA library using gene specific primers. The primers were designed such that the forward and reverse primers contain *EcoRI* and *XhoI* restriction sites, respectively, at their ends. The resulting PCR product was cloned in a pMOS

cloning vector by blunt end cloning (ECoRV digested) and its sequence was verified by automated sequencing. The OPTN cDNA was excised with specific restriction enzyme digestion and cloned in the mammalian expression vector pcDNA 3.1 (HA) and pACT2 yeast two-hybrid vector. For cloning in the pGBKT-7 yeast two hybrid expression vector, optineurin was excised from pcDNA 3.1 (HA) with *BamHI* and *XhoI* and ligated in *BamHI* and *SalI* sites of pGBKT-7. The primers used for cloning optineurin are listed in Table 2.2.

Table 2.2: List of primers used for cloning optineurin

Primer	Sequence	Information Accession - AF420371
Forward Primer	5'-CGGAATTCCTGCAATGTCCCATCA ACCTCTC- 3'	**Optineurin cloning primers; 62°C; 36 cycles. (vent polymerase with 4mM $MgSO_4$ used).**
Reverse Primer	5'-CCGCTCGAGACATCAACACTTAAA TGATGCAATCC-3'	
Sequencing Primer	5'-GGTCAGTAAAAGAAATCAAG-3'	**Used for sequencing.**
RT-PCR Primer	5'-GCTGCAAATGGATGAAATGAA GCA-3'	**Used for sequencing. Also used along with Reverse primer; 65°C; 412 bp.**

2.2.17 Other Expression Vectors

A) Rab8: Full length human Rab8 was cloned using RT product from the A549 cell line with gene specific primers containing *ECoRI* and *XhoI* sites in forward and reverse primers respectively. The resulting PCR product was cloned in pMOS blue blunt end vector and its sequence was verified by automated sequencing. The Rab8 cDNA was excised with specific restriction enzymes and cloned in *ECoRI* and *XhoI* sites of pcDNA 3.1 (HA) vector and pACT2 vector and *ECoRI* and *SalI* sites of pEGFP-C3 vector. For cloning in pGBKT-7 yeast two hybrid expression vector, optineurin was excised from

pcDNA 3.1 (HA) with *BamHI* and *XhoI* and ligated in *BamHI* and *SalI* sites of pGBKT-7. The primers used for Rab8 cloning are listed in Table 2.3.
Activated Rab8 (Q67L) and dominant negative Rab8 (T22N) were constructed by site directed mutagenesis by Dr.Nishant Jain in our lab.
Activated Rab8 and dominant negative Rab8 were cloned in yeast two-hybrid expression vector pGBKT-7 using the same procedure used for wild type Rab8.

B) IK-cytokine: Full length and partial human IK-cytokine were cloned using the RT product from the A549 cell line with gene specific primers containing *ECoRI* and *XhoI* sites in forward and reverse primers respectively. The resulting PCR product was cloned in pMOS blue blunt end vector and its sequence verified by automated sequencing. The IK-cytokine cDNA was excised with specific restriction enzymes and cloned in *ECoRI* and *XhoI* sites of pcDNA 3.1 (HA) vector and *ECoRI* and *SalI* sites of pEGFP-C3 vector. The primers used for IK-cytokine cloning are listed in Table 2.3.

C) Other constructs: The pcDNA3.0-MnSOD vector was a kind gift from Joseph J. Cullen, University of Iowa College of Medicine. Mutant caspase-1 was prepared by replacing Cys 285 (TGC) with Ala (GCC) by PCR-based site-directed mutagenesis (Gupta *et al*., 2002) Caspase-9S is a splice variant of caspase-9 and is missing most of the large subunit of caspase-9, including the catalytic site, but has the intact prodomain and small subunit (Seol *et al*., 1999). These two mutant caspases are the dominant negatives of their respective caspases.

Table 2.3 List of primers used for cloning Rab8 and IK-cytokine

Gene	Primer	Sequence	Information	
Rab8 Accession X56741	**RAB-F**	5'- CGGAATTCCCAATATGGCGAAG ACCTACGATTAC-3'	68°C, 30 cycles	
	RAB-R	5'-CCGCTCGAGGGCGGTGTTCCTC ACAGAAGAAC-3'		
IK-cytokine Accession NM_006083	**IK-For.P**	5'-CCG GAA TTC AAA TGC CGG AGC GAG ATA GTG AG-3'	Primers for cloning full length IK-cytokine; 65°C; 33 cycles	
	IK-Rev.P	5'-CCG CTC GAG TAG TGA TTA GTA TTT TGG TCT TTT GAC-3'		Primers for cloning partial IK-cytokine; 65°C; 33 cycles
	IK-IntP	5'-CCG GAA TTC CCA GCA AAG AGA AAG AGG AAG AGG-3'		

2.2.18 Construction of Mutations in Optineurin cDNA by Site Directed Mutagenesis

Mutagenic primers containing the desired nucleotide changes were purified by urea-PAGE and mutations were generated by PCR using Quik change site directed muatgenesis (Stratagene) protocol. The primers were generally 35-45 bp and designed to have mutations in the middle of the primer sequence. All the primers had a minimum 40% GC content and the T_m of the primers was greater than or equal to 78°C. The T_m was calculated by the formula: 81.5 + 0.41(%GC) -675/N - % mismatch, where N is the primer length in base pairs. Typically, 25μl PCR reaction was set up using 10-20ng of DNA template, 125ng of the mutagenic primers, 200μM of dNTPs, 2.5μl of 10X *Pfu* buffer and 1.25 units of *Pfu* Turbo DNA polymerise which has proof reading activity. The cycling conditions were: initial denaturation at 95°C for 2 minutes, followed by 16-18 cycles of 95°C for 30 seconds, annealing at 60°C for 30 seconds, extension at 68°C for required time (calculated according to 2

minutes extension per Kb of plasmid). The final extension was given at 72°C for 7 minutes. The PCR product (5μl) was run on 0.8% gel to confirm amplification. The PCR product (10μl) was digested with DpN I enzyme (2.5 units) at 37°C for 4 hours. 5μl of digested product was then used for transformation of ultra competent DH5-α cells and colonies were allowed to grow overnight in a 37°C incubator. Since DpN I digests the methylated DNA, all parental plasmid gets digested leaving the newly synthesized unmethylated DNA strand. For this, along with the newly synthesized strand, the control parental plasmid of equal concentration was also digested with DpN I and then used for transformation to assess the efficiency of digestion as in principle no colonies must grow on plate transformed with parental plasmid after digestion. These colonies were picked and plasmids made which were checked by PCR using check primers (these primers are designed in a way that they end at 3' mutated nucleotide), which will amplify only that cDNAs which have mutation in it and not the unmutated cDNA.

The list of all the mutagenic primers and corresponding check primers is given below in Table 2.4.

2.2.19 Sequence Analysis

The following programs, available online from different sources, were used in this study.

1) From NCBI:

Blast n: for nucleotide level homology to a nucleotide database.

Blast p: for protein level homology to a protein database.

Blast2 sequences: to align two nucleotide sequences based on their similarity.

Genomic blast sequence: to align with the human genome based on similarity.

Table 2.4: List of primers used for site directed mutagenesis

Primer	Sequence	Information
KF-P	5'-GATGAAAGAGCTCCTGACC**AAG**AACCACCAGCTGAAAG-3'	55°C; 16 cycles; mutation from GAG→AAG OPTN E50→K
KR-P	5'- CTTTCAGCTGGTGGTT**CTT**GGTCAGGAGCTCTTTCATC-3'	
KC-P*	5'-TTCTTTCAGCTGGTGGTTCTT-3'	Check primer; 72°C, 180 bp
QF-P	5'-CTGAGGACAGGGACTGG**CAG**CAACAGCGGAATATTCC-3'	55°C; 16 cycles; mutation from CGG→CAG OPTN R545→Q
QR-P	5'-GGAATATTCCGCTGTTG**CTG**CCAGTCCCTGTCCTCAG-3'	
QC-P*	5'-CGGAATATTCCGCTGTTGCT-3'	Check primer; 72°C, 331 bp
H26D-FP	5'-GGAAATGGACCCCCC**GAC**CTGGCCCACCCAAAC-3'	55°C; 16 cycles; mutation from CAC→GAC OPTN H26→D
H26D-RP	5'-GTTTGGGTGGGCCAG**GTC**GGGGGGTCCATTTCC-3'	
H26D-CP	5'-CAGGAAATGGACCCCCCG-3'	Check primers; 66°C; 231 bp
H26D-REV	5'-GACGCTCTTTTGCTTCTTTGC-3'	
H486R-FP	5'-GCAGCGAGAGAGAAAATT**CGT**GAGGAAAAGGAGCAACTG-3'	55°C; 16 cycles; mutation from CAT→CGT OPTN H486→R
H486R-RP	5'-CAGTTGCTCCTTTTCCTC**ACG**AATTTTCTCTCTCGCTGC-3'	
H486R-CP*	5'-CAGTTGCTCCTTTTCCTCAC-3'	Check primer;154 bp

*
KC-P was used with OPTN forward primer
QC-P was used with OPTN RT-PCR primer
H486R-CP was used with OPTN RT-PCR primer

2) Webcutter 2.0

This software was used to analyse the restriction sites in various cDNAs.

3) Amplify 1.2

This Mac-based program was used for designing and checking primers for PCR.

2.2.20 Yeast Strains, Media and Solutions used for Yeast Two Hybrid Screening

2.2.20.1 Yeast strain PJ69-4A: MATa trp1-901 leu2-3, 112 ura3-52 his3-200 gal4Δ, gal80Δ,LYS2: :GAL1-HIS3,GAL2-ADE2, met2: : GAL7-lacz (James *et al*., 1996).

2.2.20.2 YPAD is the optimal medium for growth of most strains of *Saccharomyces cerevisiae*. It is a complex medium used for general, non-selective growth. One litre YPAD contains 20 g peptone, 10 g yeast extract, 20 g dextrose, 100 mg adenine and 1.7 % agar.

2.2.20.3 YC is the minimal defined medium for yeast. One litre YC contains 6.7 g yeast nitrogen base with ammonium sulphate, 10 g succinic acid, 6 g NaOH, 20 g glucose along with 100 mg of adenine, arginine, cysteine, leucine, lysine, threonine, tryptophan, uracil and 50 mg of aspartic acid, histidine, isoleucine, methionine, phenylalanine, praline, serine, tyrosine, valine and 1.7 % agar-agar powder.

2.2.20.4 Preparation of YC medium

To make YC (Yeast Complex) medium yeast nitrogen base with ammonium sulphate (0.67 g), succinic acid (1 g) and NaOH (0.6 g) are dissolved in 80 ml of double distilled water and adjusted to pH 5.7 with NaOH

and volume is made up to 85 ml. Agar powder 1.7 gm is added and autoclaved at 15 lbs, 121°C for 20 min. It is then cooled to 50°C and 5 ml of glucose (40% solution) is added and 10 ml aminoacid solution [10X] without leucine, tryptophan, and adenine. 1ml of Leu/Trp/Ade is added whenever required from 100X stock solutions.

2.2.20.5 Preparation of YC medium plates containing X-gal

To check for β-galactosidase gene activation, an *in vivo* plate assay is done in which YC media plates are prepared containing X-gal (80 mg/ml) and 1X BU salts. BU salts are included in the medium to maintain the optimum pH for β-galactosidase and to provide the phosphate needed for the assay. The X-gal is incorporated into the medium before the plates are poured since X-gal is heat-labile. X-gal is used as a substrate for β-galactosidase.

2.2.20.6 Solutions used for yeast two hybrid screening

10X aminoacid solution: contains 100 mg of arginine, cysteine, lysine, threonine, uracil and 50 mg of aspartic acid, isoleucine, methionine, phenyl alanine, proline, serine, tyrosine and valine are dissolved in a final volume of 100 ml with double distilled water and sterilized by autoclaving.

100X aminoacid solution: For 10 ml stock, 100 mg of adenine or leucine or tryptophan are dissolved in double distilled water and sterilized by autoclaving.

10X BU salts: For 1 litre, 70 g of $Na_2HPO_4.7H_20$, 30 g of NaH_2PO_4 are dissolved and pH adjusted to 7.0.

10X TE: 100mM Tris and 10mM EDTA solution adjusted to pH 7.5.

10X LiAc: 1M lithium acetate solution adjusted to pH 7.5 with dilute acetic acid.

40 % PEG-3350/ 1X TE/ 1X LiAc: 40% PEG-3350 solution containing 1X TE and 1X lithium acetate.

Carrier DNA solution: Sodium salt of salmon sperm DNA is dissolved at 2mg/ml concentration in 1X TE, boiled and chilled immediately in ice water to maintain it in single standard condition.

2.2.20.7 Methods Involved in Yeast Two Hybrid Assays

2.2.20.7.1 Growth and maintenance of yeast strains

The PJ69-4A strain of *Saccharomyces cerevisiae* was regularly grown and maintained on YPAD plates. Strains with plasmids were maintained on yeast YC media plates supplemented with amino acids as required by the auxotrophs but for the one in the plasmid to prevent loss of the plasmid. Cultures on plates were stored at 4°C for 1-2 months.

2.2.20.7.2 Plasmid isolation from yeast cells

A single colony of yeast was inoculated in 5 ml of YC broth (Leu^-) and grown overnight at 30°C. Cells were harvested at 2000 rpm for 5 min and the supernatant was discarded. The pellet was resuspended in 0.5 ml of 1M sorbitol, 0.1M Na_2EDTA (pH 7.5) and transferred to a 1.5 ml microfuge tube. About 0.02 ml of 2.5 mg/ml solution of Zymolyase was added and incubated at 37°C for 60 min. After incubation, the cells were pelleted down by centrifugation for 1 min. The supernatant was discarded and cells resuspended in 0.5 ml of 50mM Tris-Cl (pH 7.4), 20 mM Na_2EDTA. About 0.05 ml of 10 % SDS was added and kept at 65°C for 30 min. After incubation for 30 min, 0.2 ml of 5M potassium acetate was added. The tubes were kept on ice for 60 min and centrifuged for 5 min. The supernatant was transferred to a fresh microfuge tube and one volume of 100 % isopropanol added and

incubated at room temperature for 5 min and then centrifuged for 5 min. The supernatant was discarded and pellet resuspended in 50 μl of TE. Out of this, 5 μl was used for transformation of *E.coli* to further propagate and get higher yields of plasmid DNA.

2.2.20.7.3 Transformation of yeast with plasmid DNA

A single colony of yeast strain PJ69-4A was inoculated into 5 ml of YPAD broth and grown overnight at 30°C. OD (A_{600nm}) of overnight culture was determined and was diluted to 0.4 OD in 5 ml fresh YPAD broth and grown for another 4 hours. After 4 hours the cells were pelleted down by centrifugation at 2000 rpm for 5 min. The cells were washed once with 1X TE and resuspended in 100 μl of 1X LiAC and 0.5X TE and incubated at room temperature for 10 min. Salmom sperm DNA was denatured by boiling for 5 min followed by immediate chilling on ice and kept on ice till use. For each transformation, 100 ng of plasmid DNA, 100 μg of denatured sheared salmom sperm DNA along with 100 μl of the yeast suspension were mixed. 700 μl of 40 % PEG-3350:1X LiAC: 1X TE were added to it and vortexed briefly to mix thoroughly. Incubation at 30°C for 30 min was done with frequent tapping. After incubation, heat shock was given at 42°C for 20 min and centrifuged in a microcentrifuge for 10 seconds, and the supernatant discarded. The pellet was resuspended in 50 μl of 1X TE. The transformation mixture was plated on transformation effieciency plates (TE) which do not contain tryptophan and leucine and incubated at 30°C for 2 days.

2.2.20.7.4 Cell lysate preparation from yeast cells for western blotting

After transformation of the plasmids encoding GAL4-DNA BD fusion proteins into *Saccharomyces cerevisiae* strain PJ69-4A and incubation in

plates lacking *Trp*, single colonies were inoculated into 5 ml YC medium lacking *Trp*. At an optical density (A_{600nm}) around 0.7, the culture was centrifuged at 2500 g for 5 min, the pellet was washed in distilled water and boiled for 3 min in 200 μl of 2X Laemmelli loading buffer. 50 μl of this sample was separated by 10% SDS-polyacrylamide gel electrophoresis and blotted onto a nitrocellulose membrane and later western blotting was performed to check the expression of bait protein in yeast cells.

2.2.20.7.5 Yeast two hybrid c-DNA library screening

Full length optineurin was used as bait. Yeast strain PJ69-4A was used for two-hybrid analysis (James *et al.*, 1996). Expression of optineurin as a fusion protein with Gal4 DNA binding domain expressed by the construct in pGBKT7 vector, was checked by western blotting using lysates from yeast cultures grown in Trp dropout liquid culture. The optineurin expressing yeast strain was then transformed with human placental library. Similar transformation protocol was used except that everything was done at 10X scale. Transformants were plated on yeast dropout medium plates lacking tryptophan, leucine and adenine. A small part (0.1%) of transformant mix was plated on leucine and tryptophan dropout medium plate to check the efficiency of transformation. The routine transformation efficiency was 1x 10^5 transformants/μg of DNA. The positives obtained on Trp^-, Leu^- and Ade^- plates were checked for the activation of β-galactosidase reporter gene by plating them on plates containing Trp and Leu dropout medium containing β-galactosidase substrate (adjusted to pH 7.0). Plasmids were isolated from positive yeast colonies, propagated in *E.coli* and then sequenced. The interactions were confirmed by retransformation of positive clones with optineurin or control plasmid. Yeast colonies obtained on transformation efficiency plates (Trp^-, Leu^-) were plated onto the selection plates (Trp^-, Leu^-

and Ade^-) and (Trp^-, Leu^- and X-gal^+) to check for activation of reporter genes. The plates were incubated at 30°C for 2-3 days. Yeast colonies showing growth on (Trp^-, Leu^- and Ade^-) plates, and blue colour on (Trp^-, Leu^- and X-gal^+) were considered as positives. A schematic view of the yeast two-hybrid screening methodology is shown in Figure 2.1.

2.2.21 Cell Biology Techniques

2.2.21.1 Maintenance of cell lines

RGC-5, Cos-1, HeLa, IMR-32 and D407 cells were grown as monolayers at 37°C in Dulbecco's Minimum Essential Medium (DMEM) containing 10% FCS, 100 U/ml penicillin and 100 μg/ml streptomycin. The cells were maintained at 37°C in a humidified 5% CO_2 incubator and subcultured upon attaining 70% confluency. The medium was aspirated and the cells washed with PBS, after which they were trypsinized with 200 μl of 0.1% trypsin and 0.1% EDTA and suspended in fresh DMEM containing 10% FCS and antibiotics. The suspended cells were re-seeded at a 1:5 dilution (1:20 dilution for RGC-5 cells) and incubated at 37°C in the CO_2 incubator. For freezing cell lines, the cells were trypsinized , washed in complete DMEM (CDMEM) and suspended in freezing medium (DMEM containing 10% DMSO and 50% FCS without antibiotics) at approximately 2.5 - 5 x 10^6 cells/ml. The cells were then aliquoted as 0.5- 1 ml aliquots into 1.5 ml freezing vials (cryovials) and stored at -70°C overnight, and then transferred to a liquid N_2 container the next day for long term storage.

2.2.21.2 Transient transfection of cell lines

For Cos-1 cells, transfections were performed on cells grown as a monolayer in either 35 mm dish or coverslips using the cationic lipid DHDEAB as described (Banerjee *et al.*, 1999; Radha *et al.*, 2004). Briefly, 1 μl lipid

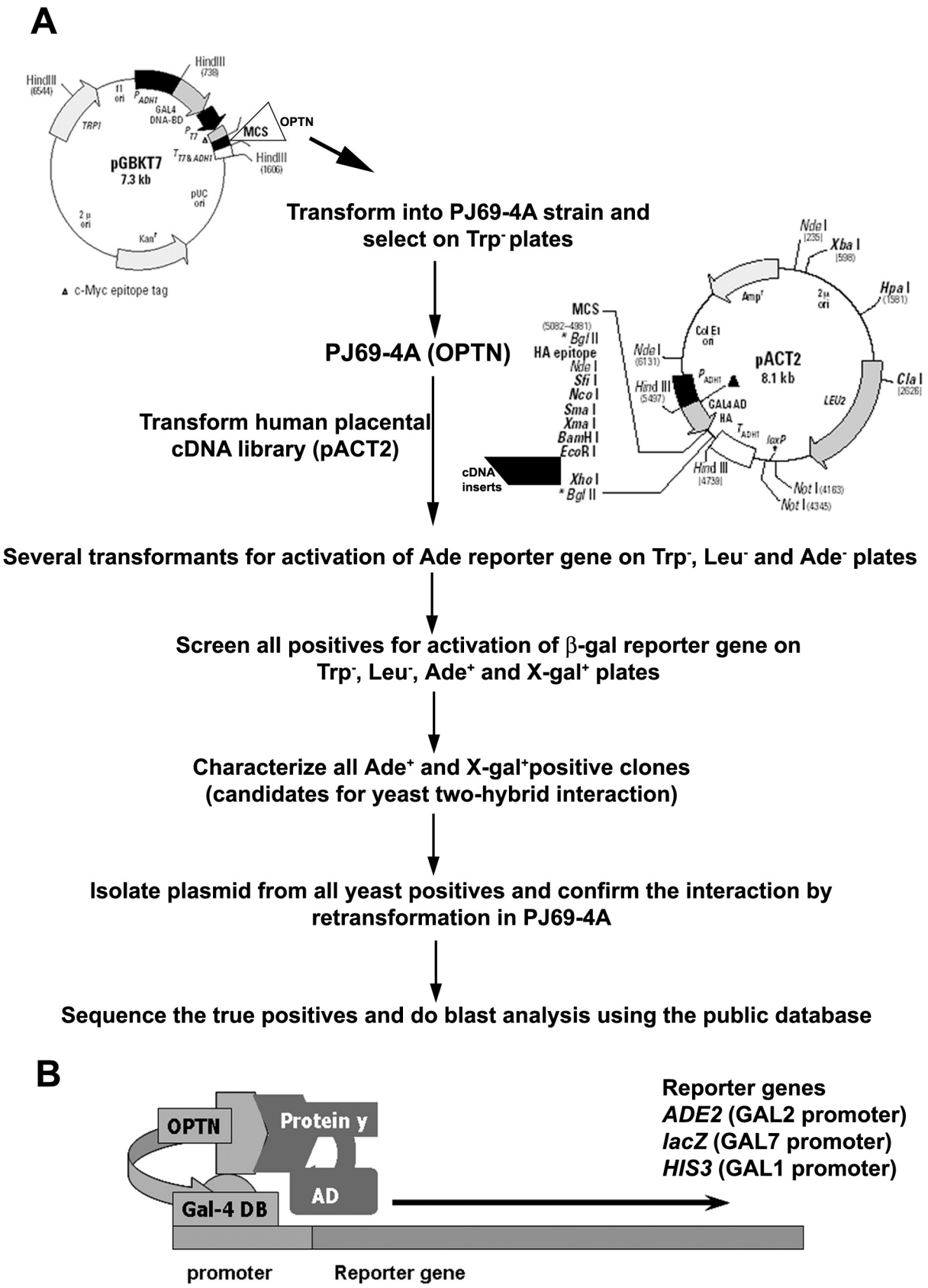

Figure 2.1: (A) Outline of the yeast two-hybrid cDNA library screening protocol. (B) Schematic diagram showing yeast two hybrid reporter gene activation by the interaction of Gal4 DNA-BD and AD fusion proteins.

diluted in 50 μl serum free DMEM was mixed with 1 μg DNA in 50 μl serum free DMEM. The mixture was kept at room temperature for 30 minutes to allow complex formation before adding to the (60%-80% confluent) cell monolayer. Transfections were stopped after 4 hours by adding complete DMEM to the cells and then harvested at indicated time points after transfection.

For RGC-5 and HeLa cells, plasmids were diluted in serum-free DMEM, mixed and PLUS reagent was then added. This was mixed and incubated for 15 minutes after which LipofectAMINE was added to DNA-PLUS complex and incubated for another 15 minutes. This complex was then added to the cells. Transfections were stopped after 4 hours by adding complete medium to the cells.

2.2.21.3 TNF-α induced cell death assays

Cells grown on coverslips were transfected with 300 ng plasmids expressing WT or E50K mutant optineurin. After 24 hours of transfection, the cells were treated with TNF-α (10 ng/mL) for 24 hours or with TNF-α and cycloheximide (20μg/ml) for 8 hours. They were then fixed and stained for optineurin. The percentage of cells undergoing cell death was quantitated in optineurin-expressing and non-expressing cells.

2.2.21.4 Antibody staining of cells

For immunofluorescence staining, the cells were grown on cover slips, transfected with required plasmids and processed as described earlier (Kamatkar *et al*., 1996; Radha *et al.*, 2004). Cells grown on coverslips were fixed in 3.7% formaldehyde in 1X PBS (Phosphate Buffered Saline), pH 7.4 for 10 min at room temperature and then washed thrice with 1X PBS. Fixed

cells were then permeabilized using 0.5% Triton-X 100 and 0.05% Tween-20 in 1X PBS for 6 minutes at room temperature. The cells were then washed thrice and incubated with PBS containing 2% BSA for 1 hour at room temperature for blocking. Following this, the cells were incubated with the primary antibody diluted in PBS containing 2% BSA for required time. Antibody was removed and the cells were washed with PBS three times. They were then incubated with fluorophore-conjugated secondary antibody in blocking solution for 1 hour at room temperature. Subsequently, the cells were again washed with PBS and mounted on glass slides in a home-made mountant.

2.2.21.5 Fluorescence and confocal microscopy

For routine checking, cells were observed using an Olympus BX60 fluorescence microscope and images were captured with a CCD camera and analysed using the Image-Pro Plus V4.1software. Colocalization was determined by observing the staining patterns using LSM 510 Meta Confocal Microscope from Carl Zeiss. Serial optical sections in the Z-axis of the cell were collected at 0.33 μm or 0.5 μm intervals with 100X oil immersion objective lens. Then 2-3 middle sections were projected and colocalization was observed in the total thickness of 1 μm using LSM 510 version 3.2 software. Immunofluorescence staining and colocalization was also observed using a Zeiss Axioplan2 microscope fitted with an Apotome. The apotome (from Carl Zeiss Microimaging) is a 3D imaging system for contrast enhancement in fluorescence microscopy. It uses structured illumination to reject signals belonging to regions of the sample that are outside the best focus position of the microscope. Images were captured using the Axiocam (Zeiss) CCD camera and processed using the Axiovision 4 software.

2.2.21.6 Apoptosis assay

Quantitative analysis of apoptotic cells was carried out as described previously (Shivakrupa *et al.*, 2003; Gupta *et al.*, 2002; Radha *et al.*, 1999). Cells grown on coverslips were transfected with the required plasmids and processed for immunostaining using appropriate antibodies for detection of expressing cells. Cells were mounted in 90% glycerol containing 1mg/ml para-phenylenediamine (antifade) and 0.5μg/ml DAPI (4'6-diamidino-2-phenylindole) for DNA staining. Cells showing immunofluorescence staining were counted and those cells that showed loss of refraction, condensed chromatin, apoptotic bodies, cell shrinkage were scored as apoptotic. At least 200 expressing cells were counted in each coverslip. The data represent the mean ± S.D. from at least three independent experiments on duplicate coverslips. Background apoptosis was determined by counting non-expressing cells in the same coverslips.

2.2.21.7 Detection of intracellular ROS levels

The intracellular accumulation of ROS (reactive oxygen species) in the E50K-transfected RGC-5 cells was assessed using 5- (and -6-)-chloromethyl-2',-7'-dichlorodihydrofluorescein diacetate (CM-H_2DCFDA; Molecular Probes, Eugene, OR). This nonfluorescent compound accumulates within cells, and, on deacetylation, H_2DCF then reacts with ROS to form fluorescent dichlorofluorescein (DCF). RGC-5 cells transfected with wild-type optineurin or E50K mutant were washed twice with Hanks balanced salt solution (HBSS) and incubated with 10 μM CM-H_2DCFDA in HBSS for 1 hour at 37°C in the dark. Cells were then washed three times with HBSS and finally examined in HBSS supplemented with 10% fetal calf serum through live cell microscopy (Axiovert inverted microscope; Carl Zeiss, Oberkochen,

Germany). Untransfected RGC-5 cells were taken as negative control, and cells treated with 600 μM H_2O_2 for 1 hour were used as a positive control.

2.2.21.8 SDS Polyacrylamide Gel Electrophoresis (SDS-PAGE)

SDS-PAGE, as described by Laemmli (1970), was carried out using a discontinuous buffer system. Stacking gel (0.125 M Tris-HCl pH 6.8, 5% acrylamide and 0.1% SDS) and the resolving gel (0.375 M Tris HCl pH 8.8, 10 or 12% acrylamide and 0.1% SDS) were polymerised using TEMED and ammonium per sulphate. The gels were run using buffer containing 0.025M Tris, 0.192M glycine and 0.1% SDS at 20 mA constant current. After stacking of proteins at the resolving front and subsequent entry into the resolving gel, current was increased to 30 mA till the end of the run.

2.2.21.9 Western Blotting

Proteins were resolved using the SDS-PAGE gel and blotted onto nitrocellulose membranes (Hybond C or Hybond ECL from Amersham) using the semidry apparatus (Pharmacia). The semidry transfer buffer containing 39 mM glycine, 48 mM Tris-HCl, 0.0375% SDS and 20% methanol was used and transfer was carried out at constant current at 0.8 mA/cm^2 for 1-2 hours. After transfer, the proteins were stained using Ponceau S solution and the positions of molecular weight markers was marked. Subsequently, blots were incubated in 5% Blotto in TBST (10 mM Tris HCl pH 8.0 buffer, 150 mM NaCl, 0.05% Tween-20) for 1 hour at room temperature. For detection of phosphotyrosine proteins, blots were blocked with 5% BSA for 1 hour at room temperature. The blots were then incubated with the required dilution of primary antibody in 0.5% Blotto in TBST for $1^1/_2$ hours at room temperature or overnight at 4^0C. Non-specifically bound primary antibody was removed by three 5-minute

washes with TBST. Subsequently, blots were incubated with appropriate dilution of secondary antibody in 0.5% Blotto in TBST for 45 minutes. After three washes with TBST, blots were processed for alkaline phosphatase reaction or enhanced chemiluminescence (ECL) detection. For alkaline phosphatase colour reaction the blot was developed with 100mM Tris HCl pH 9.0, containing 100 mM NaCl, 5mM $MgCl_2$ with 0.005% BCIP and 0.01% NBT. ECL was done using the Western lighting chemiluminescence reagent from Perkin Elmer and different exposure times were given to get the right intensity of the signal.

2.2.22 Statistical analysis

All data obtained were tested for levels of significance by the student's t-test using Microcal Origin version 4.0 (Microcal Software, Inc. USA). When significant differences were observed, P values for pairwise comparisons were calculated using the tailed t-test. P value less than 0.05 was considered significant.

Chapter 3

E50K Mutant of Optineurin Selectively Induces Death of Retinal Ganglion Cells

3.1 Introduction

Glaucoma is the second major cause of bilateral blindness in the world. The etiology of the disease is quite varied and the major risk factor is raise of intraocular pressure (IOP). Whatever may be the etiology, the ultimate cause of the disease is the death of retinal ganglion cells (RGC). Though there are many theories on how the RGC death occurs, there is no clear picture of why it occurs.

One of the genes associated not only with normal tension glaucoma (NTG) but also primary open angle glaucoma (POAG) is *OPTN,* which codes for the protein optineurin. *OPTN* is the only candidate gene reported for NTG till date. This subset of glaucoma does not show raise in IOP but yet, death of retinal ganglion cells occurs. Since there is no IOP increase, it becomes difficult to create animal models to understand this form of glaucoma. Certain missense mutations in the coding region of optineurin are associated with adult onset and juvenile onset open angle glaucoma. The mutation E50K (where glutamic acid at position 50 is mutated to lysine) is the most common disease-causing mutation of optineurin reported till date (Rezaie *et al*., 2002; Aung *et al*., 2005). However, little is known about the molecular mechanisms responsible for the pathogenesis of glaucoma caused by such mutations. Several functions for optineurin have been proposed as described earlier. However, none of these experiments explore the role of wild type optineurin or the pathogenicity of mutants in the eye, particularly retinal ganglion cells. All experiments have been done in non-ocular cell lines which do not hold patho-physiological relevance. It has been speculated that optineurin has a neuroprotective role in the eye and optic nerve (Rezaie *et al*., 2002), but it has not been demonstrated experimentally. Hence, we have conducted experiments using the retinal ganglion cell line (RGC-5), which is of

prime importance in glaucoma. Though the cell line is a rat cell line, it still holds the significance of what might be happening in the human counterpart. The retinal ganglion cell line (RGC-5) chosen for our study has all the appropriate cell characteristics, viz., Thy-1, Brn-3C, neuritin, NMDA receptor, GABA-B receptor and synaptophysin expression, and negative for GFAP, HPC-1 and 8A-1 (Krishnamoorthy *et al*., 2000).

We explored the possibility that the disease associated mutants of optineurin may inhibit the functions of, or even induce the death of retinal ganglion cells (RGCs), a cell type relevant for glaucoma. One of the mutants of optineurin, E50K, was able to induce cell death in RGCs but not in other cell lines tested. An attempt was made to characterize the cell death pathway because understanding the mechanism would help us to design treatment strategies to prevent this cell death.

3.2 Results

3.2.1 E50K mutant of optineurin induces death selectively in RGC-5 cells.

Because the primary defect in glaucoma is the death of retinal ganglion cells, we used the rat RGC cell line (RGC-5), which is a useful model to study physiology of retinal ganglion cells, to analyze the effect of optineurin mutant expression on the survival of RGCs. RGC-5 cells grown on coverslips were transfected with the plasmids expressing HA-tagged wild type optineurin (WT) or its mutants, as described in chapter 2. Transfected cells were stained with anti-HA antibody and examined by fluorescence microscopy. Expression of the mutant E50K resulted in the death of 22.6% ± 3.3% cells, as revealed by the loss of refractility, condensation of chromatin and decrease in cell size caused by the

shrinkage of cytoplasm (Figure 3.1A, 3.2A). These morphological features of E50K-induced cell death are similar to those of apoptosis. Interestingly, cells expressing other mutants, namely R545Q, H26D and H486R, which too have been linked to POAG, did not display any more cell death than the basal value shown by wild type optineurin (Figure 3.1A & 3.3). The induction of cell death by E50K was not caused by its higher level of expression as compared to WT optineurin which was confirmed by western blot analysis (Figure 3.1B). A mutant protein can induce stress in the endoplasmic reticulum because of improper folding, but the effect of E50K did not seem to be caused by ER stress because the level of calnexin (a chaperone protein induced by ER stress) did not increase upon expression of E50K (Figure 3.1B).

To understand whether E50K induced cell death is cell type specific or a common phenomenon in all cell types, experiments were done in non-ocular cell lines and one more ocular cell line. The ability of the E50K mutant to induce cell death appears to be selective to RGCs because neither this mutant nor WT optineurin was able to induce cell death in IMR32 (a neuronal cell line), HeLa or Cos-1 (Figure 3.1C, 3.2 B). The level of E50K expression in these cell lines was compared by western blot analysis. The differences in the level of E50K expression were less and were not likely to explain the selectivity of E50K to induce cell death in RGC-5 cells (Figure 3.1D). The level of endogenous protein was higher in RGC-5 cells than in other cell lines (Figure 3.1E). Moreover, in RGC-5 cells the optineurin band showed faster mobility. The effect of E50K overexpression was also checked in another ocular cell line, namely the human retinal pigment epithelial cell line or D407. Neither the wild type optineurin nor the E50K mutant was able to induce cell death in this cell line (Figure 3.1C,

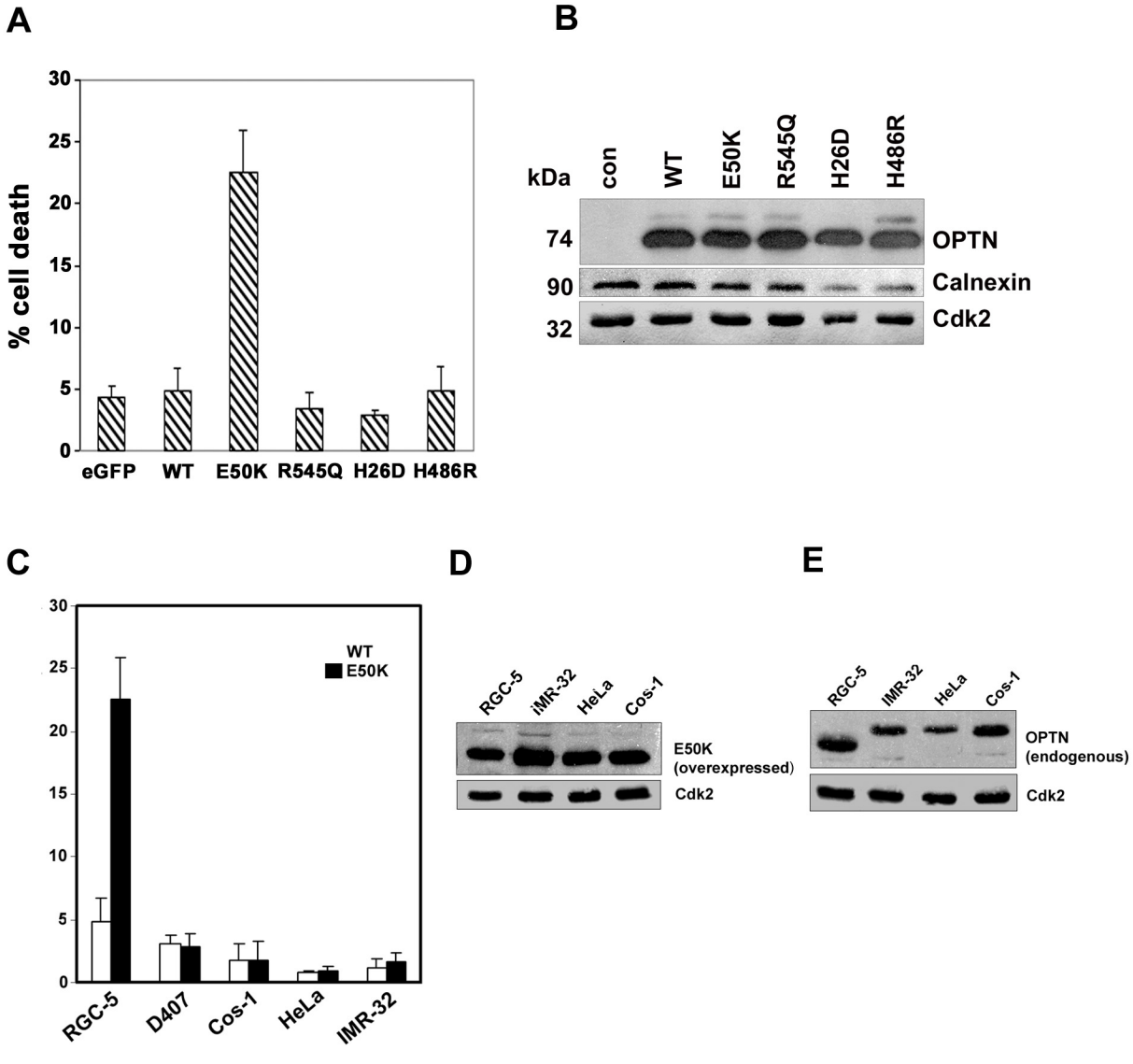

Figure 3.1: E50K mutant of optineurin selectively induces the death of RGCs.

(A) Effect of expression of various mutants of optineurin on the induction of cell death in RGC-5 cells. Cells grown on coverslips were transfected with 150 ng plasmids expressing normal optineurin (WT) or its mutants. After 32 hours of transfection, cells were fixed and stained for optineurin (HA-tag antibody) to determine cell death. Data represents cell death in expressing cells (mean ± SD of at least 4 experiments) after subtracting the background cell death observed in nonexpressing cells, which was generally 1% to 3%. GFP was used as an additional control. *P<0.01 compared with WT optineurin- expressing cells (Student's *t* test).

(B) Western blot showing expression of various mutants of optineurin and the level of expression of calnexin. Cdk2 was used as a loading control.

(C) E50K mutant does not induce cell death in D407, Cos-1, HeLa or IMR-32 cells. Cells grown on coverslips were transfected with 300 ng indicated plasmids and processed as described in (A).

(D) Western blot showing expression of E50K mutant in indicated cell lines. Cdk2 was used as loading control. Transfection conditions of E50K in various cell lines, grown in 24-well plates, were the same as those used for cell death assays.

(E) Western blot showing expression of endogenous optineurin using optineurin antibody.

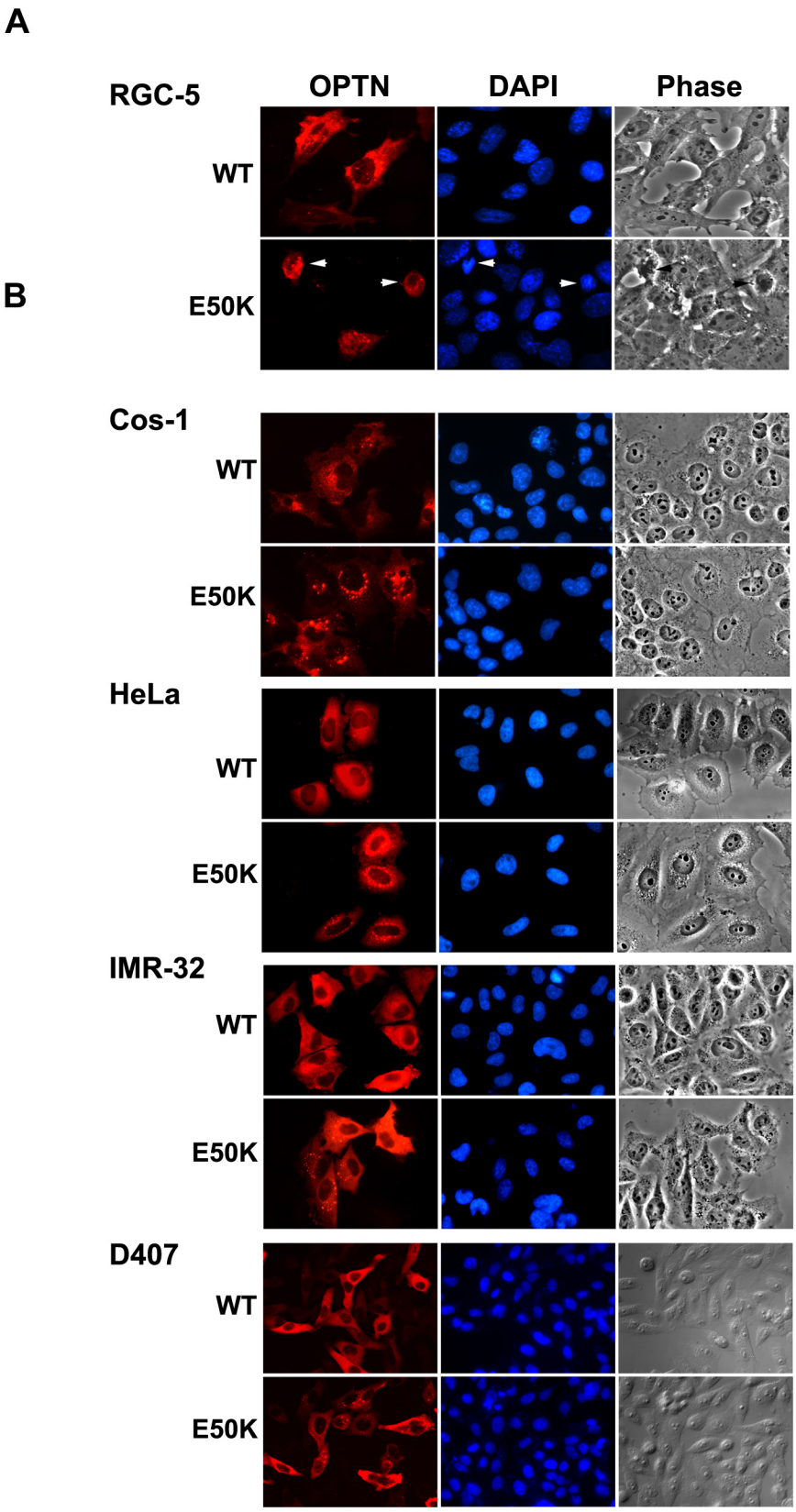

Figure 3.2: E50K mutant induces cell death only in RGC-5 and not in other cell lines (Cos-1, HeLa, IMR-32 & D407).

(A) Images of RGC-5 cells expressing WT or E50K mutant of optineurin, showing the induction of cell death by this mutant. Arrowheads: E50K-expressing dead cells.

(B) Images of Cos-1, HeLa, IMR-32 and D407 cells expressing WT or E50K mutant of optineurin.

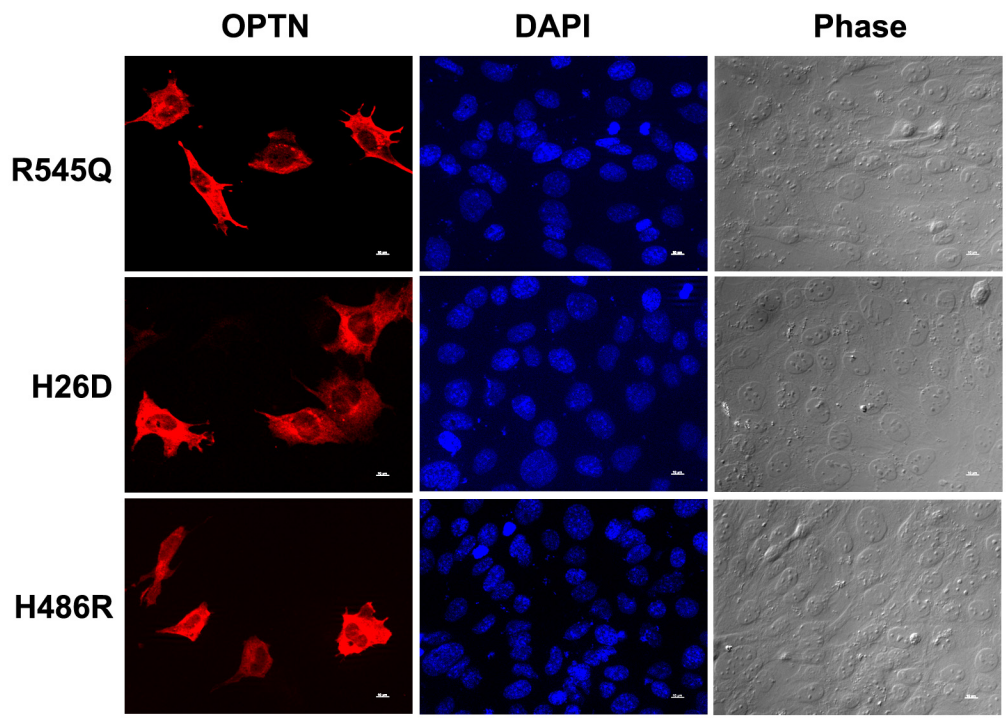

Figure 3.3: Localization of optineurin mutants in RGC-5 cells. RGC-5 cells were transfected with the mutant constructs, viz., R545Q, H26D and H486R and 32 hours after overexpression stained for optineurin with HA antibody. Images showing expression and localization of optineurin mutants, R545Q, H26D and H486R in RGC-5 cells.

3.2B).These results show that E50K mutant of optineurin selectively induces death of RGC-5 cells but not of other cell lines tested.

3.2.2 E50K induced cell death is inhibited by Bcl2 and requires caspases

Since it was observed that E50K induced cell death has features of apoptosis, the involvement of a few caspases was studied. Mutant caspase-1 (Gupta *et al*., 2002) and caspase-9s (Seol & Billiar, 1999) are dominant negatives of the respective caspases and Bcl2 is an anti-apoptotic protein present in the mitochondria. Cell death induced by E50K in RGC-5 cells was inhibited by the antiapoptotic protein Bcl2 ($p<0.05$). Expression of caspase-9s (an inactive variant of caspase-9 that inhibits caspase-9 function) and mutant caspase-1 significantly reduced the effect of E50K on cell death ($p<0.05$) (Figure 3.4A). The inhibitory effect of Bcl2, mutant caspase-1 and caspase-9s on E50K induced cell death was not caused by their effect on the expression of E50K protein as determined by western blotting (Figure 3.4B). These results suggest that caspases are required for E50K-induced cell death in RGC-5 cells. TUNEL assay of DNA fragmentation did not reveal any significant labeling of E50K-expressing cells over the control. Moreover, little activation of caspase-3 was observed on E50K mutant expression (Figure 3.5A, B).

3.2.3 Optineurin and E50K mutant potentiate TNF-α induced cell death in retinal ganglion cells

TNF-α is a cytokine that induces many signaling pathways and induces cell death in many types of cells. The expression of TNF-α and TNF-α receptor-1 is upregulated in the retina and optic nerve head in persons with glaucoma (Yan *et al*., 2000; Tezel *et al*., 2001; Yuan *et al*., 2000). Optineurin gene expression is

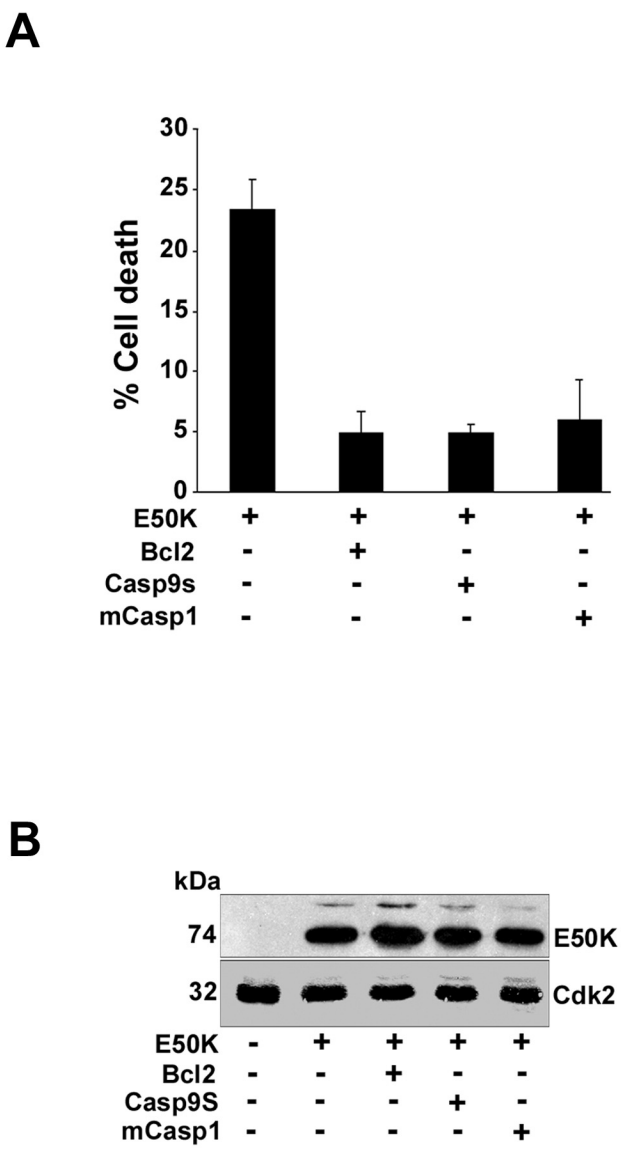

Figure 3.4: Effect of caspase inhibitors and Bcl2 on E50K-induced death of RGC-5 cells.

(A) Cells grown on coverslips were cotransfected with E50K expression plasmid (150 ng) along with plasmids expressing mutant caspase (mCasp)-1, caspase (Casp)-9s, or Bcl2 (150 ng each). After 32 hours of transfection, cells were fixed and stained with HA-tag antibody, and cell death was determined. Expression of mutant caspase-1, caspase- 9s, and Bcl2 resulted in significant inhibition ($P<0.05$) of cell death.

(B) Cells grown in 24-well plates were transfected as described in (A), and, after 32 hours, cell lysates were made for Western blotting. E50K protein level was determined using HA antibody.

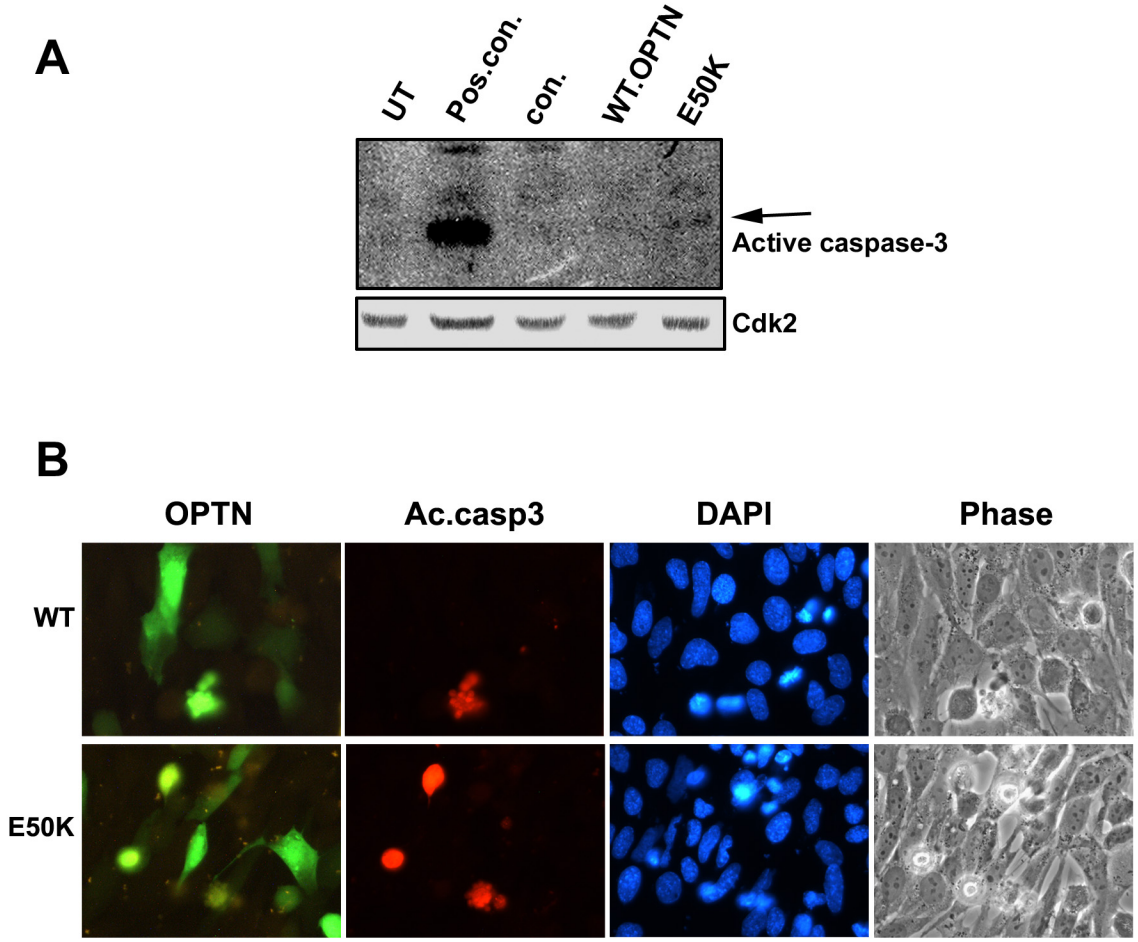

Figure 3.5: E50K expression leads to caspase-3 activation in RGC-5 cells.

(A) RGC-5 cells were transfected with 1μg of wild type optineurin or E50K mutant and allowed to express for 32 hours. Western blot showing a faint active caspase-3 band in E50K mutant transfected lane. RGC-5 cells treated with 1μM staurosporine for 7 hours was used as positive control for caspase-3 activation. Cdk2 was used as loading control.

(B) Images of RGC-5 cells showing active caspase-3 staining in E50K expressing cells undergoing cell death. Cells grown on coverslips were transfected with 150 ng plasmids expressing WT optineurin or its E50K mutant. After 32 hours of transfection, cells were fixed and stained for optineurin (HA-tag antibody, in green) and active caspase-3 (in red) to determine active caspase-3 in E50K transfected cells.

induced by TNF-α in many cells (Li *et al.*, 2000; Schwamborn *et al.*, 1998). An association between polymorphisms in the optineurin and the TNF-α genes has been suggested to increase the risk for glaucoma (Funayama *et al.*, 2004; Lin *et al.*, 2003). Therefore, we examined the effect of the expression of optineurin and E50K mutant on TNF-α induced cell death. Cells were transfected with WT optineurin or E50K and after 24 hours these cells were treated with TNF-α for 24 hours. TNF-α induced cell death was seen to be potentiated by both WT and E50K mutant; E50K expressing cells showed significantly more cell death than those expressing normal optineurin (Figure 3.6A, B). Surprisingly even wild type optineurin increased TNF-α induced death of RGC-5 cells ($P<0.05$).

3.2.4 E50K- induced cell death is inhibited by antioxidants

To understand the mechanism by which the E50K mutant induces cell death in RGC-5 cells, we investigated the possibility of E50K causing oxidative stress, which is known to lead to pathologic cell death. The ability of antioxidants to inhibit E50K-induced cell death was tested. In our experiments, three different antioxidants were used: N-acetylcysteine (NAC), Trolox (a water soluble homolog of vitamin E) and MnSOD (manganese superoxide dismutase which is a mitochondria specific enzyme). NAC is the precursor of glutathione, which is a major antioxidant in mammalian cells. Treatment with NAC resulted in an inhibition of E50K induced cell death (Figure 3.7A, B). Another antioxidant, Trolox was also able to reduce this cell death. Cotransfection of a plasmid-expressing MnSOD resulted in greater than 75% inhibition of E50K-induced cell death (Figure 3.7A, B). Interestingly, we note that the protection against cell death induced by the three different antioxidants, NAC, Trolox and MnSOD was

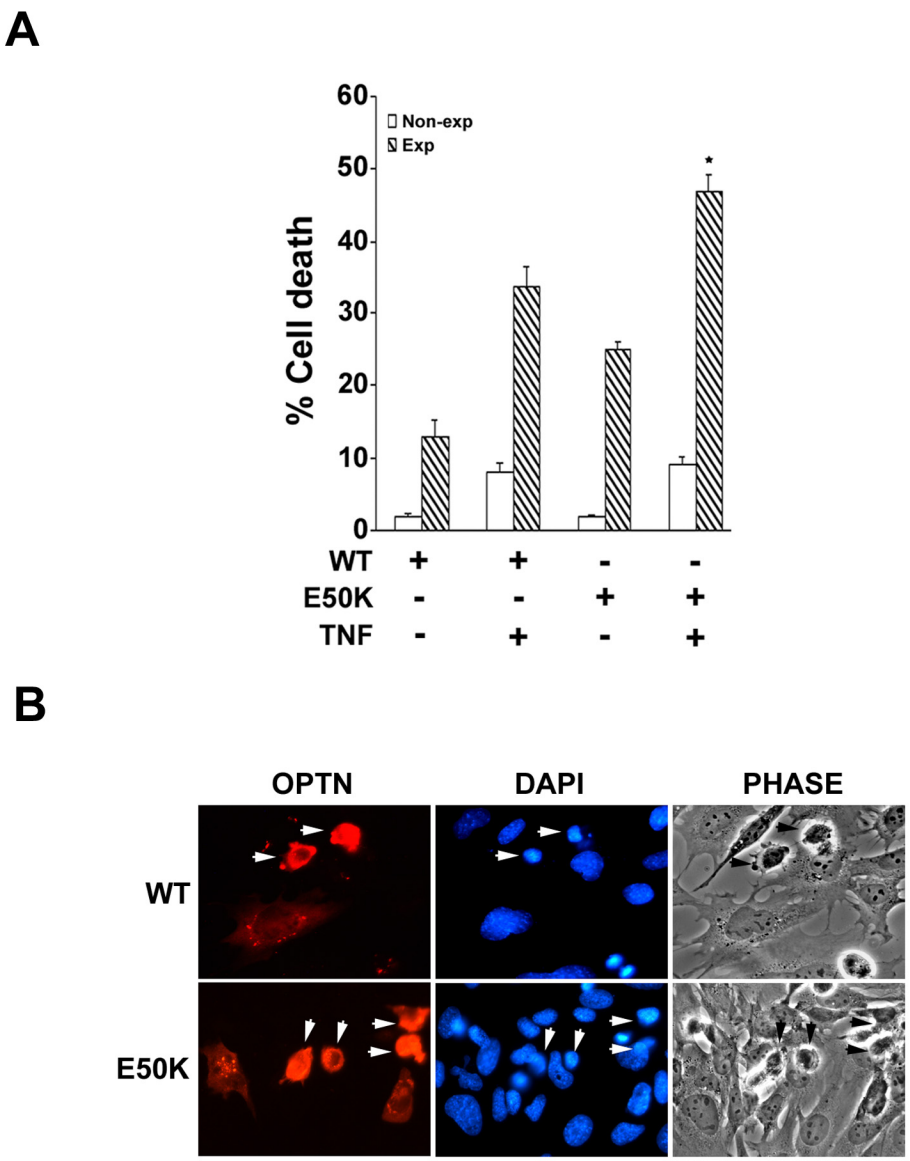

Figure 3.6: Effect of optineurin (WT & E50K) overexpression on TNF-α induced cell death in RGC-5 cells.

(A) RGC-5 cells grown on coverslips were transfected with 300ng of wild type optineurin or E50K mutant. 24 hours after transfection, cells were treated with murine TNF-α (10ng/ml) for 24 hours and later fixed and stained with HA antibody. Bar diagram showing the effect of optineurin overexpression on TNF-α induced cell death. *P< 0.05 compared with WT optineurin expressing TNF-α treated cells (Student's *t* test).

(B) Images of RGC-5 cells showing effect of WT optineurin and E50K mutant on the TNF-α induced death of RGC-5 cells.

significant ($P<0.05$). That this inhibitory effect was not caused by the reduced expression of E50K protein was shown by western blotting (Figure 3.7C). Cell death induced by E50K in the presence of TNF-α was also inhibited significantly by NAC and Trolox ($P<0.05$) (Figure 3.7D). These results suggest that oxidative stress induced by E50K plays an important role in cell death.

3.2.5 E50K overexpression increases ROS levels in RGC-5 cells

To investigate further the involvement of ROS (reactive oxygen species) in E50K-induced cell death, the levels of ROS in RGC-5 cells transfected with E50K mutant or WT optineurin were determined by using an ROS-sensitive probe, CM-H_2DCFDA. It is a non-fluorescent probe which upon entering the cell is cleaved by intracellular esterases that remove its acetate groups and shows green fluorescence on binding to ROS. Expression of E50K mutant resulted in an increase in ROS production, as shown by increased DCF fluorescence (Figure 3.8A). Treatment of E50K transfected cells with NAC and Trolox, resulted in reduced ROS production (Figure 3.8B). Cotransfection of a plasmid expressing MnSOD with E50K resulted in nearly complete loss of ROS (Figure 3.8B). These results suggest that E50K expression induces ROS production which is partially inhibited by NAC and Trolox and completely by MnSOD.

3.2.6 Sub-cellular localization of endogenous optineurin in mammalian cell lines

Altered subcellular localization of a mutant protein can affect its function. Therefore, the subcellular localization of exogenous optineurin and of E50K was examined. In addition, subcellular localization of endogenous optineurin was also analyzed. Initial studies on optineurin show that the endogenous protein localizes

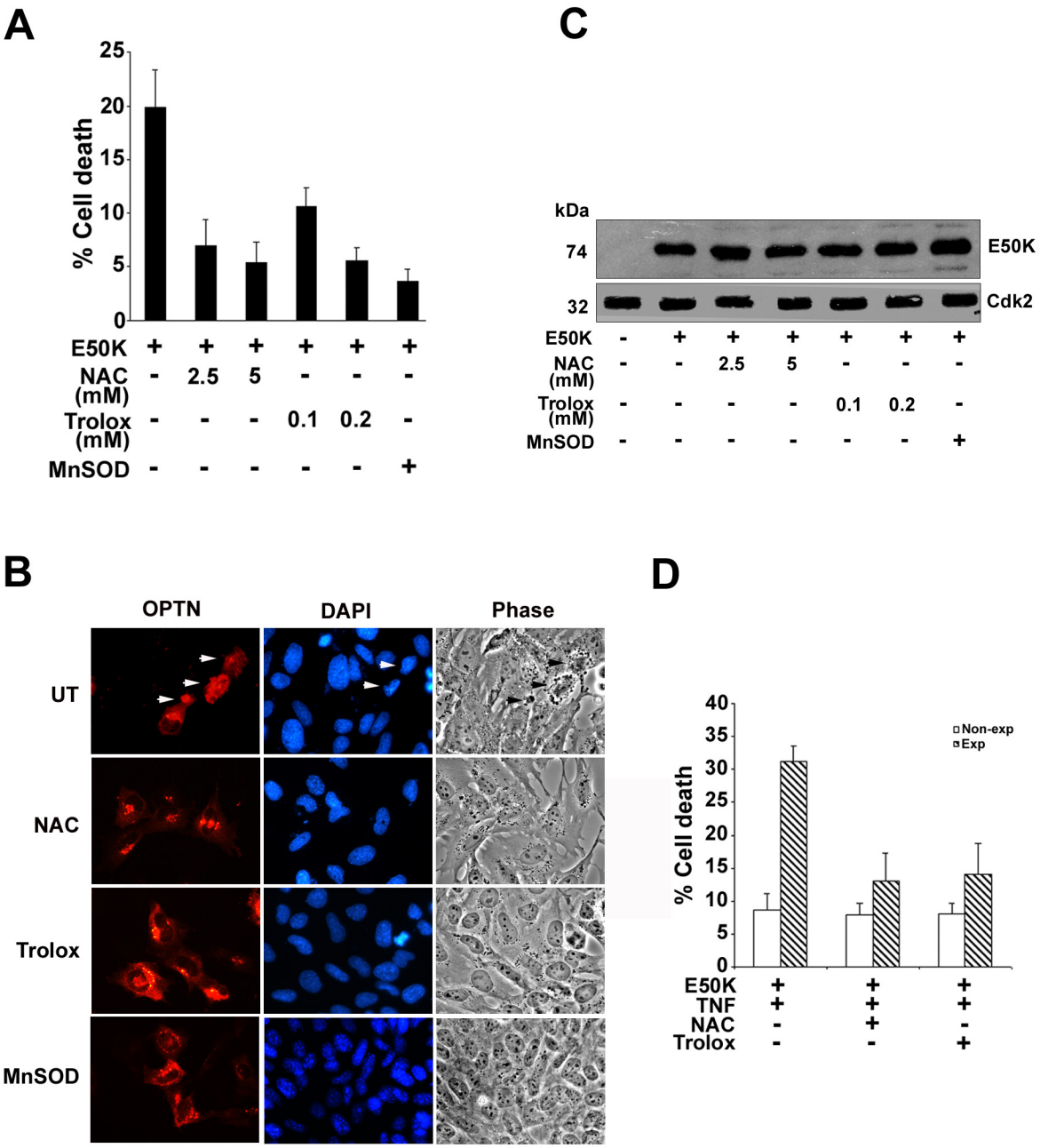

Figure 3.7: Effect of antioxidants on E50K-induced cell death of RGC-5 cells.

(A, B) NAC or Trolox was added to the medium after 6 hours of cell transfection with E50K expression plasmid. After 22 hours of transfection, medium was replaced with fresh medium containing antioxidants. Cells were fixed and stained after 32 hours of transfection.

(C) Western blot showing the level of E50K mutant in the presence of antioxidants. Cells grown in 24-well plates were transfected with E50K plasmid alone or with MnSOD. Cells were then treated with NAC or Trolox after 6 hours of transfection as in (A, B). Cell lysates were prepared after 32 hours of transfection for Western blotting.

(D) Effect of antioxidants on E50K-induced cell death in presence of TNF-α. This experiment was performed as in (A) except that after 24 hours of transfection, murine TNF-α was added.

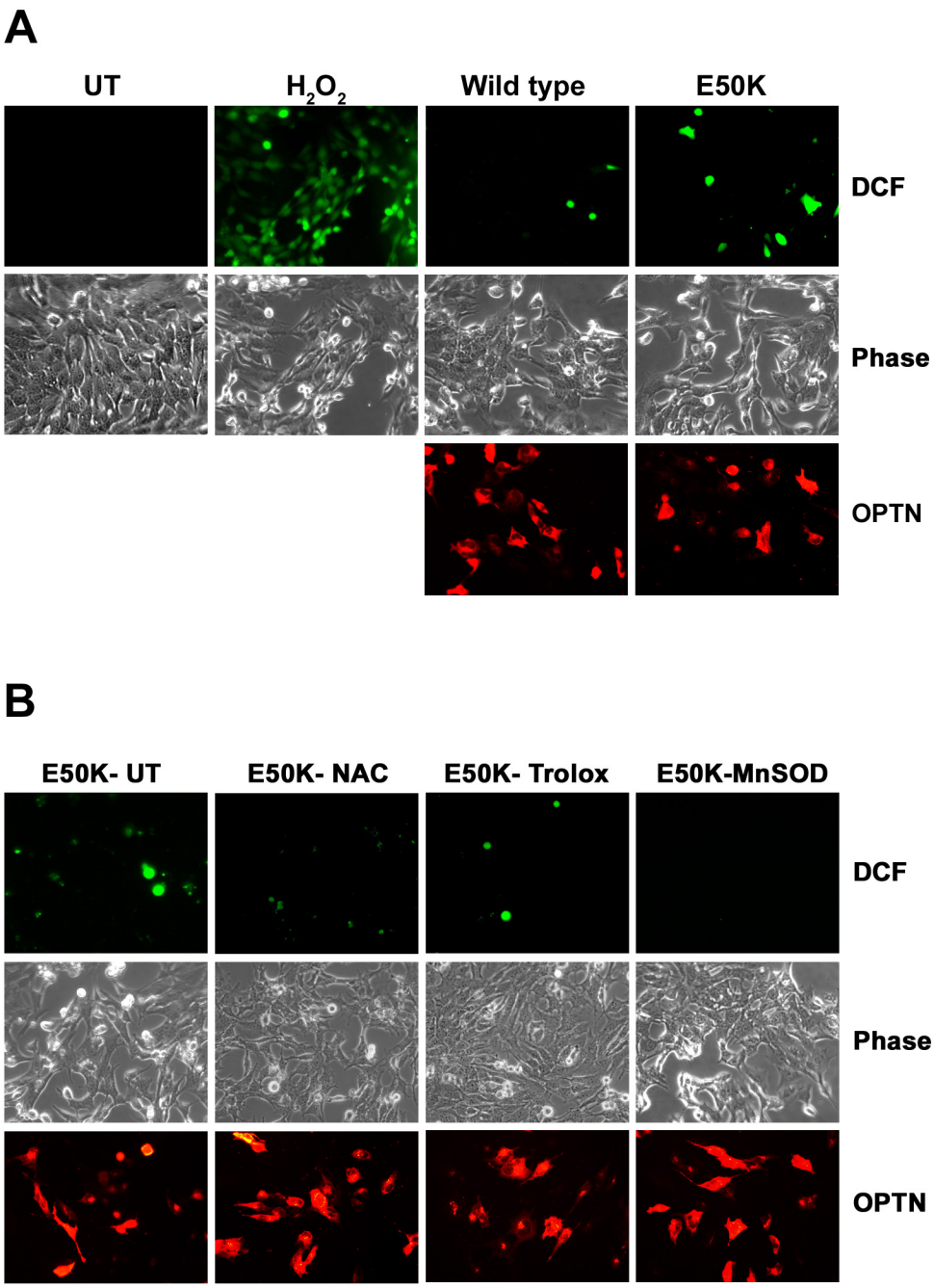

Figure 3.8: E50K mutant induces ROS production.

(A) RGC-5 cells were transfected with WT optineurin or E50K mutant plasmids. After 30 hours of transfection, cells were washed and incubated with CM-H_2DCFDA. After 1 hour, cells were washed and visualized by an inverted microscope. Representative fields showing DCF fluorescence and corresponding phase-contrast images are shown. H_2O_2-treated cells were used as positive control. UT, untreated cells. Expression of E50K and WT optineurin was confirmed in each experiment by fixing these cells and staining with HA antibody. Representative fields from the same coverslips are shown in the bottom panels.

(B) RGC-5 cells were transfected with E50K expression plasmid alone or with MnSOD. E50K-transfected cells were treated with 5 mM NAC or 0.2 mM Trolox and were subjected to ROS detection assay. Representative fields showing DCF fluorescence are shown. MnSOD-transfected cells showed no DCF fluorescence.

to the Golgi apparatus (Schwamborn *et al*., 2000; Rezaie *et al*., 2002). But a later report provides evidence contradicting the Golgi localization of endogenous optineurin (Park *et al*., 2006). Hence, experiment was done to determine the exact intracellular localization of endogenous optineurin in RGC-5 cells. RGC-5 cells were transfected with GFP- p23 (plasmid codes for a mature form of rat p23 tagged with GFP at the N-terminus), which has been shown to localize to the Golgi network and intermediate compartment (Blum *et al*., 1999). The cells were then fixed and stained for endogenous optineurin. Majority of the endogenous optineurin showed diffuse distribution in the cytoplasm and a detectable amount of the protein colocalizes with GFP- p23 (Figure 3.9A). We also tested this using another ocular cell line, D407, by double staining the cells with optineurin and Giantin (another Golgi marker) antibodies. Unlike in RGC-5, we found here that apart from uniform distribution of the protein in the cytoplasm, a prominent localization in the Golgi (Figure 3.9B) was also seen as observed by colocalization with Giantin. Optineurin localization was checked by staining with optineurin antibody in the non-ocular cell lines Cos-1, HeLa and IMR-32. In Cos-1, besides a detectable amount of the protein in the cytoplasm, substantial amount of the protein was seen localizing in the Golgi region, which is in the perinuclear position whereas in HeLa and IMR-32, optineurin shows a similar distribution pattern like in RGC-5 (Figure 3.10). The above results indicate that optineurin localizes and distributes in a cell type-specific manner; in a few cell lines it shows diffuse distribution in the cytoplasm along with Golgi while in some others it shows prominent localization in the Golgi apart from cytoplasmic distribution.

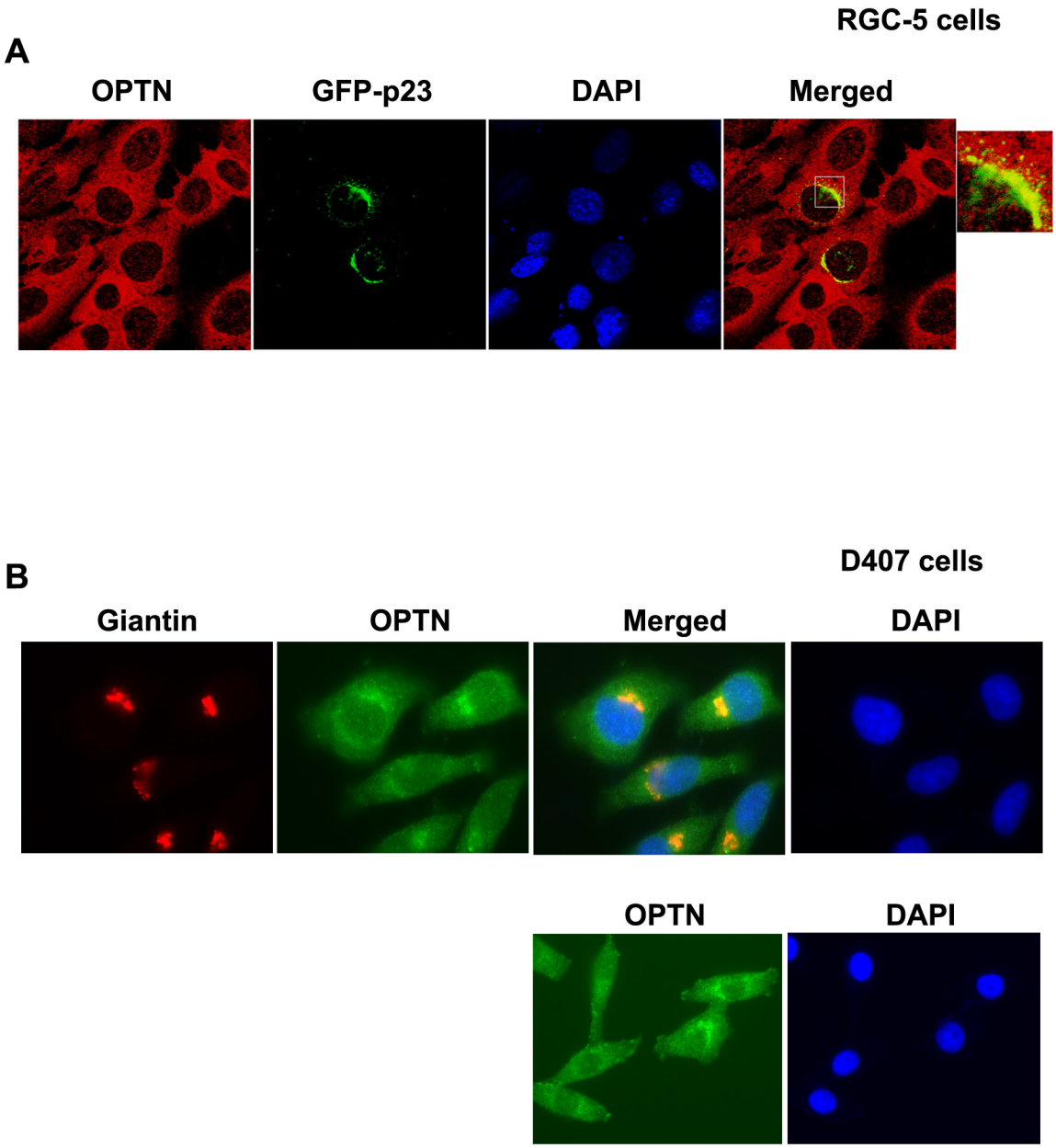

Figure 3.9: Sub-cellular localization of endogenous optineurin in ocular cell lines.

(A) RGC-5 cells transfected with GFP-p23 (a known Golgi marker) were stained with optineurin antibody. Confocal sections show diffused distribution of optineurin in the cytoplasm. Colocalization of optineurin with the Golgi marker was also observed as yellow colour in merged images. Nuclear staining is shown in blue in the images.

(B) D407 cells were co-stained with Giantin (a Golgi marker) and optineurin antibodies. Optineurin showed distribution in the cytoplasm and a prominent staining in the Golgi as shown by yellow colour in merged images. One coverslip was stained with only optineurin to show that the staining pattern remains unaltered when stained with Giantin and there is no cross reactivity among the secondary antibodies.

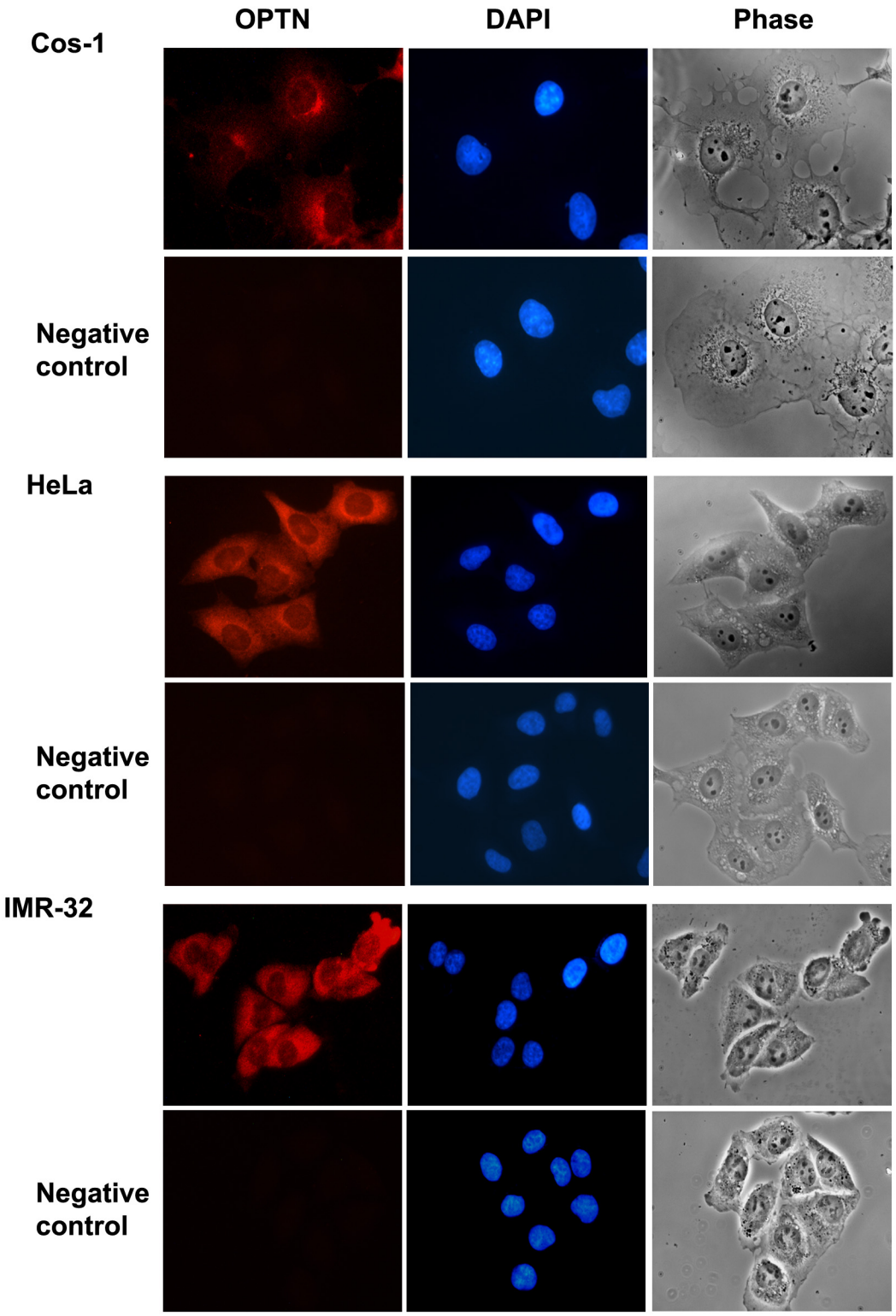

Figure 3.10: Sub-cellular localization of endogenous optineurin in non-ocular cell lines.

Cos-1, HeLa and IMR-32 cell lines were plated on coverslips and after 24 hours stained with optineurin antibody. Immunofluorescence pictures showed that the protein has cytoplasmic distribution and in Cos-1 there is a prominent staining at the perinuclear position likely to be Golgi. Images also show negative controls for Cos-1, HeLa and IMR-32 where only secondary antibody staining was performed.

3.2.7 Expression and localization of overexpressed optineurin and its mutants

Since we found that endogenous optineurin shows cytoplasmic distribution along with Golgi localization, our next experiment was to see whether overexpressed optineurin and its mutants also behaved the same way. WT optineurin cloned in the pcDNA 3.1-HA vector was transfected in RGC-5 and stained with anti-HA antibody. Overexpressed optineurin showed diffused distribution in the cytoplasm (Figure 3.11A). The mutants of optineurin, viz., E50K, R545Q, H26D and H486R behaved like wild type optineurin in their expression and localization (Figure 3.3), except that the E50K mutant showed large vesicular structures distributed in the cytoplasm. However, the large vesicular structures seen in E50K transfectants were generally concentrated in the vicinity of Golgi region (Figure 3.11A).

To check whether the HA-tag is interfering with the localization pattern of optineurin, vectors were made which expressed optineurin and E50K mutant without any tag and the transfected cells were stained with optineurin antibody. Optineurin and E50K showed the same localization as in the HA-tagged vector (Figure 3.11B). It can thus be concluded that the HA-tag does not affect the localization pattern of optineurin and E50K.

3.3 Discussion

It has been suggested that optineurin has a cytoprotective function that is disrupted by mutations leading to glaucoma (Rezaie *et al.,* 2002). Although this function of optineurin in RGCs is yet to be established, our results suggest that the E50K mutant has acquired the ability to induce cell death selectively in RGCs

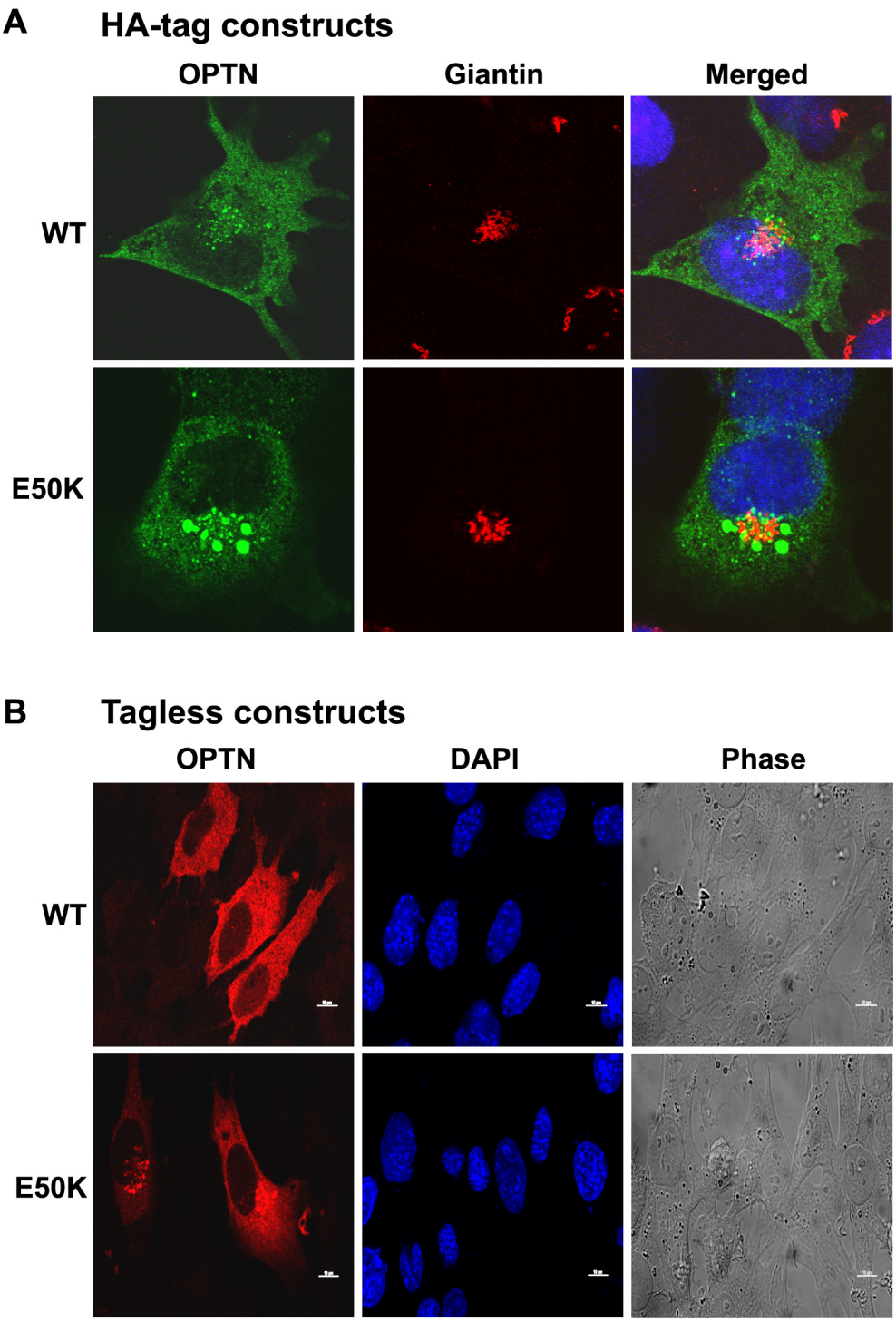

Figure 3.11: Subcellular localization of overexpressed optineurin and its mutant E50K in RGC-5 cells.

(A) RGC-5 cells were transfected with pcDNA3.1-HA-optineurin or E50K mutant and stained with HA and Giantin antibodies. Confocal sections show very little colocalization of overexpressed optineurin (WT) or E50K (green) with Golgi marker giantin (red) as seen by lack of yellow colour in the merged images. Optineurin shows diffused distribution in the cytoplasm. Nuclear DNA staining with DAPI is shown in blue in merged images. E50K forms large vesicular structures, which are usually concentrated in Golgi region.

(B) RGC-5 cells were transfected with pcDNA3.0-OPTN/E50K and stained with optineurin antibody. The staining pattern is similar to the tagged vectors of optineurin.

but not in other cells. This selectivity has relevance to the disease condition because even though optineurin shows ubiquitous expression in various tissues of the body, patients with a mutation in optineurin gene suffer from glaucoma alone, and are not reported to have any other disease history. The ability of E50K to potentiate TNF-α induced death of RGCs points to the role of environmental, as well as genetic factors in causing glaucoma. The finding that E50K mutant-induced cell death is mediated by oxidative stress indicates the potential of antioxidants in preventing or delaying glaucoma.

Interestingly, only the E50K mutant of optineurin was able to induce the death of RGC-5 cells; three other mutants were unable to do so. E50K is a unique mutation that has been found only in British patients or in patients of British descent. It has been suggested that a founder effect accounts for the E50K mutation frequency in British patients (Alward *et al.,* 2003). It appears that E50K mutation alone is able to induce cell death when expressed at elevated levels. Glaucomas are generally multifactorial and are perhaps affected by multiple interacting loci (Libby *et al.,* 2005). It is likely, therefore, that other mutants (H26D, H486R) of optineurin may require interaction with genetic modifiers for inducing cell death in RGCs.

Oxidative stress in a cell may occur because of an imbalance between the production and removal of ROS, and it has been implicated in nerve cell death in the eye (Maher & Henneken, 2005a, b). Cell death induced by oxidative stress can be prevented or reduced by blocking specific steps in the cell death cascade. Cell death induced by E50K in RGC-5 cells was inhibited by two structurally unrelated antioxidants (NAC and Trolox), which act by different mechanisms, suggesting that this cell death was mediated by oxidative stress. This suggestion

is further supported by the observations that E50K expression results in increased production of ROS, which is reduced by NAC and Trolox. MnSOD completely abolished ROS production by E50K and inhibited cell death. These results suggest that the inhibition of E50K-induced cell death by NAC and Trolox is mediated, at least in part, by their ability to reduce ROS levels. Cell death induced by oxidative glutamate toxicity in RGC-5 cells has features of classic apoptosis and oxytosis (Maher & Henneken, 2005b). This type of cell death has morphologic features of apoptosis (rounding of cells, shrinkage of cytoplasm) but does not involve DNA fragmentation or caspase-3 activation (Maher & Henneken, 2005b). E50K-induced cell death is morphologically similar to apoptosis but does not show any significant increase in DNA fragmentation. Only a small increase in caspase-3 activation was seen. Taken together, these results suggest that the E50K mutant induces a type of cell death in RGC-5 cells that has characteristics of classic apoptosis and oxytosis.

How does the E50K mutant induce cell death in RGC-5 cells? Optineurin interacts with many proteins and the Rab8 interaction domain (amino acids 58-209) (Hattula & Peranen, 2000) is present in the vicinity of the E50K mutation site. It is thus likely that a conformational change induced by E50K mutation alters its interaction with Rab8. It has been reported that in response to a high level of oxidative stress (25 mM H_2O_2), optineurin translocates to the nucleus in a Rab8-dependent manner, whereas the E50K mutant is unable to do so (De Marco *et al*., 2006). Whether the loss of interaction with Rab8 or a gain of interaction with some other protein is responsible for the ability of E50K mutant to induce cell death in RGC-5 cells will require further investigation. A cytoprotective role of optineurin has been suggested in the retina, though this remains to be

demonstrated. In NIH 3T3 cells, optineurin (but not the E50K mutant) protects against cell death induced by a high level of oxidative stress (De Marco *et al*., 2006). Thus, it is likely that under certain conditions of stress, optineurin may have a cytoprotective function. However, our results suggest that a high level of WT optineurin can increase the TNF-α-induced death of RGC-5 cells, indicating that optineurin might not have a generalized cytoprotective function in these cells.

The mechanism of selectivity of E50K-induced cell death in RGC-5 cells (compared with other cells tested) is unclear. This selectivity is not the result of a higher level of E50K expression in RGC-5 cells. Earlier studies with neonatal rat retina have shown that, compared with other retinal cells, RGCs were more resistant to oxidative stress-induced cell death (Kortuem *et al*., 2000). In another report (Maher & Henneken, 2005b), it was observed that RGC-5 cells were less sensitive to oxidative stress-induced cell death than the hippocampal cell line HT22. Therefore, differential sensitivity of RGC-5 cells to oxidative stress is not likely to be the reason for the selectivity of E50K-induced cell death, which would require further investigation.

Earlier evidence regarding endogenous optineurin distribution were quite contradictory; some reports show that endogenous optineurin has Golgi localization (Schwamborn *et al.,* 2000; Rezaie *et al*., 2002), whereas another reports argues that optineurin is not present in Golgi (Park *et al*., 2006). A recent report also shows localization of endogenous optineurin in Golgi (De Marco *et al*., 2006). We have shown that endogenous optineurin shows diffused cytoplasmic distribution which includes Golgi too, as shown by using two different Golgi markers, i.e., GFP- p23 and Giantin in two different cell lines- RGC-5 and D407.

Moreover, staining for optineurin in Cos-1, HeLa and IMR-32 also showed similar distribution pattern like in RGC-5 and D407 cell lines. On the other hand, overexpressed optineurin showed uniform cytoplasmic distribution and did not colocalize with Giantin. Other mutants, viz., H26D, H486R and R545Q also behaved similar to wild type optineurin. The most common mutation E50K showed large vesicular structures in the cytoplasm and most of them lie in the vicinity of Golgi. Overall the results suggest that although some amount of endogenous optineurin is present in Golgi, this is dependent on cell type.

3.4 Conclusion

The results described in this chapter show that

- **E50K mutant of optineurin has acquired the ability to induce cell death selectively in retinal ganglion cells.**
- **E50K induced cell death is inhibited by antioxidants, suggesting the potential of antioxidants to prevent or delay some forms of glaucoma, particularly NTG and**
- **optineurin affects TNF-α induced cell death, suggesting that it may be a component of TNF-α signaling pathway.**

Chapter 4

Identification of Optineurin Interacting Proteins by Yeast Two-Hybrid Screening

4.1 Introduction

Optineurin is speculated to play a neuroprotective role (Rezaie *et al.*, 2002). Although several functions for optineurin have been proposed, their relevance to glaucoma is currently speculative. How do mutations in optineurin contribute to glaucoma? Which functions of optineurin are altered in glaucoma-associated mutants is not known. Since optineurin does not show any enzymatic activity, its functions are likely to be mediated by interaction with other cellular proteins. Those optineurin-interacting proteins, which show altered interaction with mutants of optineurin need to be identified. Therefore, to understand the cellular/ *in vivo* functions of optineurin and to identify proteins which interact with it specifically, yeast two-hybrid screening method was used. The yeast two-hybrid system offers several advantages over classical biochemical approaches to detect protein-protein interactions such as a) immediate availability of the cloned gene of the interacting protein, b) requirement of only a single plasmid construction, c) *in vivo* detection of interaction, d) detection of weak and transient interactions and e) accumulation of a weak signal over time (Chien *et al.,* 1991). Biochemical techniques such as protein cross-linking, co-immunoprecipitation and chromatographic fractionation may permit the isolation of proteins that physically associate with the protein of interest; however, determining the identity of these proteins can be challenging (McNabb and Guarente, 1996).

4.2 The Yeast two hybrid method

Yeast two hybrid method is based on the fact that transcription factors are generally bimodular in nature having distinct DNA binding domain (DNA-BD) and transcription activation domains (AD). The DBD binds to a defined promoter

sequence upstream of a gene and the AD interacts with RNA polymerase II complex. The DBD and AD can function in close proximity to each other without direct binding to activate transcription. The yeast two-hybrid assay takes the advantage of the modular set up of a transcription factor. If we fuse these two domains separately with two different proteins of interest which interact with each other, it will lead to the reconstitution of a functional transcription factor (Fields & Song, 1989). This functional transcription factor can be used to activate the transcription of its effector gene which in case of yeast two-hybrid can be a reporter gene such as β-galactosidase gene. This activation of reporter gene indicates the physical interaction between these two proteins which are fused along with transcription factor domains. Both the domains are required for normal activation of reporter gene.

In yeast two hybrid assay we come across two terms: 'bait' and 'hunter' fusion proteins. The 'bait' fusion protein is the protein of interest (X) linked to DNA-BD and the 'hunter' is the potential binding partner (Y) which is linked to AD. An entire library of hybrids with the AD can also be constructed to search for new or unknown proteins that interact with the bait protein. The strain used for yeast two hybrid screening should be a knock out for this transcription factor and contain some marker genes (for efficient maintenance of the plasmids coding for the genes being tested for interaction in yeast). The two hybrids are cotransformed into a yeast host strain leading to activation of adenine reporter gene which can be detected by growth on minimal media. Later on positives obtained by selection on adenine dropout medium are confirmed by checking for the activation of β-galactosidase gene by colour formation assay.

For our work, we have used the yeast strain *PJ69-4A* that contains three easily assayed reporter genes each under the control of a different inducible promoter (James *et al*., 1996). This strain is auxotrophic for His, Leu, Trp, Ade and Ura and contains an additional β-galactosidase gene down stream of Gal4 responsive promoter sequences. The major concern in yeast two hybrid assay is the number of false positives which is circumvented by using three different promoters responsive to Gal4 transcription factor. His, Ade and β-gal genes are downstream of Gal4 responsive promoters Gal1, Gal2 and Gal7 respectively. These three Gal4 responsive genes enable enhanced sensitivity and less background of false positives.

4.3 Results

4.3.1 Expression of optineurin in yeast

Optineurin was amplified using gene specific primers (*ECoRI* site in forward primer & *XhoI* site in reverse primer) from human placental cDNA library (Clontech). Resultant PCR product was first cloned in pMOS blue vector with the help of pMOS blunt end ligation and then sequenced from both ends. After confirming the sequence, the cDNA coding for full length optineurin was excised with the help of specific restriction sites (*ECoRI & XhoI* in this case) from pMOS and cloned in-frame in the respective sites of pcDNA 3.1-HA vector. Full length optineurin gene was excised from pcDNA 3.1-HA vector with specific restriction sites (*BamHI& XhoI*) and cloned in *BamHI and SalI* sites of pGBKT-7 yeast two hybrid expression vector (Figure 4.1A). The mutants of optineurin were cloned similarly from pcDNA-HA contructs in pGBKT-7 vector. pGBKT-7 contains kanamycin gene and Trp gene for selection in *E.coli* and yeast respectively and

on the other hand pACT2 contains ampicillin gene and Leu gene for selection in E.coli and yeast respectively.

Yeast expression vector, pGBKT-7 containing human optineurin cDNA was transformed into PJ69-4A yeast strain using the lithium acetate transformation protocol as described in Methods, section 2.2.20.7.3. The transformed yeast cells were selected on Trp^- yeast selection media plates. Single colonies of transformed yeast cells were picked, grown in Trp^- liquid yeast selection media and protein lysates were made. These protein lysates were electrophoresed on 8% SDS-PAGE and transferred on to nitrocellulose membrane and expression of optineurin was checked by western blotting using anti-myc mouse monoclonal antibody and ALP- conjugated rabbit anti-mouse secondary antibody (Figure 4.1B). Mutants of optineurin, viz., E50K, R545Q, H26D and H486R were also cloned in a similar way like wild type and protein expression was checked. (Figure 4.1B&C).

4.3.2 Identification of optineurin interacting proteins by yeast two hybrid cDNA library screening

PJ69-4A strain expressing optineurin was transformed with human placental cDNA library in pACT2. Transformants were plated on yeast dropout medium plates lacking Trp, Leu and Ade. A small part (0.1%) of transformation mix was plated on the Trp and Leu dropout medium plate to determine the efficiency of transformation. Colonies were obtained on these selection plates after 2-3 days of incubation at 30°C. Upon incubation for a week these selection plates yielded many slow growing positives also. These positives were patched on Ade dropout medium plates to confirm the activation of adenine reporter gene.

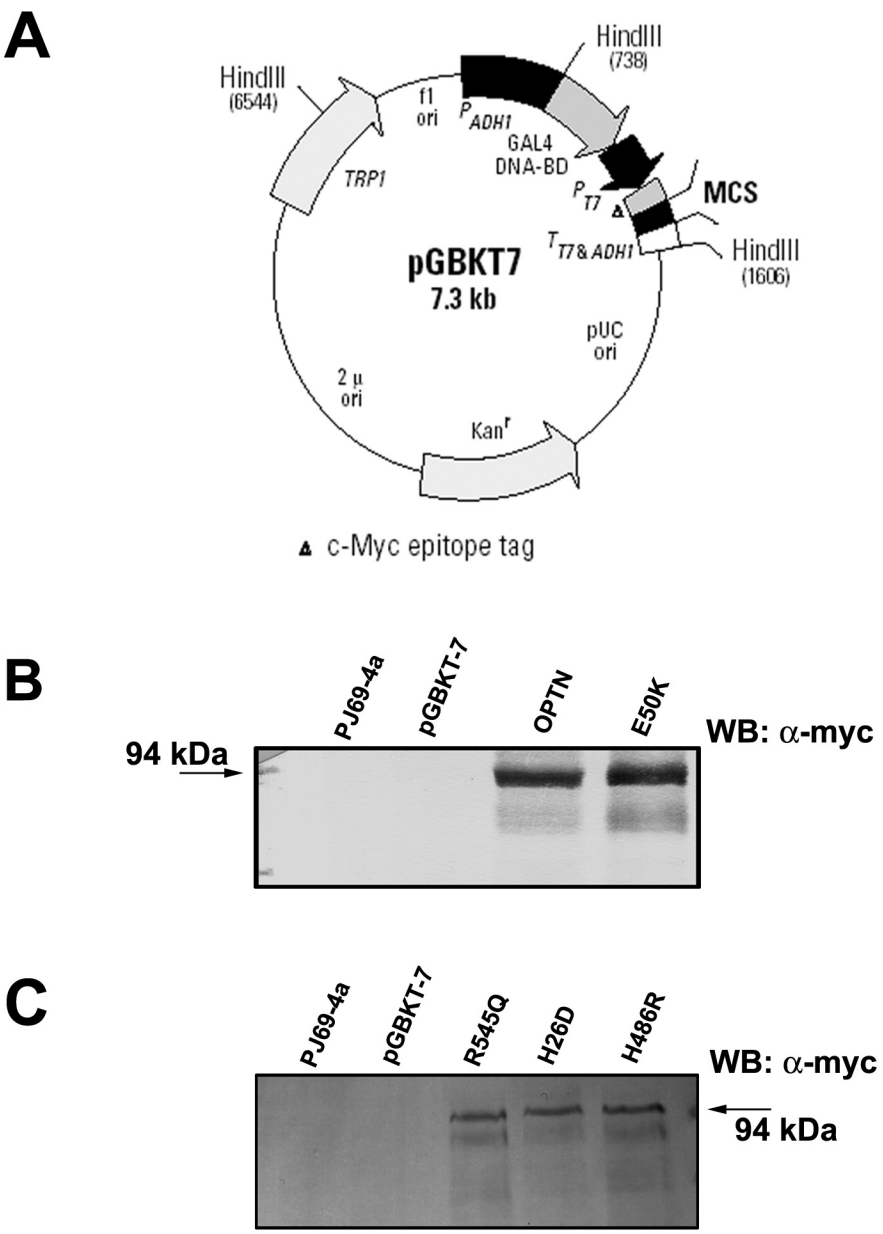

Figure 4.1: Cloning of human optineurin in DNA-BD pGBKT-7 yeast two-hybrid vector.

(A) Vector map of yeast two-hybrid DNA-BD expression vector pGBKT-7. cDNAs coding for optineurin and its mutants were cloned in *BamHI-SalI* sites present in MCS (multiple cloning site region) of pGBKT-7.

(B) Western blot showing expression of wild type optineurin and E50K mutant bait DNA-BD fusion proteins in yeast cell lysates.

(C) Western blot showing expression of optineurin mutants, R545Q, H26D and H486R bait DNA-BD fusion proteins in yeast cell lysates.

For checking activation of β-gal reporter gene, positives were plated on Trp, Leu dropout medium plates containing β-galactosidase substrate X-gal. By screening of ~ 2x 10^6 transformants, 25 positives were obtained for adenine reporter gene, out of which 23 were positive for β-galactosidase reporter gene.

Out of these 25 yeast two hybrid positives, 23 clones which were able to activate the reporter genes Ade and β-gal were chosen for further analysis. The plasmids were isolated from these positives by spheroplast method. Then these plasmids isolated from yeast were transformed in E.coli DH5α cells and the transformants were selected on LB plates containing ampicillin. Plasmids were isolated by alkaline lysis method from colonies growing on LB amp plates (containing the plasmid coding for interacting protein). The presence of inserts was confirmed by restriction digestion with *Bgl II*.

To confirm that these isolated plasmids show interaction in yeast with our bait gene specifically, these were transformed in parent strain PJ69-4A along with optineurin or empty pGBKT7 vectors. Transformants showing activation of reporter genes (Ade and LacZ) only in the presence of optineurin and not with empty DNA-BD vector were considered to be true positives. Plasmids showing reproducible interaction with optineurin were used for automated sequencing and obtained sequences were compared against public database available at http://www.ncbi.nlm.nih.gov/ for known genes using BLASTN.

Many yeast two hybrid positives were obtained by various selection criteria (their ability to grow on adenine deficient plates and also by their ability to turn blue in the presence of β-galactosidase substrate) and by confirming interaction by repeated co-transformation. Ten out of sixteen clones were

confirmed to be true positives after re-interaction studies. They belonged to different categories like regulators of NF-κB, RabGTPase member, members of immune response etc. and each of them is described below.

4.3.2.1 *CYLD* as an interacting partner of optineurin

The tumor suppressor gene, *CYLD* codes for a deubiquitinating enzyme which is a negative regulator of the transcription factor NF-κB. The gene is located to chromosome *16q12-13* and it was initially discovered associated with cylindromatosis also called turban tumor syndrome (Bignell *et al*., 2000). CYLD is an evolutionarily conserved protein of 956 aminoacids (120kDa) and is a unique member of DUB family (deubiquitinase activity). CYLD contains few distinct domains, like the catalytic domain at the C-terminus composed of two conserved subdomains containing active cysteine and active histidine which form the catalytic pocket. In addition, it contains three CAP-Gly motifs at the amino terminus that regulate microtubule dynamics (Gao *et al.,* 2008). The negative regulation of NF-κB by *CYLD* requires the deubiquitinating activity of *CYLD* on upstream signaling molecules or TNFR family members like TRAF2, TRAF6, NF-κB essential modulator NEMO (Brummelkamp *et al*., 2003) and BCl-3 (Massoumi *et al*., 2006). Inhibition of *CYLD* by RNA-mediated interference causes increased NF-κB activity and tumorigenesis (Courtois, 2008). CYLD also has a role in regulating cellular entry into mitosis (Stegmeier 2007). The participation of CYLD in NF-κB signaling was identified by various strategies one of it being yeast two-hybrid screening. In a yeast two-hybrid assay with NEMO as the bait, CYLD was identified as an interacting partner. Apart from regulating NF-κB activity, CYLD also negatively regulates JNK signaling pathway and MAPK pathway which

participate in diverse cellular programs like proliferation, differentiation and apoptosis. Knock out studies show that cyld$^{-/-}$ mice, though viable have several immune system related abnormalities (Courtois, 2008).

CYLD was one of the strongest yeast two-hybrid positives obtained in the screening (Figure 4.2). The cDNA clone obtained during the screening study was a partial clone and codes for the C-terminal 553 aminoacids (403-956 aa). This suggests that the optineurin-binding site on CYLD lies after 402 amino acids. The protein expressed by control plasmid pGBKT-7 (Gal4 DNA binding domain) did not show any interaction with CYLD (Figure 4.2).

4.3.2.2 Optineurin

Yeast two-hybrid screening helped us to identify optineurin itself as the interacting partner and we obtained optineurin as two out of the ten interacting partners (20%). The cDNA clones obtained during screening codes for 412 amino acids (165-577aa). The optineurin clones obtained did not interact with empty pGBKT-7 vector (Figure 4.2).

4.3.2.3 FLJ12168 (TBC1D17):

The Rab family of Ras-related small GTPases are key regulators of membrane trafficking and are conserved in all eukaryotic cells. More than 60 different Rabs of approximately 40 different Rab subfamilies are present in human and mice Pfeffer, 2001). Rab GTPases function as molecular switches, naturally cycling between the GDP-bound “off” state and GTP- bound “on” state at intrinsically slower rates. These slow rates of hydrolysis and nucleotide exchange of Rab proteins, i.e. GDP/GTP-cycling of Rabs may be dramatically

enhanced or suppressed by guanine nucleotide exchange factors (GEFs) and GTPase-activating proteins (GAPs). Rabs have been implicated in cargo selection, vesicle motility, vesicle tethering and membrane fusion. This wide range of GTP-Rab functions are mediated by an extraordinary diversity of effector molecules. According to recent studies, GAPs have been found to bind cargo and known coat proteins as well as directly contribute to vesicle formation (Nie and Randazzo, 2006).

A Rab-Gap member TBC1D17 (FLJ12168) was identified as one of the optineurin interacting partners in our yeast two-hybrid study. It is a TBC domain (Tre2/Bub2/Cdc16) containing protein like many other Rab-GAPs which is conserved from yeast to mammals (Itoh *et al*., 2006). The TBC domain consists of approximately 200 amino acids and is known to be present in a variety of proteins in humans. TBC1D17 is a cytosolic protein and a recent study shows that it may be a GAP for Rab21. It regulates trafficking of shiga toxin from cell surface to the Golgi along with two other Rab-GAPs EV15, RN-tre/USP6NL and TBC1D10A-C (Fuchs *et al.,* 2007). An earlier study shows that FLJ12168 weakly, but specifically recognizes Rab5 subfamily (Itoh *et al.,* 2006).

The cDNA clone obtained in our study was a full length construct of 649 amino acids along with 2 amino acids from the 5'-UTR. The protein expressed by control plasmid pGBKT-7 did not show any interaction with TBC1D17 (Figure 4.2).

4.3.2.4 IK-cytokine:

IK-cytokine was originally isolated from the conditioned culture medium of the K562 erythroleukemic cell line as a factor that inhibits IFN-γ induced

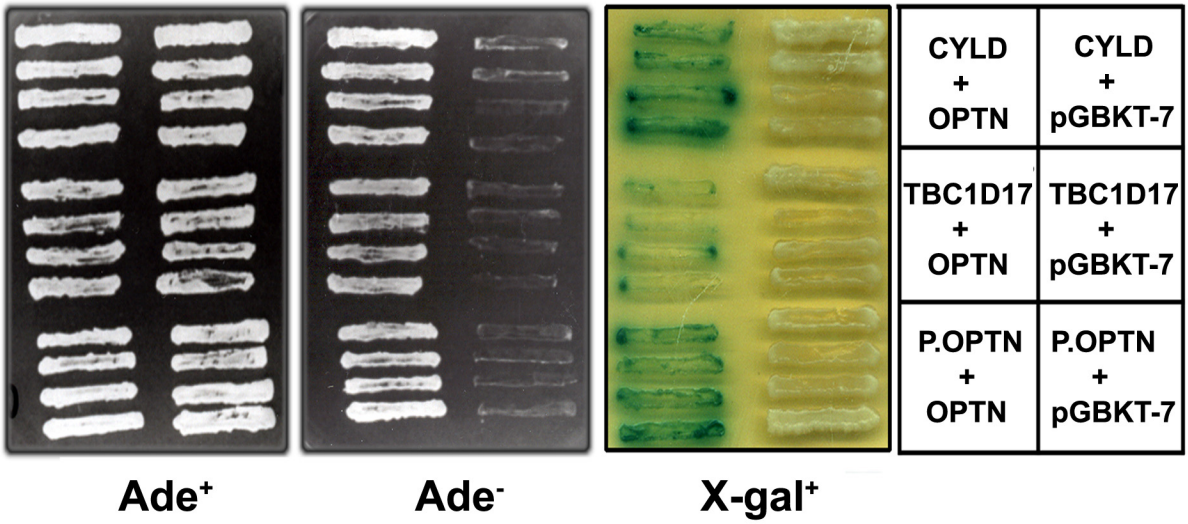

Figure 4.2: Interaction of optineurin with CYLD, TBC1D17 and optineurin.

Yeast two-hybrid interaction of optineurin with CYLD, TBC1D17 and optineurin. Interactions were confirmed by re-interaction studies after initial screening. These three proteins were the strongest positives obtained. pGBKT-7 represents empty Gal4 DNA-binding domain containing yeast two hybrid expression vector.

expression of MHC-II antigen (Krief *et al*., 1994). IK factor is infact a part of a larger protein called RED, encoding a 557 amino acid protein. The protein is termed RED because of repetitive arginine/ glutamic acid/ aspartic acid tripeptides. The gene is mapped to chromosome 5q22-q23 (Assier *et al.*, 1999). It is a 80 kDa protein and immunofluorescence studies show that the protein is localized to the nucleus as multiple nuclear dots excluding the nucleoli. Functional studies on IK cytokine are limited. Aberrant expression of class II MHC antigens has been recognized in auto immune diseases. Autoimmune diseases in MRL/*lpr* mice resemble human SLE and are characterized by dysregulation of both cellular and humoral immunity. It was demonstrated that a truncated form of IK cytokine (translated from methionine at 315 position) when transfected into nonmetastatic fibroblastoid cell line and then subcutaneously injected into MRL/lpr mice, show reduced renal damage as compared with control mice. Also, a significant decrease in macrophage and T cell infiltration was found in the kidneys which in turn resulted in decreased IFN-γ and IL-2 production (Muraoka *et al*., 2006).

The cDNA clone obtained in the screening study was a partial clone of 379 amino acids (178-557 aa) (Figure 4.3A). This suggests that the optineurin binding region in IK-cytokine lies after amino acid 178. The protein expressed by control plasmid pGBKT-7 (Gal4 DNA binding domain) did not show any interaction with IK cytokine explaining the specificity of interaction.

The partial construct (178-557 aa) obtained in yeast two-hybrid screening and the full length gene (557aa) were cloned in pEGFP-C3 vector using sequence specific primers with restriction sites giving rise to GFP-full length IK cytokine and GFP-partial IK-cytokine. On transfecting these constructs in Cos-1

cells, both the proteins showed nuclear localization as shown earlier (Assier *et al*., 1999). The full length construct showed multiple nuclear dots excluding the nucleolus whereas the partial construct showed diffused nuclear localization, and the foci were less in number (Figure 4.3B). The partial construct apart from nuclear distribution also showed cytoplasmic localization in few cells. The vector expressing partial IK-cytokine was cotransfected with wild type optineurin and colocalization was observed in the cytoplasm in very few cells (Figure 4.3C). The percent of cells with co-localization might be less because of transient interaction between the two proteins.

4.3.2.5 A20 (TNF-α Inducible Protein-3):

A20 (also called TNFAIP3) was the second negative regulator of NF-κB obtained in the screening analysis. Apart from negative regulation of NF-kB, A20 also inhibits TNF-α induced programmed cell death. It is a cytoplasmic zinc finger protein that was originally identified as a TNF-α inducible gene product in HUVEC (Human umbilical vein endothelial cells), in response to various stimuli (Dixit *et al*., 1990). It contains N-terminal ovarian tumor (OTU) domain and seven novel zinc finger structures at its C-terminus (Opipari *et al*., 1990). Yeast two-hybrid analysis shows that A20 interacts with both TRAF1 and TRAF2 and the negative feed back regulation of TNF-α induced NF-κB activation observed by A20 might be through the protein's interaction with TRAF2-TRAF1 complex (Song *et al*., 1996). TRAF2 and TRAF1 form an oligomeric complex and associate with cytoplasmic domain of TNF receptor during NF-κB activation. A20 has two distinct catalytic domains necessary for the negative regulation of NF-κB activity, both of which co-operate to downregulate NF-kB signalling: the N-

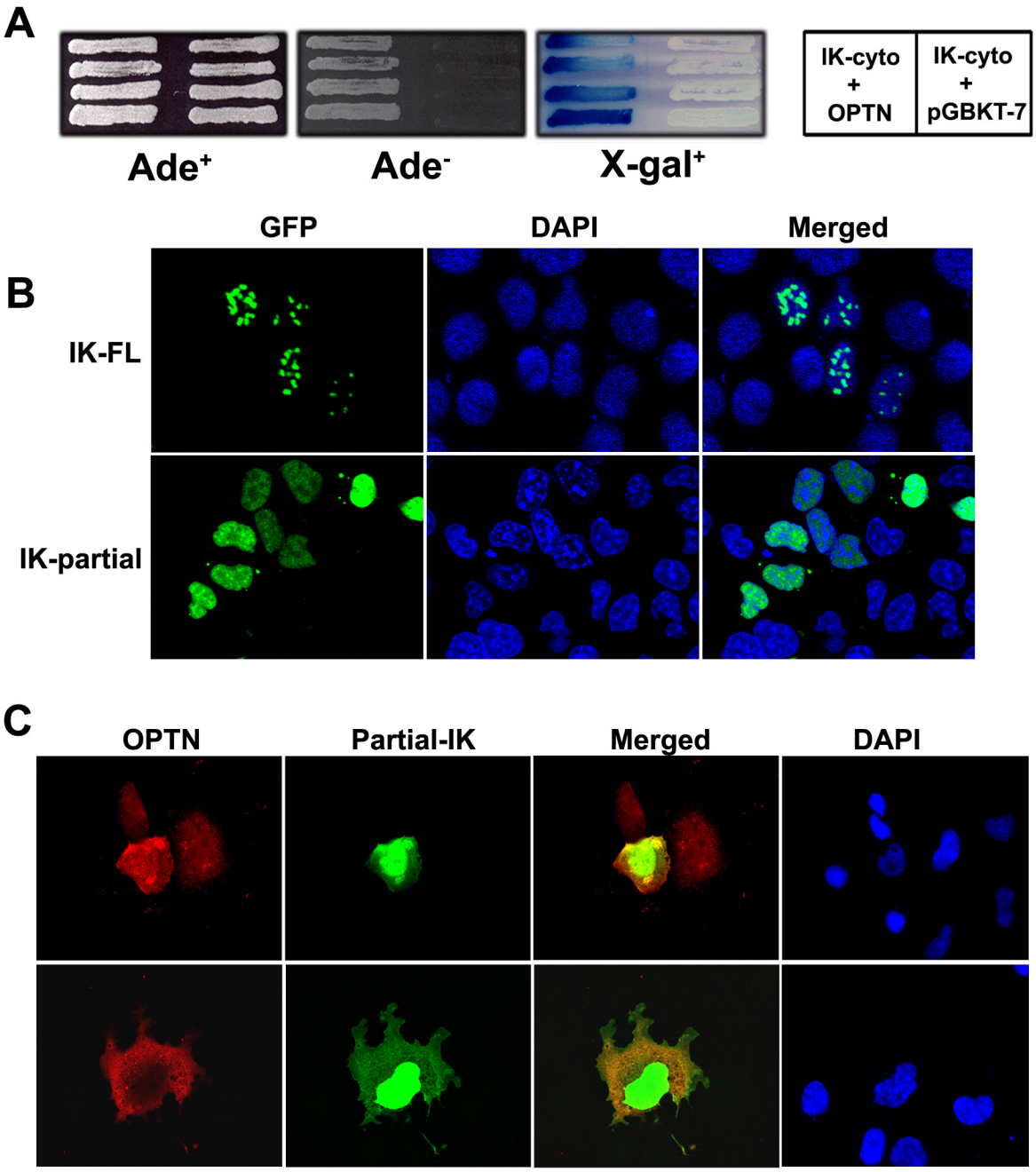

Figure 4.3: Interaction of optineurin with IK-cytokine in yeast and Cos-1 cells.

(A) IK-cytokine was obtained as a moderate interacting partner of optineurin in yeast two-hybrid screening. IK-cytokine did not show any interaction with empty pGBKT-7 vector.

(B) GFP constructs of IK-FL (full length) or partial IK-cytokine were transfected in Cos-1 cells and overexpressed for 30 hours. Full length IK-cytokine showed speckled pattern only in the nucleus while partial construct shows diffused nuclear staining.

(C) Cos-1 cells were co-transfected with wild type optineurin and partial IK-cytokine. Merged image shows good colocalization as shown by yellow colour.

terminal OTU domain removes K63-linked ubiquitin chains from active RIP making it inactive, which then permits the C-terminal ZnF region to target RIP for proteasomal degradation through K48-linked polyubiquitination (Wertz *et al*., 2004). Also, A20 physically interacts with ABIN1, an adaptor protein, which recruits it to the NEMO for further downstream activity (Mauro *et al*., 2006).

The cDNA clone obtained during screening codes for the C-terminal 235 amino acids (position 555-790 aa). A20 did not show any interaction with control vector indicating the specificity of interaction with optineurin (Figure 4.4). This result also shows that the C-terminus of A20 is the region necessary for interaction with optineurin.

4.3.2.6 HIBADH

3-hydroxyisobutyrate dehydrogenase (3-hydroxy-2-methylpropanoate:NAD(+) oxidoreductase, EC 1.1.1.31) is a dimeric mitochondrial enzyme that catalyzes the NAD(+)-dependent, reversible oxidation of 3-hydroxyisobutyrate, an intermediate of valine catabolism, to methylmalonate semialdehyde. Not much research has been carried out on this enzyme. The human protein is 336 amino acids in length and the rat protein is 300 amino acids long with an N-terminal nucleotide binding domain (Rougraff *et al*., 1988, Rougraff *et al*., 1989). The amino acid sequence shows similarity to several other mammalian pyridine nucleotide-dependent dehydrogenases. Northern blot analysis detected expression of an approximately 2.0-kb transcript in all rat tissues examined, which included kidney, liver, heart, and muscle. The rat protein shows mitochondrial localization as shown by double labeling of astroglial cells with

HIBADH and a marker for mitochondria, pyruvate dehydrogenase. Also, HIBADH shows ubiquitous expression among neural cells in culture (Murin *et al*., 2008).

The cDNA clone obtained was a full length protein coding for 336 amino acids along with some 5'-UTR. The protein did not show any interaction with empty pGBKT-7 vector (Figure 4.4).

4.3.2.7 UXT

UXT is a ubiquitously expressed transcript and has been suggested to be involved in human tumorigenesis (Schroer *et al*., 1999). Computer modeling predicted that UXT is a prefoldin like protein (Gstaiger *et al*., 2003). The gene is localized to human X chromosome X*p*11; composed of seven exons and codes for a 157 amino acid protein with three potential phosphorylation sites. The mouse homologue shares 90% identity with the human counterpart and has all the three phosphorylation sites conserved. explaining that these sites have some functional importance. Functional work on UXT was limited until quite recently. Recent investigations show that it binds to the N-terminus of the androgen receptor and regulates androgen receptor responsive genes that are important in prostrate growth suppression and differentiation (Markus *et al*., 2002; Taneja *et al*., 2004). UXT is hence called ART-27. UXT is also a component of centrosome and plays a role in cell viability (Zhao *et al.,* 2005); and is an integral component of the NF-kB enhanceosome and is essential for its nuclear function. It is speculated that UXT functions as a molecular chaperone for NF-κB in this process and positively regulates it (Sun *et al*., 2007).

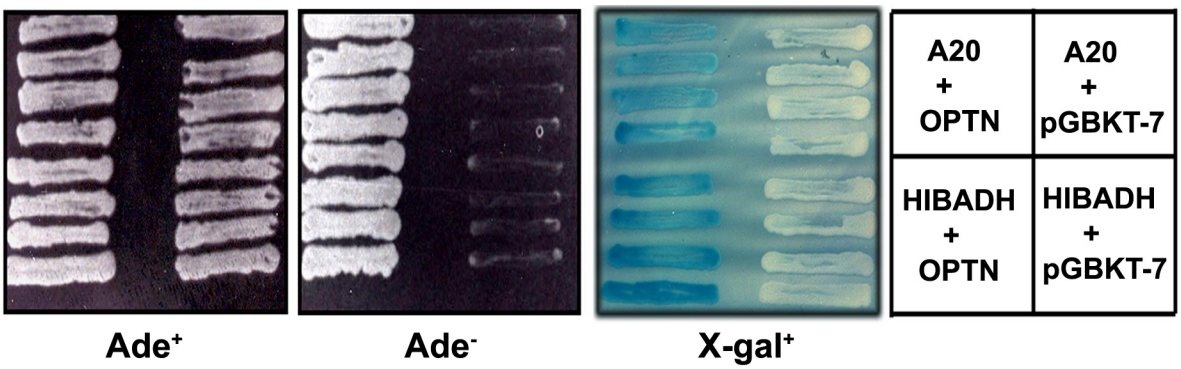

Figure 4.4: Interaction of optineurin with A20 and HIBADH.
Yeast two-hybrid interaction of optineurin was performed with A20 (TNFAIP3) or HIBADH and these proteins were the moderate interacting partners of optineurin obtained.

The cDNA clone obtained in our screening studies is a full length clone of 157 amino acids with some amount of 5'-UTR. UXT did not show any interaction with control vector (pGBKT-7) (Figure 4.5).

4.3.2.8 ZBTB33

Kaiso is a ubiquitously expressed BTB/POZ (broad complex, Tramtrack, Bric à brac/pox viruses and zinc fingers) transcription factor that was originally identified in a yeast-two-hybrid screen for binding partners of the multifunctional Armadillo-repeat containing protein p120-catenin (Daniel and Reynolds, 1999). Like other BTB/POZ proteins, Kaiso has the characteristic N-terminal protein-protein interaction POZ domain and it is through this domain that Kaiso homodimerizes and heterodimerizes with other BTB/POZ proteins (Daniel and Reynolds, 1999). In addition, Kaiso contains three C-terminal Kruppel-like C_2H_2 zinc fingers that mediate DNA binding (Daniel and Reynolds, 1999; Daniel *et al*., 2002). Kaiso is generally described as transcriptional repressor (Yoon *et al*., 2003; Ruzov *et al*., 2004) and majority of the candidate genes linked to it so far, i.e. CDH1 (E-cadherin), S100A4 (mts-1), matrilysin (MMP7), MTA2, and Wnt11 are linked to development and cancer.

The cDNA clone obtained in our screening studies is a partial clone of 477 amino acids (195-672 aa). This suggests that the optineurin binding region of HIBADH lies after the first 195 amino acids. ZBTB33 did not show any interaction with control vector (pGBKT-7) (Figure 4.5).

4.3.2.9 HLA-B associated transcript 4 (BAT4):

The gene BAT4 along with the other members of the family, viz., BAT1, 2, 3 & 5 is located in the vicinity of TNF-α and β within the major histocompatibility complex class III region (Spies *et al*., 1989). Structural and functional studies on BAT4 are limited but the protein is speculated to be involved in some aspects of immunity.

The cDNA clone obtained in our screening studies codes for the protein from 4 -356 amino acids. BAT4 did not show any interaction with control vector (pGBKT-7) (Figure 4.5).

The other interacting partners obtained after the initial screening analysis were confirmed to be false positives after re-interaction studies as they showed interaction with empty pGBKT-7 vector by either showing growth on SP plate or colour on X-gal plate.

4.3.3 Interaction studies of optineurin mutants with the yeast two-hybrid positives obtained

Having obtained nine different interacting partners for optineurin, the next aim was to check whether the optineurin mutants (E50K, H26D, H486R and R545Q) show any alteration in interaction with the optineurin interacting partners. Alteration in interaction would help us to understand the involvement of the concerned aminoacid in binding with yeast two-hybrid interacting partners and may provide probable clue for the defect in the patients with glaucoma carrying the OPTN mutation.

4.3.3.1 Interaction of E50K and R545Q with CYLD, TBC1D17 and optineurin:

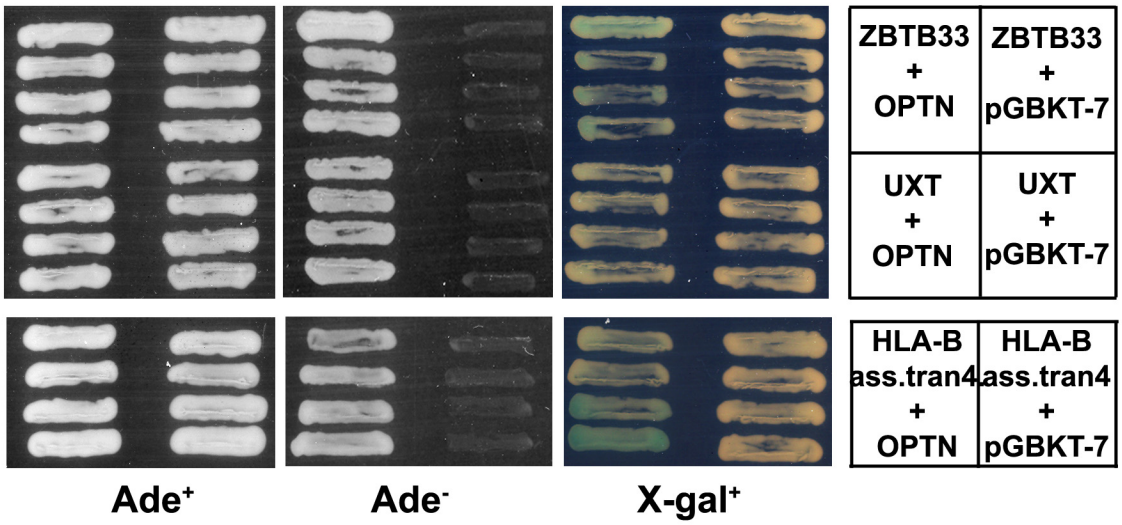

Figure 4.5: Interaction of optineurin with ZBTB33, UXT and HLA-B associated transcript 4.

ZBTB33, HLA-B associated transcript 4 and UXT were the weak interacting partners obtained after screening and re-interaction studies. pGBKT-7 represents empty Gal4 DNA-binding domain containing yeast two hybrid expression vector.

The three proteins mentioned above are the strongest optineurin interacting partners. E50K or R545Q mutant was co-transformed with either CYLD or OPTN or TBC1D17. Wild type optineurin interaction with each of the three positives also was repeated as a positive control and also for a comparison of the mutant's interaction. Interaction studies with E50K and R545Q revealed that these two mutants do not show any alteration in interaction with the three interacting partners mentioned. The two mutants show good growth on SP plate and equally good colour on X-gal plate similar to wild type optineurin (Figure 4.6 A, B &C).

4.3.3.2 Interaction of optineurin mutants with

a. IK-cytokine

To understand whether optineurin mutants would show any alteration in interaction with IK-cytokine, yeast two-hybrid assay was done between IK-cytokine and wild type optineurin or its mutants. R545Q, H26D did not show any alteration in interaction with the IK. While E50K showed weak interaction with IK-cytokine, H486R showed very weak interaction as observed by less growth on SP plate and weak colour on X-gal plate (Figure 4.7A)

b. HIBADH

In the case of HIBADH, E50K again shows very weak interaction as shown by less colour intensity on X-gal plate and H486R does not interact at all with HIBADH. R545Q and H26D behave like wild type optineurin (Figure 4.7B)

c. UXT

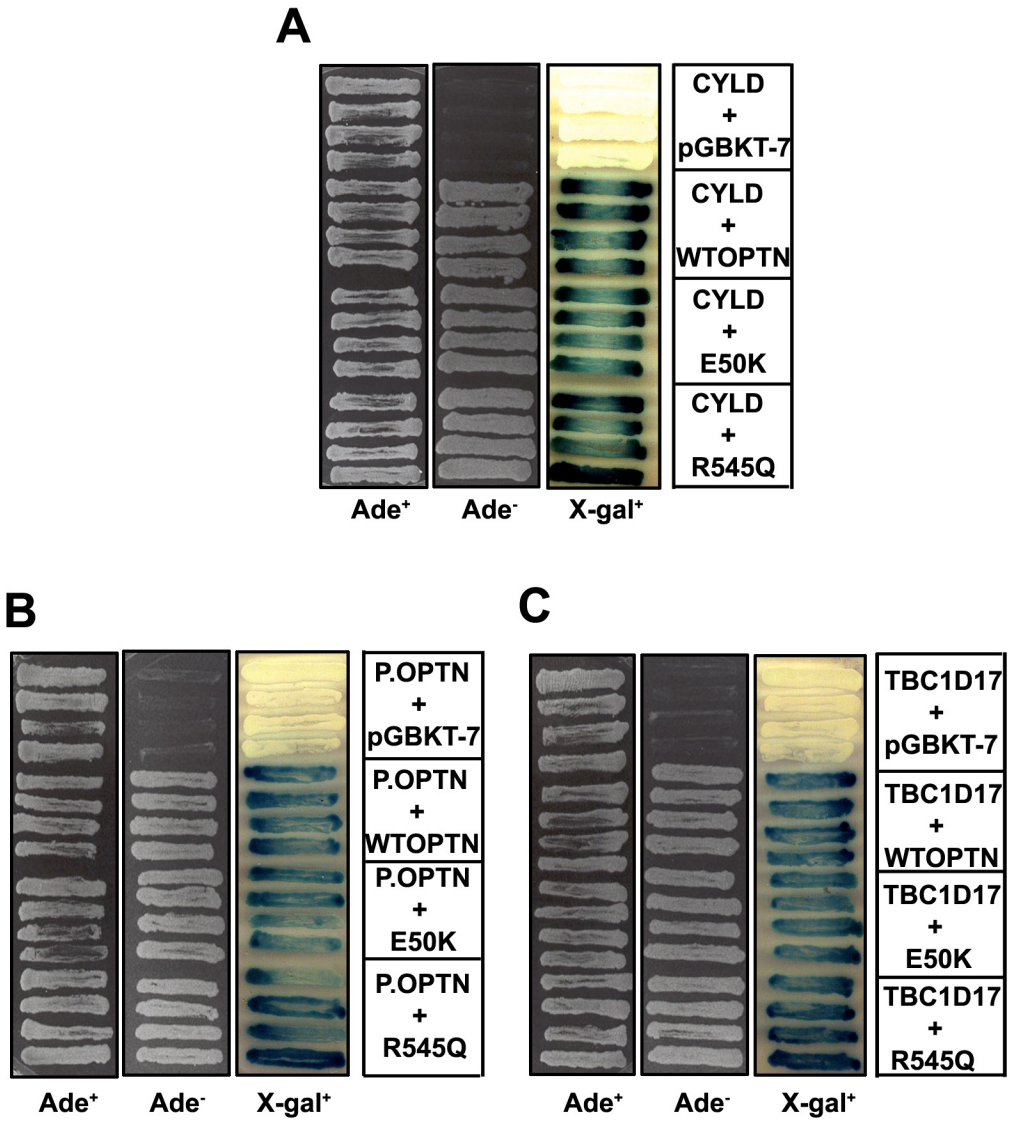

Figure 4.6: Interaction of optineurin mutants with CYLD, partial optineurin and TBC1D17.

Yeast two-hybrid analysis was performed between optineurin mutants, E50K or R545Q and CYLD(A) or optineurin(B) or TBC1D17(C). Optineurin mutants equally interact with the yeast two-hybrid positives like wild type and do not show any alteration in interaction. Ade^+, Ade^- or $X\text{-}gal^+$ are yeast media plates showing interaction between cotransformants. pGBKT-7 represents empty vector used as negative control. Wild type optineurin was used as a positive control for yeast interaction.

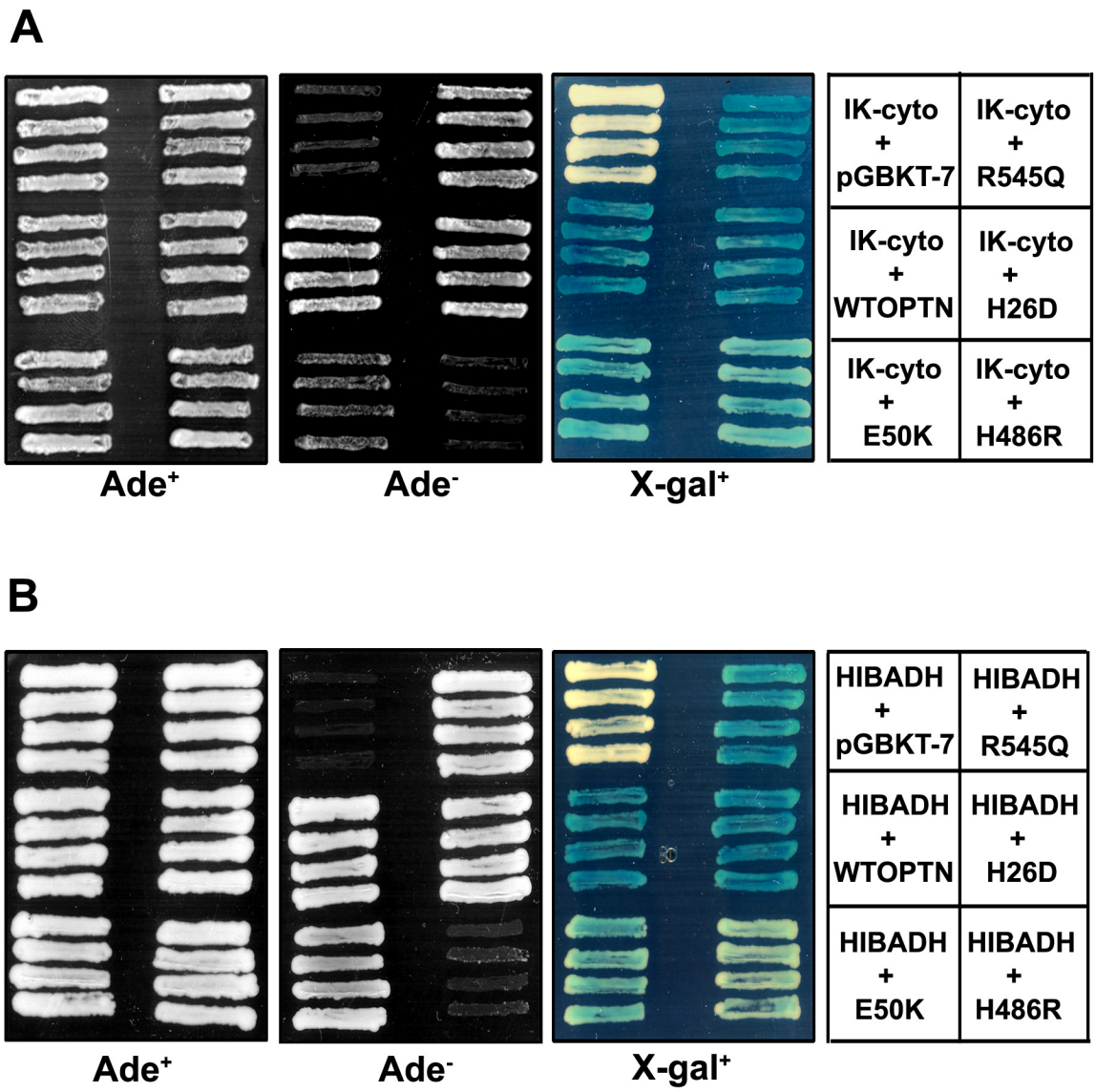

Figure 4.7: Interaction of optineurin mutants with IK-cytokine and HIBADH.

(A) Yeast two-hybrid analysis was performed between optineurin mutants and IK-cytokine. While H486R showed very weak interaction as shown on ade$^-$ plate, E50K showed weaker interaction compared to that of wild type. Other mutants behaved like wild type optineurin.

(B) Yeast two-hybrid analysis was performed between optineurin mutants and HIBADH. While H486R showed very weak or no interaction as shown on ade$^-$ plate, E50K showed weaker interaction compared to that of wild type (X-gal$^+$). Other mutants behave like wild type optineurin.

To check for the interaction status between UXT and mutants of optineurin, yeast two-hybrid assay was experimented between UXT and OPTN mutants. Both E50K and H486R showed weak interaction with UXT compared to wild type optineurin as shown by less growth on selection plate and less colour on X-gal plate. Here again, R545Q and H26D did not show any alteration in interaction with UXT (Figure 4.8A).

d. ZBTB33

To check for optineurin mutants' interaction with ZBTB33, yeast two hybrid interaction was done between ZBTB33 and optineurin or its mutants. We observed that H486R does not interact with ZBTB33 while E50K and other mutants showed interaction (Figure 4.8B).

e. HLA-B associated transcript 4 (BAT4)

All the mutants of optineurin interact equally well like wild type optineurin with HLA-B associated transcript 4 (Figure 4.9), shown by equal growth on SP plate.

4.4 Discussion

Although the gene encoding optineurin (FIP-2) was identified almost a decade ago (Li *et al*., 1998 & Rezaie *et al*., 2002), the normal function of the protein and the precise mechanisms by which mutations in optineurin cause glaucoma remains a subject of intense inquiry. It is speculated that optineurin has a neuroprotective function, but there is no clear cut evidence to show it. To understand the role of optineurin, it would be advantageous if we know its interacting partners, because the identity of the interacting proteins may provide

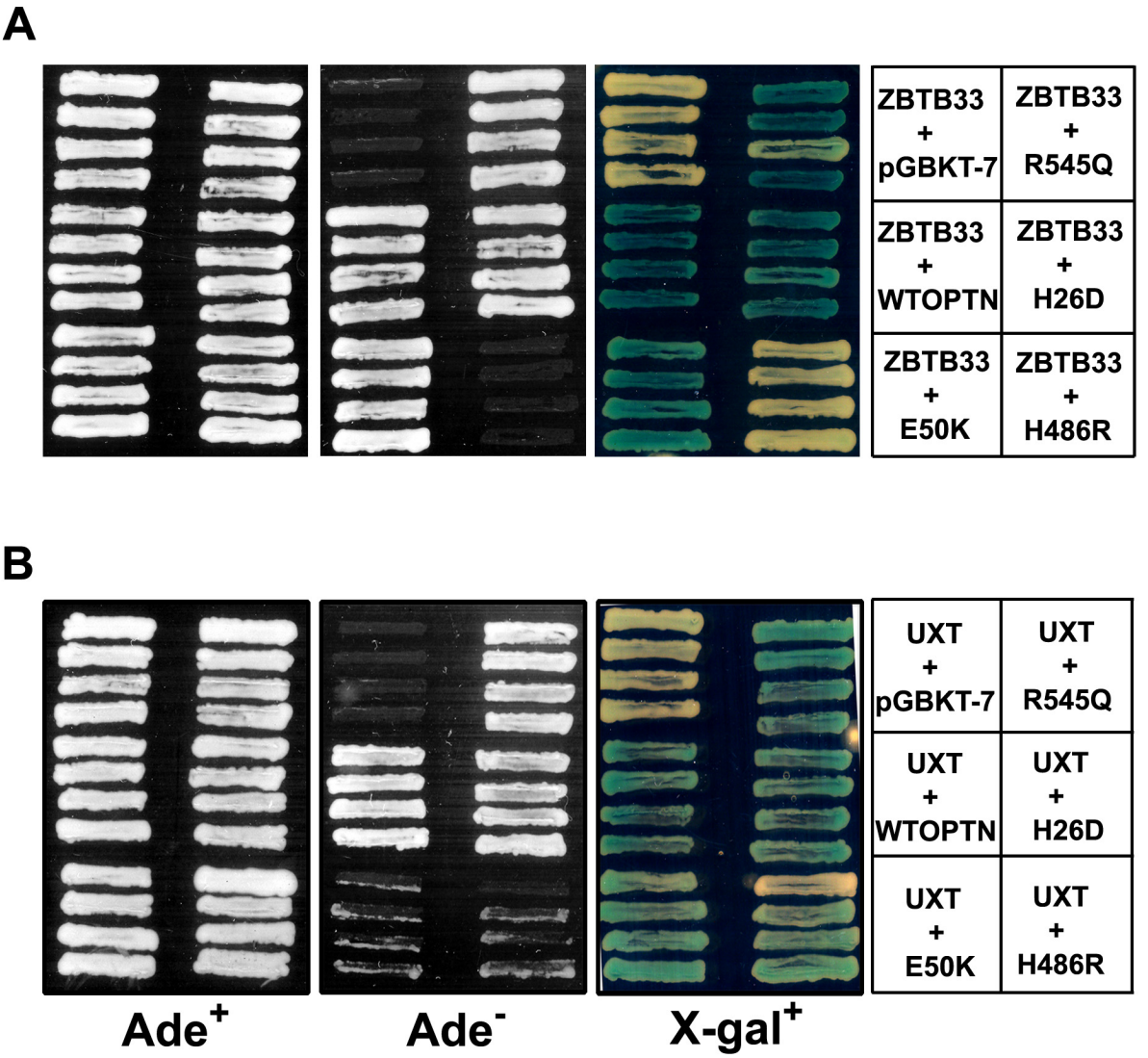

Figure 4.8: Interaction of optineurin mutants with ZBTB33 and UXT.

(A) Yeast two-hybrid analysis was performed between optineurin mutants and ZBTB33. H486R did not show interaction with ZBTB33. Other mutants behaved like wild type optineurin.

(B) Yeast two-hybrid analysis was performed between optineurin mutants and UXT. Both E50K and H486R showed partial interaction with UXT as shown on ade$^-$ plate, Other mutants behaved like wild type optineurin.

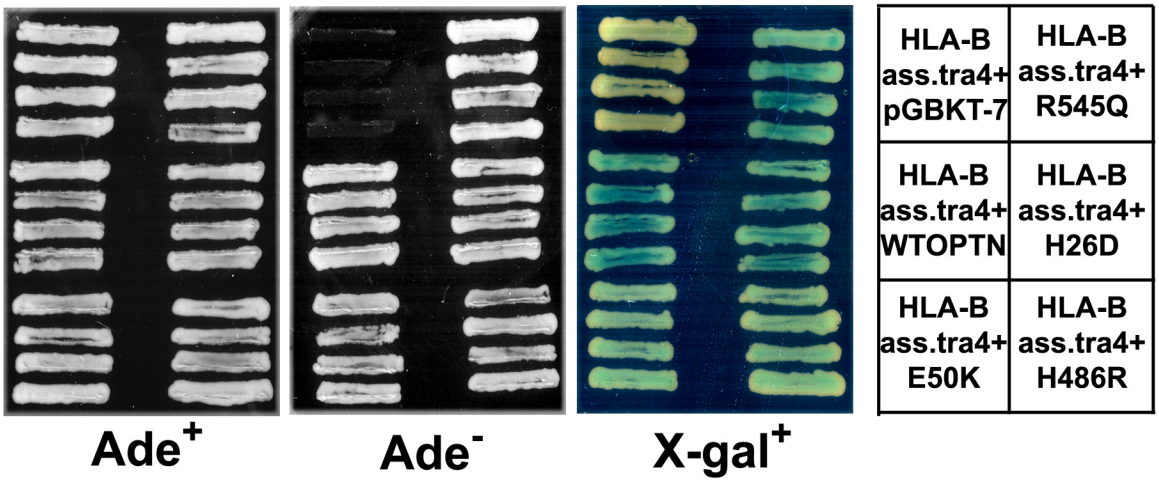

Figure 4.9: Interaction of optineurin mutants with HLA-B associated transcript 4.

Yeast two-hybrid analysis was performed between optineurin mutants and HLA-B associated transcript. All the mutants showed good interaction with the protein and did now show much alteration in interaction compared to that of wild type optineurin.

clues about the possible function of optineurin. Hence, to identify novel interacting partners of optineurin, yeast based two-hybrid screening was employed. Although initially we got a set of 25 potential interactors, subsequent re-interaction studies resulted in a total of 10 positive clones representing 9 different genes. The set of optineurin interacting partners and the degree of interaction with OPTN are listed in Table 4.1.

4.4.1 Optineurin interacts with diverse cellular proteins

The interacting partners fall under different categories based on their functions.

1. Proteins involved in NF-κB signaling pathway (CYLD, A20 & UXT).
2. Protein involved in vesicular trafficking (TBC1D17)
3. Proteins having a role in immunity (IK-cytokine, BAT4).
4. Other proteins- HIBADH & ZBTB33.

4.4.1.1 Optineurin interacts with three of the NF-κB regulators

The yeast two-hybrid screening showed that three of the optineurin interacting partners are NF-κB regulators. Among them, CYLD and A20, which were observed as strong positives, are negative regulators and UXT, a weak interacting partner of optineurin, is a positive regulator of NF-κB. NEMO, a regulatory subunit of IKK complex which plays a central role in NF-κB activation is known to interact with CYLD as shown by yeast two-hybrid analysis and co-immunoprecipitation experiments (Trompouki *et al.,* 2003); our study here shows that optineurin which has substantial amount of amino acid similarity with NEMO (53% similarity) (Schwamborn *et al*., 2000) also interacts with CYLD. But earlier reports show that optineurin has no role in TNFα- induced NF-κB activation

pathway and it stays in a high molecular weight complex different from IKK complex and is not associated with IκBα kinase activity. Also optineurin cannot reconstitute the NEMO deficient cell line (Schwamborn *et al*., 2000). But recent evidences suggest that optineurin does have a role in NF-κB regulation.

Overexpression of optineurin inhibits TNF-α induced NF-κB activation (Zhu *et al*., 2007). NEMO has a domain which can bind to K63-linked polyUb chains and this interaction facilitates recruitment of IKK complex to K63-pUb-RIP (Receptor Interacting Protein) in response to TNF-α. This interaction is necessary for the downstream NF-κB activation. The K63-polyUb-binding region of NEMO is conserved in optineurin and hence optineurin also binds to K63-linked polyUb-chains *in vitro* and to K63-poly Ub-RIP in TNF-α stimulated cells. Optineurin competitively antagonizes binding of NEMO to polyUb-RIP which results in inhibition of NF-κB activation by optineurin. A mutation in the ubiquitin binding region of optineurin, D474N (equivalent to D311N in NEMO) fails to do so. It can also be supported by earlier report that pre-treatment of cells with TNF-α upregulates optineurin mRNA and protein levels (Schwamborn *et al*., 2000), and it is this treatment time point that has been shown to reduce subsequent TNF-α induced NF-κB activation (Laegreid *et al*., 1995).

TBK1 is another member of IκB kinase (IKK) superfamily of protein kinases and is most similar to IKKε, with which it shares 73% amino acid similarity. TBK1 (TRAF- associated NF-κB activator (TANK)-binding kinase-1), an IKK-related kinase was recently shown to interact with optineurin. It is speculated that one function of optineurin is to recruit TBK1 to the K63-polyUb-RIP in response to TNF-α or other K63-polyUb chains in response to various

agonists. A striking observation here is that a well known mutant of optineurin, E50K binds much more strongly to TBK1 than optineurin (Morton *et al*., 2008). However, the functional significance of this enhanced interaction was not shown.

Based on the interactions obtained by us and observations made by others, a few speculations can be made about the functional importance of optineurin interaction with CYLD and A20. CYLD interacts with NEMO and TRAF2 and regulates disassembly of K63-linked polyubiquitin chains from these proteins, leading to inhibition of TNF-α induced NF-κB activation (Kovalenko *et al*., 2003). A20 interacts with RIP and sequentially deubiquitinates (K63 linked Ubs) and ubiquitinates (K48-linked polyUbs) leading to its degradation, thereby leading to NF-κB inhibition (Wertz *et al.,* 2004). A20 also binds to TRAF2, NEMO and ABIN-1 and-2 (Song *et al*., 1996; Zhang *et al*., 2000; Huffel *et al*., 2001; Heyninck *et al.*, 2005); ABIN-1 and-2 are A20-binding inhibitors of NF-κB. Both CYLD and A20 act upstream of NEMO and inhibit activation of NF-κB signaling. A common feature between optineurin and NEMO is that they have ubiquitin binding domain (UBD) like ABIN proteins, ABIN-1 and -2. (Wagner et.al., 2008). Optineurin has a UBD at amino acid position 424-509 through which it binds polyUb-RIP. Since, ABIN-1 which also has UBD, is known to physically interact A20 to polyubiquitinated NEMO and deubiquitinate it (Mauro *et al.,* 2006) leading to inhibition of NF-κB activity, it can be speculated that optineurin might provide a platform or acts like an adaptor protein for A20 to perform the ubiquitination and deubiquitination activities on RIP. This is only an assumption and needs further investigations to confirm our hypothesis. This hypothesis might be true for CYLD also, where optineurin might help in recruiting CYLD to polyubiquitinated proteins whereby CYLD associates with the complex of optineurin and polyubiquitinated

proteins (such as RIP) and deubiquitinates it. UXT is a molecule which interacts with NF-κB in the nucleus and positively regulates it (Sun *et al*., 2006), moreover it is a centrosomal protein and also plays a key role in cell viability (Zhao *et al*., 2005). But to achieve a clear picture of the functional role of optineurin in binding to UXT, a further investigation is needed.

Optineurin as discussed earlier is a candidate gene for normal tension glaucoma, and the importance of NF-κB in the pathogenesis of glaucoma is further emphasized by an investigation with mice deficient in *NF-κB p50* gene which showed optic neuropathy in the absence of IOP elevation (Takahashi *et al*., 2007). An autoimmune response which might interfere with long term survival of RGCs is speculated to be one of the reasons for optic neuropathy in p50-deficient mice.

4.4.1.2 Interaction of optineurin with proteins involved in membrane trafficking

The second category of optineurin interacting protein includes the one which has a role in vesicular trafficking, viz., TBC1D17 or FLJ12168 (Rab-GAP). Two other optineurin-interacting proteins, Rab8 and huntingtin are known to be involved in vesicular trafficking (Hattula and Peranen, 2000; Sahlender *et al*., 2005). But how TBC1D17 and optineurin together might play a role is not understood. Optineurin might be playing a crucial role during the TBC1D17 mediated activation of its Rab-GTPase. It is already known that optineurin interacts with Rab8, a GTPase protein involved in vesicular trafficking. In the case of Rab8, the Rab-GAP is unknown. One interesting thing would be to see if

TBC1D17 is the concerned GAP of Rab8. Also optineurin's interaction with Rab5 and Rab21 (TBC1D17 specific Rab-GTPases) can be studied.

4.4.1.3 Oligomerization of optineurin

Optineurin interacts with optineurin itself and this suggests that the protein oligomerizes on itself though the degree of oligomerization is not known. Interaction of E50K and R545Q mutants with optineurin suggests that these mutants are not defective in interacting with optineurin. Interaction of E50K with optineurin raises the possibility that E50K might function as a dominant negative to disrupt the cytoprotective function of normal optineurin. However, this does not rule out the possibility that E50K is a dominant gain of function mutation.

4.4.1.4 Interaction of optineurin with proteins involved in immune response

IK-cytokine and BAT4 are the two immunity related proteins which were obtained as optineurin interacting proteins. There is no direct or indirect evidence of the involvement of optineurin in immunity and none of the interacting partners reported till date have a role in immune related functions. There have been suggestions that in glaucoma, particularly, where non-IOP dependent damage to RGC occurs there is a sign of immune dysfunction (Weinreb *et al*., 2004). Moreover, astrocytes of glaucoma patients express MHC-II complexes indicating that there might be some communication between astrocytes and immune system (Flammer *et al*., 2007). There is a severe upregulation of autoantibodies against ocular antigens in the serum of glaucoma patients (Romano *et al*., 1995; Tezel and Wax, 2000b; Grus *et al*., 2006). Cop-I, which is used as a immunosuppressive drug in patients with autoimmune disease, multiple sclerosis has been successfully used as a vaccination against glutamate induced

neurotoxicity (Schori *et al*., 2001). Autoimmune response interfering with the long term survival of RGC in p50-deficient mice was mentioned earlier (Takahashi *et al*., 2007). Moreover, the antibody production reported here has been showed earlier in glaucoma patients suggesting the pathological relevance of autoimmunity in RGC degeneration of glaucoma. Our results provide the first evidence that optineurin, a protein involved in normal tension glaucoma, interacts with proteins having roles in immune response, viz., IK-cytokine and BAT4, but further functional significance of this interaction needs to be explored. Altered interaction of H486R mutant with IK cytokine leads to us to suggest that H486R mutant may induce glaucoma by an indirect mechanism involving immune dysfunction.

4.4.1.5 Optineurin interacts with mitochondrial protein

HIBADH is a mitochondrial enzyme involved in valine oxidation. There is not much functional characterization of the protein and the functional significance of its interaction with optineurin has to be explored closely. However, mitochondrial dysfunction has been linked with glaucoma, where patients with POAG have mitochondrial abnormalities (Abu-Amero *et al*., 2006). Moreover patients with POAG also have mitochondrial complex I defect causing release of ROS and finally leading degeneration of trabecular meshwork (He *et al*., 2008). Since H486R mutant of optineurin shows no interaction with HIBADH, it is likely that this mutant might contribute to mitochondrial dysfunction.

4.4.2 Behaviour of optineurin mutants with optineurin interacting partners

The interactions of the optineurin mutants with Y2H partners are tabulated in Table 4.2. E50K and R545Q did not show any variation in interaction with

three of the optineurin interacting partners, CYLD, OPTN and TBC1D17, showing that these point mutations do not have any affect on the interactions studied. But when we have conducted experiments with few other interacting partners, we got interesting results. We observed that E50K shows partial interaction with IK-cytokine and HIBADH as shown by less growth on selection plate and less colour on X-gal plate. H486R does not show interaction with HIBADH and ZBTB33 at all and shows very weak interaction with IK-cytokine. In the case of interaction with UXT, a positive regulator of NF-kB, both E50K and H486R showed weak interaction when compared to that of wild type optineurin. Other mutants H26D and R545Q did not show any alteration in interaction with any of the yeast two-hybrid positives tested.

Overall, the results presented in this chapter provide a basis for exploring the role of optineurin in diverse cellular functions. It would be important to confirm the interactions by co-immunoprecipitation and co-localization experiments. The interaction of optineurin with two of the interacting partners, CYLD and TBC1D17 has been confirmed by co-immunoprecipitation in our laboratory. These optineurin interacting partners along with chromosomal locations and accession numbers are listed in Table 4.3.

4.4.3 Are TBC1D17 and IK-cytokine candidate genes for glaucoma?

One interesting fact is that, two of the proteins, viz., TBC1D17 and IK-cytokine lie in the same region of known glaucoma loci. One of the glaucoma loci is positioned at 19q12-14 (Wiggs *et al*., 2000) and TBC1D17 lies on the chromosomal position 19q13.33 which overlaps with the above mentioned glaucoma locus. In the case of IK-cytokine, the position of the gene is 5q22-23

(Assier *et al*., 1999) and another glaucoma locus at 5q22.1 is at this position implying that these genes might be responsible for the disease. So, it would be worthwhile to screen the glaucoma patients for mutations in these two genes.

4.5 Summary and Conclusions

1. **Eight novel interacting partners of optineurin are identified.**
2. **Three of the optineurin interacting partners are NF-kB regulators, emphasizing the importance of optineurin in this pathway.**
3. **Two of the optineurin interacting partners (IK-cytokine and BAT4) are involved in immune response, suggesting a role for optineurin in immune response. Interaction with IK-cytokine might be relevant for glaucoma because H486R and E50K mutants show altered interaction with IK-cytokine.**
4. **Two of the interacting partners, viz., TBC1D17 and IK-cytokine, lie in the region of glaucoma loci and hence there exists a possibility that these genes might be causative genes for the disease.**
5. **E50K and H486R mutations show altered interaction with some of the optineurin interacting partners suggesting the relevance of these interactions for glaucoma.**

Interaction with various proteins suggests that optineurin is a multifunctional protein which is likely to be involved in NF-κB regulation, vesicular trafficking, immune response and transcriptional regulation.

Table 4.1

Optineurin interacting proteins obtained by Y2H assay

Name	WT.OPTN		No. of clones	Function
	Ade$^-$	β-gal		
CYLD	+++	+++	1	Negative regulator of NF-κB
TBC1D17	+++	+++	1	Rab-GAP member
OPTN	+++	+++	2	Neuroprotective function?
A20	++	++	1	Negative regulator of NF-κB
IK-cyto	++	++	1	Down regulator of HLA-II
HIBADH	++	++	1	Involved in valine metabolism
ZBTB33	+	+	1	Cell growth & development
UXT	+	+	1	Positive regulator of NF-κB
HLA-B associated transcript 4	+	+	1	Involved in immunity

+++ strong interaction **++** good interaction **+** weak interaction

Table 4.2 Interaction of optineurin mutants with the wild type OPTN interacting partners (comparison of intensities is with wild type)

Bait / Prey	E50K		R545Q		H26D		H486R	
	Ade$^-$	β-gal	Ade$^-$	β-gal	Ade$^-$	β-gal	Ade$^-$	β-gal
CYLD	+++	+++	+++	+++				
OPTN	+++	+++	+++	+++				
TBC1D17	+++	+++	+++	+++				
IK-cytokine	++	++	+++	+++	+++	+++	+	+
HIBADH	++	++	+++	+++	+++	+++	-	-
ZBTB33	+++	+++	+++	+++	+++	+++	-	-
UXT	+	++	+++	+++	+++	+++	+	++
HLA-B associated transcript 4	+++	+++	+++	+++	+++	+++	+++	+++

Here, +++ indicates equal interaction like wild type

++ indicates moderate interaction compared to wild type

+ indicates weak interaction compared to wild type

- indicates no interaction

Table 4.3: Interacting partners of optineurin, their chromosomal locations, accession numbers

Clone name& synonyms	Chromosomal location	Accession no.	CDS length
Optineurin FIP-2, NRP, HYPL	*10p15-14*	AF420371	1733 bp
CYLD EAC, CDMT, CYLD1, CYLDI, USPL2, HSPC057, FLJ20180	*16q12-q13*	BC012342	2861 bp
TBC1D17 (FLJ12168)	***19q13.33***	**NM_024682**	**1946 bp**
A20 (TNFAIP3) OTUD7C, TNFA1P2, MGC104522, MGC138687,	*6q23*	NM_006290	2372 bp
IK Cytokine (down regulator of HLA II) RED, CSA2, MGC59741	***5q22-q23***	**NM_006083**	**1673 bp**
Homo sapiens 3-hydroxyisobutyrate dehydrogenase (HIBADH) NS5ATP1, MGC40361	*7p15.2*	NM_152740	1010 bp
zinc finger and BTB domain containing 33 (ZBTB33) ZNF348, ZNF-kaiso	*Xq23*	NM_006777	2018 bp
Ubiquitously-expressed transcript (UXT) ART-27	*Xp11.23-p11.22*	NM_004182.2	473 bp
HLA-B associated transcript 4 D6S54E, GPANK1, ANKRD59, GPATCH10, BAT4	*6p21.3*	NM_033177	1070 bp

Proteins with loci indicated in **bold** are the ones which overlap with known glaucoma loci

Chapter 5

Attempt to Understand the Mechanism of E50K-Induced Cell Death in RGC-5 Cells

5.1 Introduction

Chapter 3 shows that E50K induces cell death selectively in retinal ganglion cells and not in other ocular and non-ocular cell lines tested. This cell death was shown to be, at least in part due to an increase in reactive oxygen species levels; treatment of E50K overexpressing cells with antioxidants rescued RGCs from E50K induced cell death. Now the next major query was what makes retinal ganglion cells specifically vulnerable under the conditions tested. Does that mean RGC-5 is defective in responding to oxidative stress caused by E50K? Moreover E50K mutant of optineurin uniquely forms large vesicular structures in the cytoplasm and none of the other mutants studied or wild type shows them.

The role of oxidative stress in glaucoma has been documented. It has been demonstrated *in vivo* in humans that oxidative damage to DNA is significantly higher in the trabecular meshwork (TM) cells of glaucoma patients (Izzotti *et al*., 2003). The possible pathogenic role of oxidative stress in POAG is further supported by the increased expression of the endothelial-leukocyte adhesion molecule (ELAM-1) in the TM of glaucoma patients but not in unaffected controls. ELAM-1 expression, which is controlled by the autocrine feedback mechanism of activation of IL-1 through NF-κB, is a complex mechanism for protecting against oxidative stress (Wang *et al*., 2001). Results described in chapter 3 are the first direct evidence of a mutant of glaucoma candidate gene generating ROS and causing cell death.

We have therefore attempted to understand the mechanism of E50K induced cell death using various approaches. The first attempt was to see if the RGC-5 cell line is defective in responding to oxidative stress. This was explored

by looking at the expression of various genes which are normally induced in response to oxidative stress. The fate of these genes on E50K overexpression was checked. We also checked whether E50K mutant shows any defect in interaction with Rab8, a molecule involved in vesicular trafficking and see if the transport of proteins like VSVG-GFP is hampered in the presence of E50K.

5.2 Results

5.2.1 Responsiveness of RGC-5 cells to oxidative stress and antioxidants.

Since we have observed that E50K specifically induces cell death of rat retinal ganglion cells and not the other cell lines tested (chapter 3), there remains a doubt whether the RGC-5 cell line is defective in responding to oxidative stress and antioxidant response. Hence, the effect of hydrogen peroxide (a well known ROS generator) and antioxidants NAC and Trolox was tested on the mRNA expression levels of various genes which are normally induced in response to oxidative stress, viz., PGC1α, HO-1 and MnSOD.

PGC1α (Peroxisome proliferator gamma induced coactivator-1 alpha) is a transcriptional coactivator and a potent stimulator of mitochondrial biogenesis and respiration. PGC1α gets co-induced along with other ROS-detoxifying enzymes in the presence of oxidative stress (St-Pierre *et al*., 2006). Moreover, it is required for the induction of many ROS-detoxifying enzymes like GPx1 and MnSOD.

Hemoxygenase-1 (HO-1) or HSP32 is the inducible isoform of heme oxygenase which catalyzes the NADPH, O_2 and cytochrome P450 reductase

dependent oxidation of heme to carbon monoxide, iron and billiverdin that is immediately reduced to bilirubin (Ryter *et al*., 2006; Lin *et al*., 2007).

RGC-5 cells were treated with H_2O_2 at concentrations of 0.1, 0.2, 0.4 & 1.0mM for 2 hours and at the end of 2 hours fresh DMEM without H_2O_2 was added and left for another 2 hours as recovery time. Later, RNA was prepared and 2μg of RNA was taken for RT-PCR and the mRNA levels of PGC1α, HO-1 and MnSOD were studied by semi-quantitative PCR (Figure 5.1). Table 5.1 shows the mRNA levels of the three genes on H_2O_2 treatment.

a) **PGC1α:** The mRNA levels of PGC1α showed increase with increasing concentration of H_2O_2 with maximum induction of 2.08 fold at 0.2mM and gradually decreasing at 0.4mM and 1.0mM.
b) **HO-1:** HO-1 also showed increased mRNA levels with increasing concentrations of H_2O_2 and maximum increase of 2.57 fold was seen at 0.2mM.
c) **MnSOD:** MnSOD showed only marginal increase with maximum of 1.5 fold at 1.0mM H_2O_2.

Table 5.1: mRNA levels of various oxidative stress response genes on H_2O_2 treatment

mRNA	Untreated	0.1mM	0.2mM	0.4mM	1mM
***PGC1α**	1.00	1.52	2.08	2	1.72
***HO-1**	1.00	1.74	2.57	1.96	0.83
***MnSOD**	1.00	1.18	1.08	1.24	1.15
*Actin mRNA levels were used as internal control and the numbers in the table indicate the relative intensity normalized to actin. The above figures are the average of two experiments.					

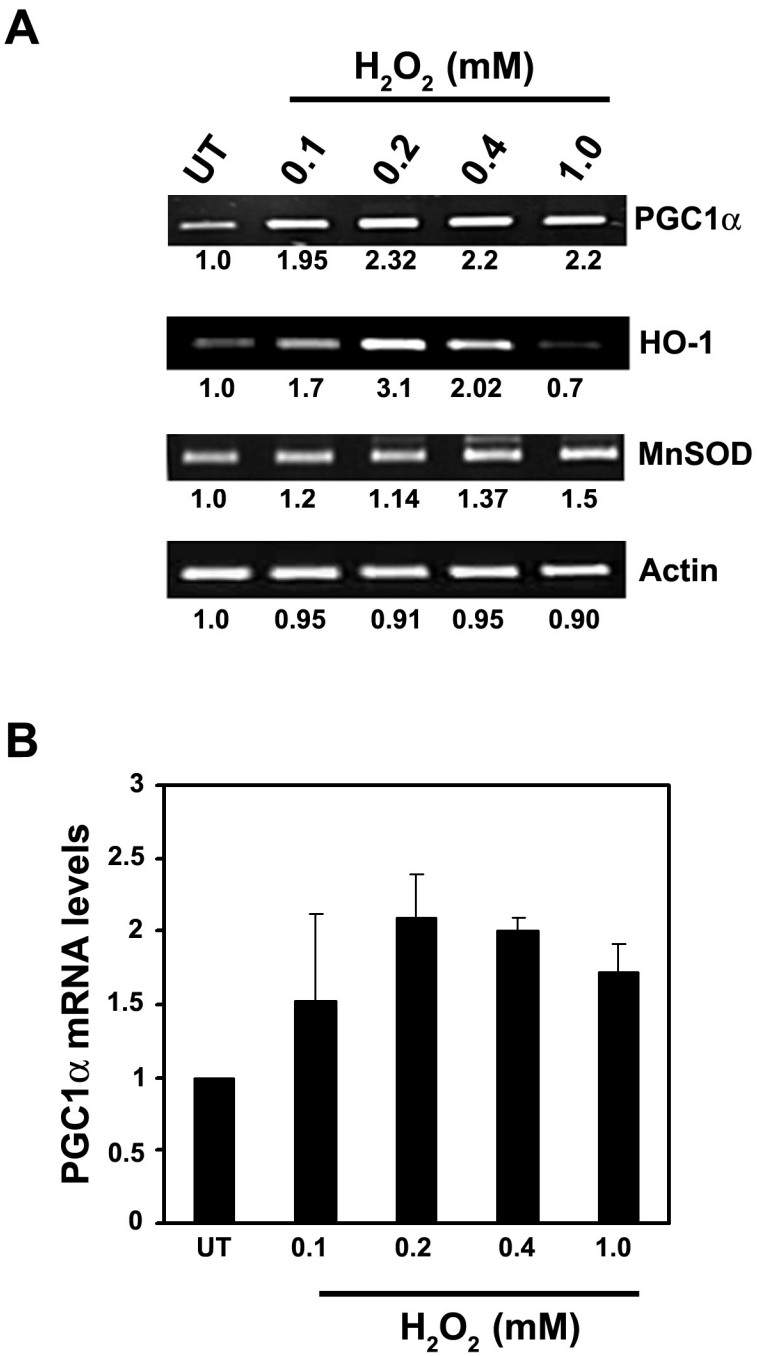

Figure 5.1: Effect of H_2O_2 treatment on mRNA levels of PGC1α, HO-1 and MnSOD in RGC-5 cell line.

(A) RGC-5 cells were treated with four different concentrations of H_2O_2 for 2 hours followed by 2 hours of recovery. Total RNA isolated was subjected to RT-PCR for PGC1α , HO-1 and MnSOD. Actin mRNA was used as an internal control. The numbers at the bottom of each panel indicate the relative intensity normalized to actin for PGC1α, HO-1 and MnSOD gene expression upon H_2O_2 treatment.

(B) Bar diagram representing the mRNA levels of PGC1α on H_2O_2 treatment in RGC-5 cells. The data represents average of two experiments.

For the effect of antioxidant treatments on these genes, RGC-5 cells were treated with two different antioxidants at two different concentrations. N-acetyl cysteine was used at 2.5 and 5.0 mM concentrations and Trolox was used at concentrations of 0.1 and 0.2 mM. The treatment time was 26 hours after which RNA was isolated and RT-PCR was done to check the mRNA levels of the three genes (Figure 5.2).

a) **PGC1-α:** Both NAC and Trolox show increased mRNA levels of PGC1α and the levels are high at higher concentration of antioxidants used.
b) **HO-1:** HO-1 also showed increased mRNA levels with increasing concentrations of NAC and Trolox.
c) **MnSOD:** Surprisingly MnSOD levels remained unaltered at the concentrations tried. Only marginal changes in mRNA levels were observed.

Table 5.2 mRNA levels of various oxidative stress response genes on antioxidant treatments

mRNA	Untreated	2.5mM NAC	5.0 mM NAC	0.1mM Trolox	0.2mM Trolox
***PGC1α**	1.00	1.51	2.07	1.47	2.17
***HO-1**	1.00	1.68	1.59	1.77	1.46
***MnSOD**	1.00	1.05	0.88	0.88	0.93
*Actin mRNA levels were used as internal control and the numbers in the table indicate the relative intensity normalized to actin. The above figures are the average of two experiments.					

5.2.2 E50K overexpression reduces PGC1α mRNA levels in RGC-5 cells.

Our earlier experiments showed that RGC-5 cell line responds to oxidative stress and antioxidant treatments. Next, the mRNA levels of these genes were

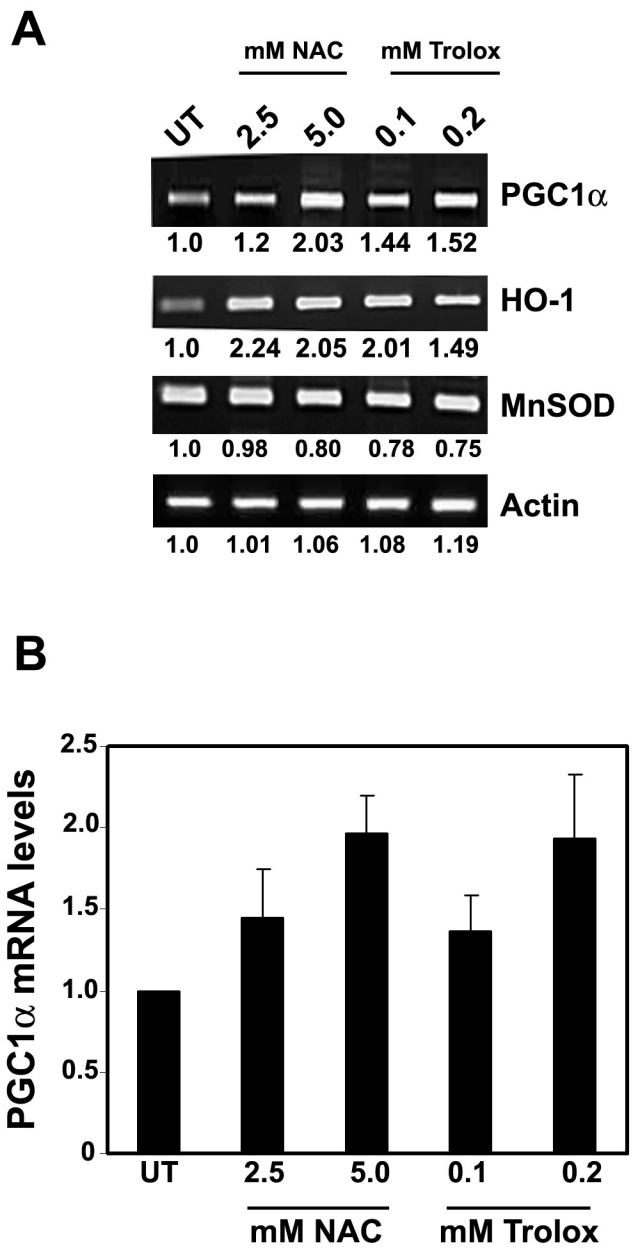

Figure 5.2: Effect of antioxidants treatment on mRNA levels of PGC1α, HO-1, MnSOD in RGC-5 cells.

(A) RGC-5 cells were treated with two different concentrations of NAC and Trolox for 26 hours. Total RNA isolated was subjected to RT-PCR for PGC1α , HO-1 and MnSOD. Actin mRNA was used as internal control. The numbers at the bottom of each panel indicate the relative intensity normalized to actin for PGC1α, HO-1 and MnSOD gene expression upon antioxidants treatment.

B) Bar diagram representing the mRNA levels of PGC1α on antioxidants treatment in RGC-5 cells. The data represents average of two experiments.

tested upon wild type (WT) optineurin and E50K overexpression. RGC-5 cells were infected with adenoviral constructs of optineurin and E50K for 30 hours. At the end of 30 hours, RNA isolation was done and 2 μg of RNA was taken to perform RT-PCR of PGC1α, HO-1 and MnSOD. Also optineurin levels were checked. E50K overexpression decreases PGC1α mRNA levels significantly by 25% whereas WT optineurin increases it by 15%. HO-1 levels were not affected by E50K over expression but WT increases the mRNA levels by 24%. MnSOD mRNA levels were not altered by either WT or E50K (Figure 5.3 and Table 5.3).

Table 5.3: mRNA levels of various oxidative stress response genes on WT and E50K expression in RGC-5 cell line

mRNA	Uninfected	Control	Wild type	E50K
*PGC1α	0.71	1.00	1.15	0.78
*HO-1	0.84	1.00	1.24	1.02
*MnSOD	1.23	1.00	1.05	1.01
*Actin mRNA levels were used as internal control and the numbers in the table indicate the relative intensity normalized to actin. The above figures are the average of two experiments except MnSOD which is from one experiment.				

5.2.3 E50K shows subtle alteration in interaction with Rab8

Optineurin interacts with several proteins and binding sites for these proteins map to different regions of optineurin. Since binding site for Rab8 is close to the E50K mutation, we examined the possibility that E50K mutation might alter interaction with Rab8. Yeast two-hybrid assay was done to check whether E50K shows alteration in interaction with Rab8.

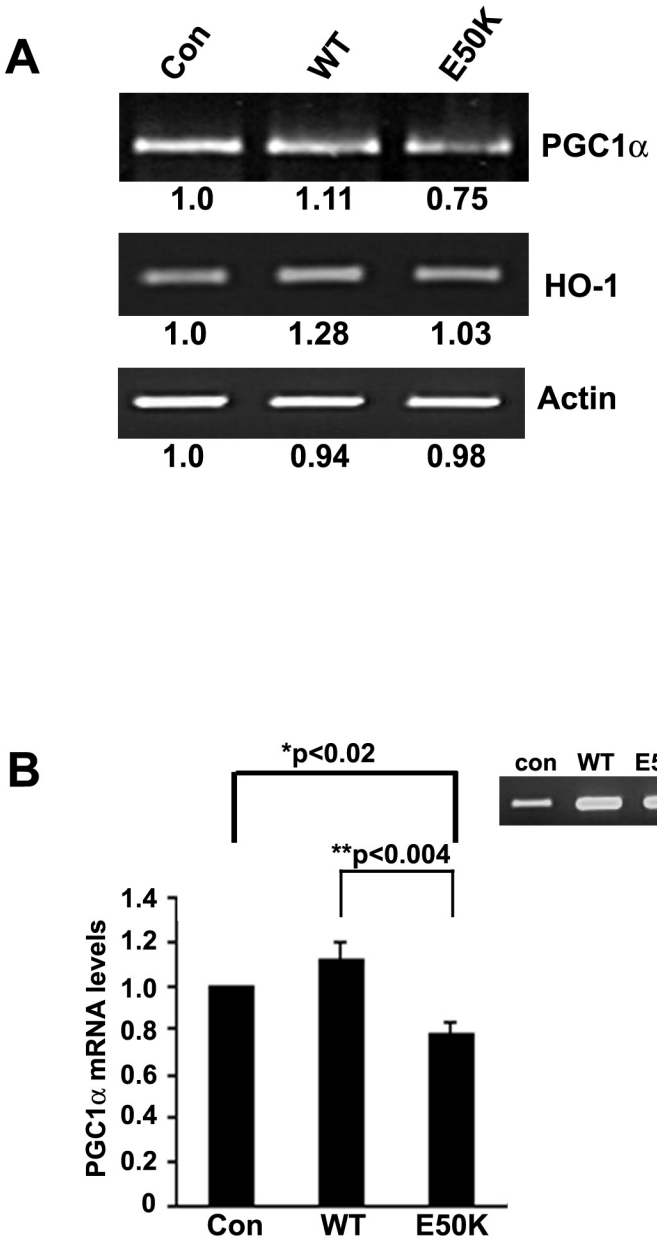

Figure 5.3: Effect of optineurin and E50K expression on PGC1α and HO-1 mRNA levels in RGC-5 cell line.

(A) RGC-5 cells were infected with control/ optineurin/ E50K adenoviral constructs and allowed to overexpress for 30 hours. Total RNA isolated was subjected to RT-PCR for PGC1α, HO-1 and OPTN. Actin mRNA was used as internal control. The numbers at the bottom of each panel indicate the relative intensity normalized to actin for PGC1α and HO-1 gene expression upon control /WT /E50K adenoviral infections.

(B) Bar diagram representing the changes in mRNA levels of PGC1α on wild type and E50K overexpression. Note that the optineurin mRNA levels are the same on WT and E50K infections.

For expression of Rab8 in yeast, the cDNA of Rab8, constitutively activated Rab8 (Q67L) and dominant negative Rab8 (T22N) were cloned in pGBKT-7 vector and the expression of the proteins was checked by western blot (Figure 5.4A). Yeast two-hybrid assay was performed by cotransforming Rab8/ Q67L/ T22N (in bait vector pGBKT-7) with optineurin or E50K (in pACT2) and interaction was checked by growth on selection plate and colour on X-gal plate. WT Rab8 showed interaction with WT optineurin as already known but not with the E50K mutant (Figure 5.4B). In contrast, both WT optineurin and E50K mutants interacted with activated Rab8 (Figure 5.5). Dominant negative Rab8 neither interacted with WT optineurin nor E50K mutant (Figure 5.6). The protein expressed by the control plasmid pACT2 did not show interaction with Rab8 or its mutants. The other mutants of optineurin, viz., H26D, H486R and risk-associated alteration R545Q showed good interaction with both WT Rab8 and activated Rab8 (Figure 5.4C, 5.5). Based on the results obtained in yeast two-hybrid assay, experiments were done to check for the co-localization in the mammalian cell line RGC-5. RGC-5 cells were cotransfected with optineurin/ E50K and Rab8/ activated Rab8. As expected, wild type optineurin colocalizes with Rab8 and activated Rab8 (Figure 5.7). In contrast to observations in yeast, E50K showed colocalization with both Rab8 and activated Rab8. But with activated Rab8 colocalization was much better than with Rab8 (Figure 5.7).

5.2.4 E50K does not interact with Rab11, another recycling endosome marker.

To test whether optineurin interaction with Rab8 is specific or seen with other Rab family members, yeast two-hybrid analysis was done between optineurin/ E50K and Rab11. Rab11 was selected for this purpose because it is

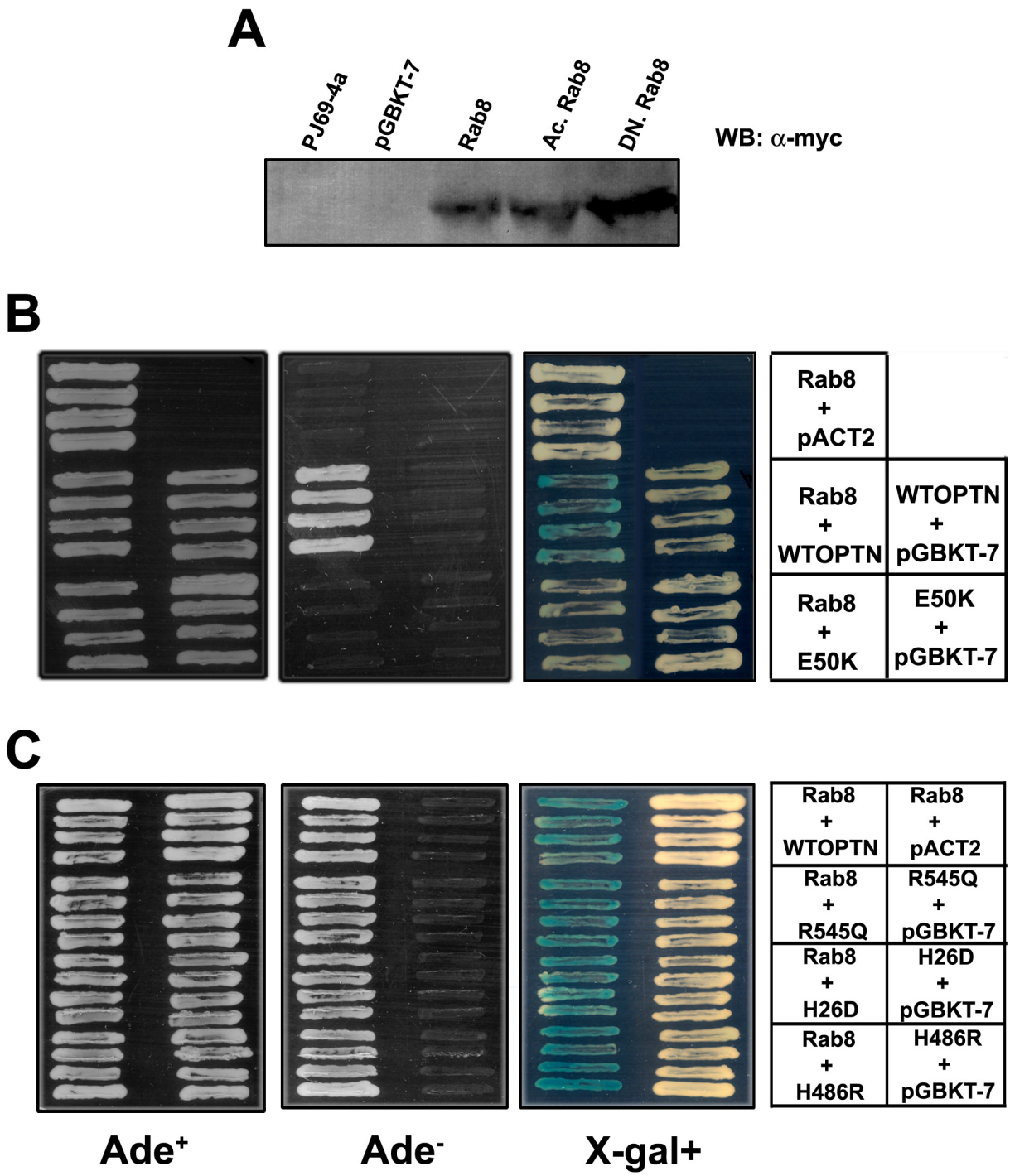

Figure 5.4: Interaction of WT OPTN and mutants with Rab8.

Yeast two-hybrid analysis was performed between human Rab8 and wild type optineurin or its mutants. Rab8 is full length human Rab8 (1-212 amino acids) fused with the DNA-BD of Gal4 in pGBKT-7. Optineurin is full length human OPTN (1-577 amino acids) fused with the DNA-AD of Gal4 in pACT2. Optineurin mutants were also contructed similar to wild type optineurin. pGBKT-7 and pACT2 are the empty Gal4 DNA- binding domain and Gal4 activation domain containing yeast two hybrid expression vectors respectively.

(A) Western blot showing expression of wild type Rab8 and its mutants activated Rab8 (Ac. Rab8) and dominant negative Rab8 (DN. Rab8) bait DNA-BD fusion proteins in yeast cell lysates.

(B) Wild type optineurin interacts with Rab8 but E50K mutant does not.

(C) Interaction of optineurin mutants, R545Q, H26D and H486R with Rab8.

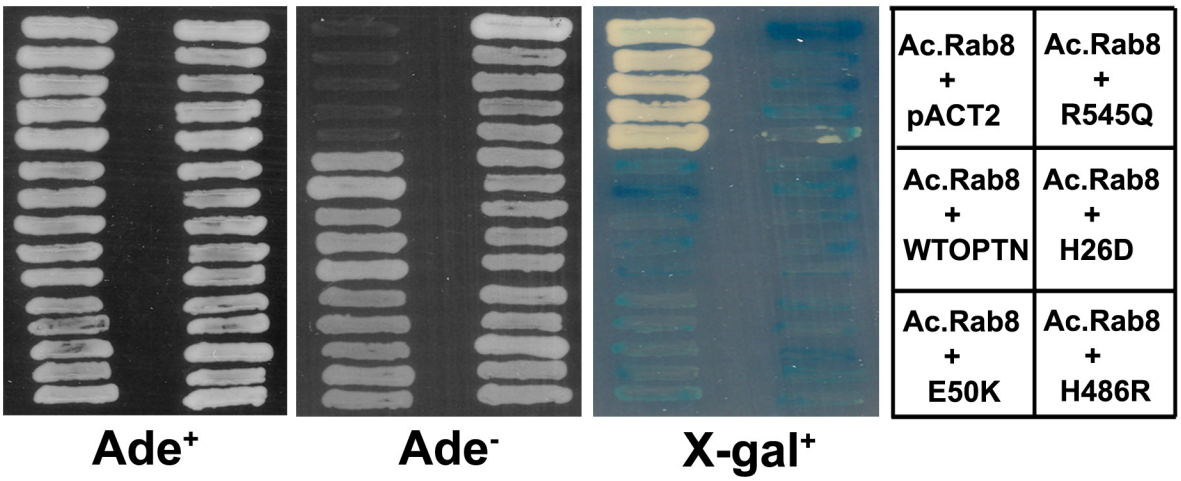

Figure 5.5: Interaction of optineurin and its mutants with activated Rab8.

Yeast two-hybrid analysis was performed between wild type optineurin or its mutants and activated Rab8. WT optineurin as well as all the mutants showed interaction with activated Rab8.

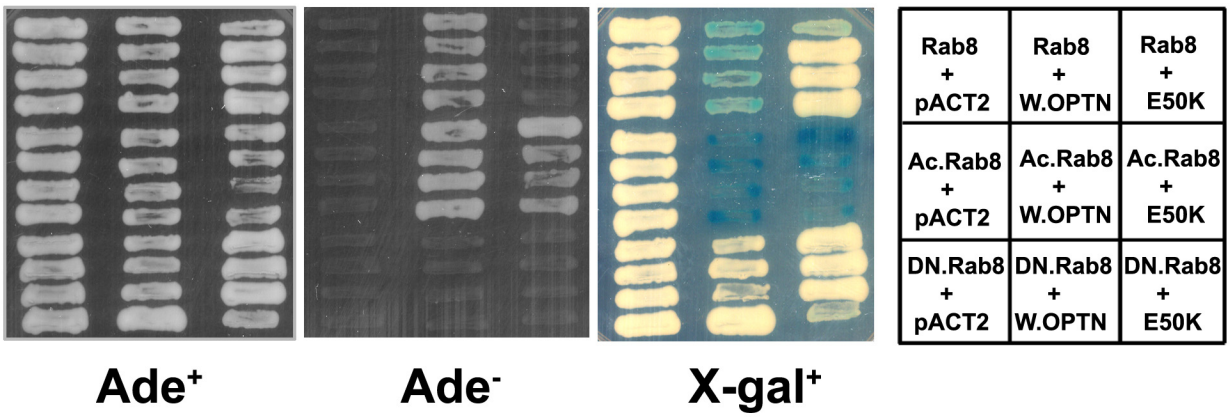

Figure 5.6: Comparison between optineurin and E50K interactions with various forms of Rab8.

Yeast two-hybrid analysis was performed between wild type optineurin or E50K and various forms of Rab8, wild type Rab8, activated Rab8 and dominant negative Rab8. Wild type optineurin interacts with wild type and activated Rab8 but not with dominant negative Rab8. E50K mutants shows interaction with activated Rab8 only and not with wild type and dominant negative Rab8.

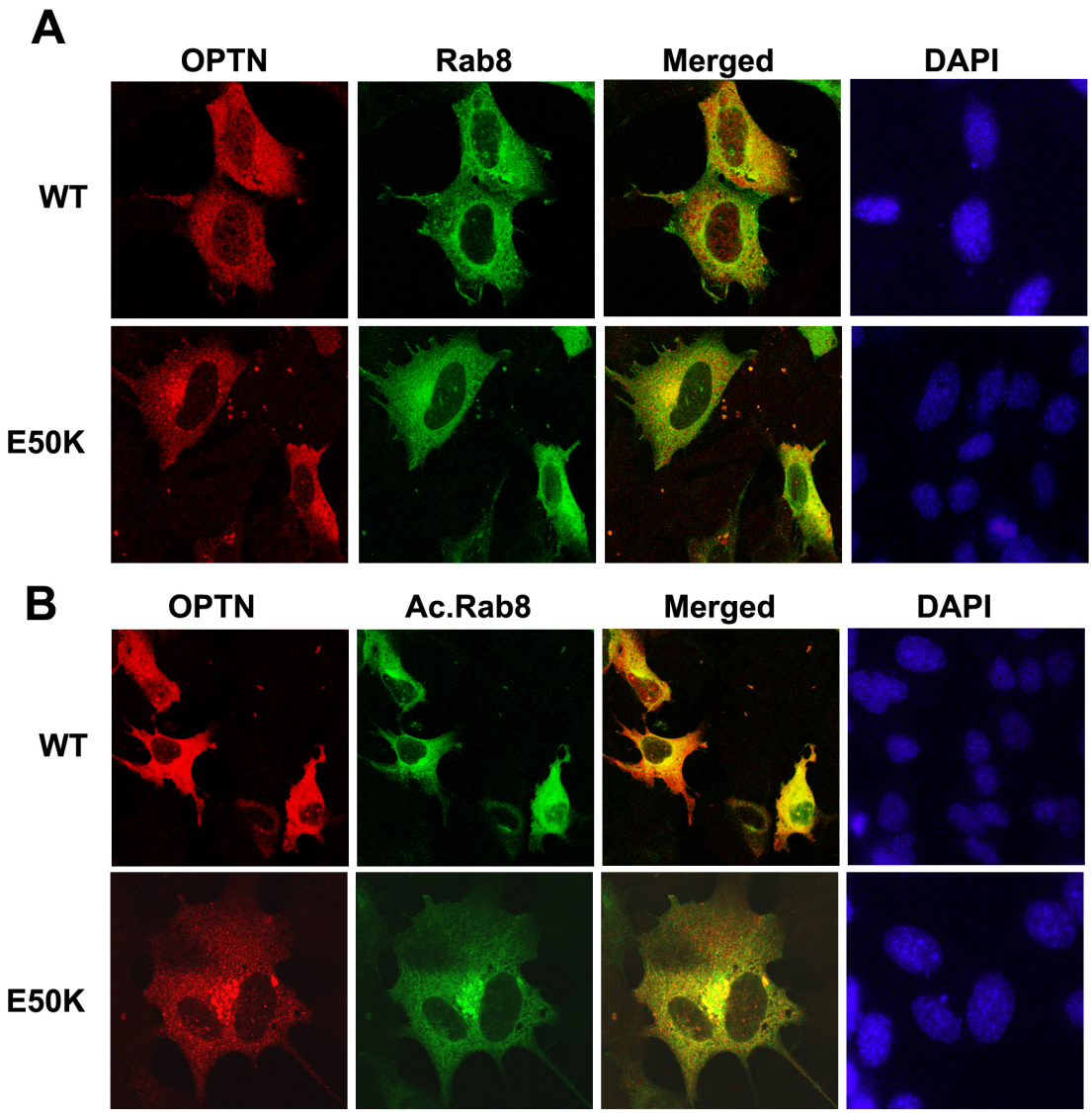

Figure 5.7: Colocalization of optineurin and E50K with wild type Rab8 and activated Rab8 in RGC-5 cell line.

(A) Wild type optineurin or E50K mutant and GFP-Rab8 are co-transfected in RGC-5 cell line and stained with anti-HA antibody. Confocal images show co-localization of optineurin/ E50K (red) with Rab8 (green) as shown by yellow colour in merged images.

(B) Wild type optineurin or E50K mutant and GFP- activated Rab8 are co-transfected in RGC-5 cell line and stained with anti-HA antibody. Confocal images show co-localization of optineurin/ E50K (red) with activated Rab8 (green) as shown by yellow colour in merged images.

present in recycling endosomes where Rab8 is also present. For this, Rab11 was cloned in pGBKT-7 vector and expression was checked by western blot using anti-myc antibody (Figure 5.8A). In yeast two-hybrid assay, we observed that neither wild type optineurin nor E50K mutant interacted with Rab11 (Figure 5.8B), suggesting that optineurin specifically interacts with Rab8 and not with Rab11.

5.2.5 Effect of E50K overexpression on VSVG-GFP transport to the plasma membrane

The thermosensitive mutant (VSVG-GFP-ts045) of G-protein of Vesicular Stomatitis Virus (VSVG) has been used to study anterograde biosynthetic vesicular protein transport from ER to Golgi and Golgi to plasma membrane. This membrane protein misfolds and is retained in the ER at 39.5° C (or higher), but upon a temperature shift to 32°C, or below, it can fold properly and as a synchronized wave it gets transported in forward direction towards ERGIC, Golgi complex and subsequently to the plasma membrane. In the presence of any other protein or inhibitor which can affect forward transport this transport is perturbed and leads to accumulation of VSVG-GFP in one of the compartments (Presley *et al*., 1997). We checked the effect of optineurin or particularly E50K expression on the trafficking of VSVG. Cos-1 cells were transfected with VSVG-GFP alone or cotransfected with optineurin or E50K mutant and VSVG-GFP and shifted to 40° C for 22 hours. A set of coverslips were fixed at the end of 22 hours using prewarmed formaldehyde (40°C). Another set of coverslips were shifted to 30°C for 2 hours and fixed. We observe that VSVG-GFP alone at 40°C shows majorly ER localization and also Golgi to some extent. But when shifted to 30°C,

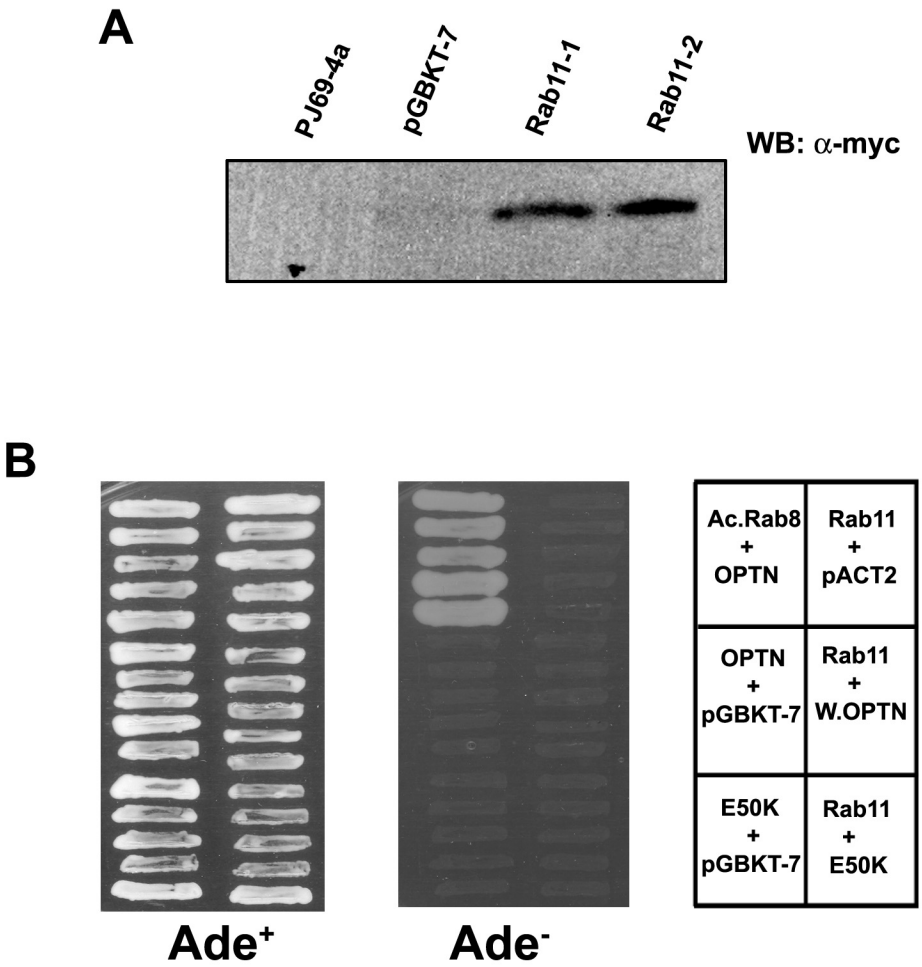

Figure 5.8: Interaction of Rab11 with optineurin and E50K.
(A) Western blot showing expression of Rab11 in DNA-BD pGBKT-7 bait vector. (B) Yeast two-hybrid analysis was performed between wild type optineurin or E50K and human Rab11. Rab11 did not interact with either WT OPTN or E50K mutant. Activated Rab8 interaction with WT OPTN was used as a positive control.

the protein moves completely to Golgi and subsequently plasma membrane (Figure 5.9). In the presence of wild type optineurin also the VSVG-GFP behaves in a similar way. But we observed that E50K mutant traps the VSVG protein in its vesicular structures in the cytoplasm. Here, even though protein movement is still there to membrane, a very obvious entrapment of VSVG protein in the E50K induced vesicular structures was seen (Figure 5.9). This explains that the mutant shows a subtle defect in transport of the protein to the membrane.

5.3 Discussion

Optineurin induces cell death selectively in retinal ganglion cells and not in other cell lines tested. Hence, there is a need to understand what makes retinal ganglion cells susceptible to undergo cell death in the presence of E50K. Since there is an increase in reactive oxygen species; the first striking thing is whether the cell line is unable to defend itself from ROS. Hence, we checked the response of the cell line to oxidative stress and antioxidant treatments. The effect of oxidative stress on the mRNA levels of genes coding for ROS- detoxifying proteins was investigated. PGC1α is a transcriptional coactivator and is a potent stimulator of mitochondrial biogenesis and respiration. PGC1α gets co-induced along with other ROS-detoxifying enzymes in the presence of oxidative stress (St-Pierre *et al*., 2006). Moreover, it is required for the induction of many ROS-detoxifying enzymes like GPx1 and MnSOD. It is also known that PGC1α shows ubiquitous expression; it is expressed in the retina and also in retinal ganglion cells though to a lesser extent (Braissant *et al*., 1996). Hence, an attempt was made to investigate the changes in mRNA levels, if any, on E50K overexpression.

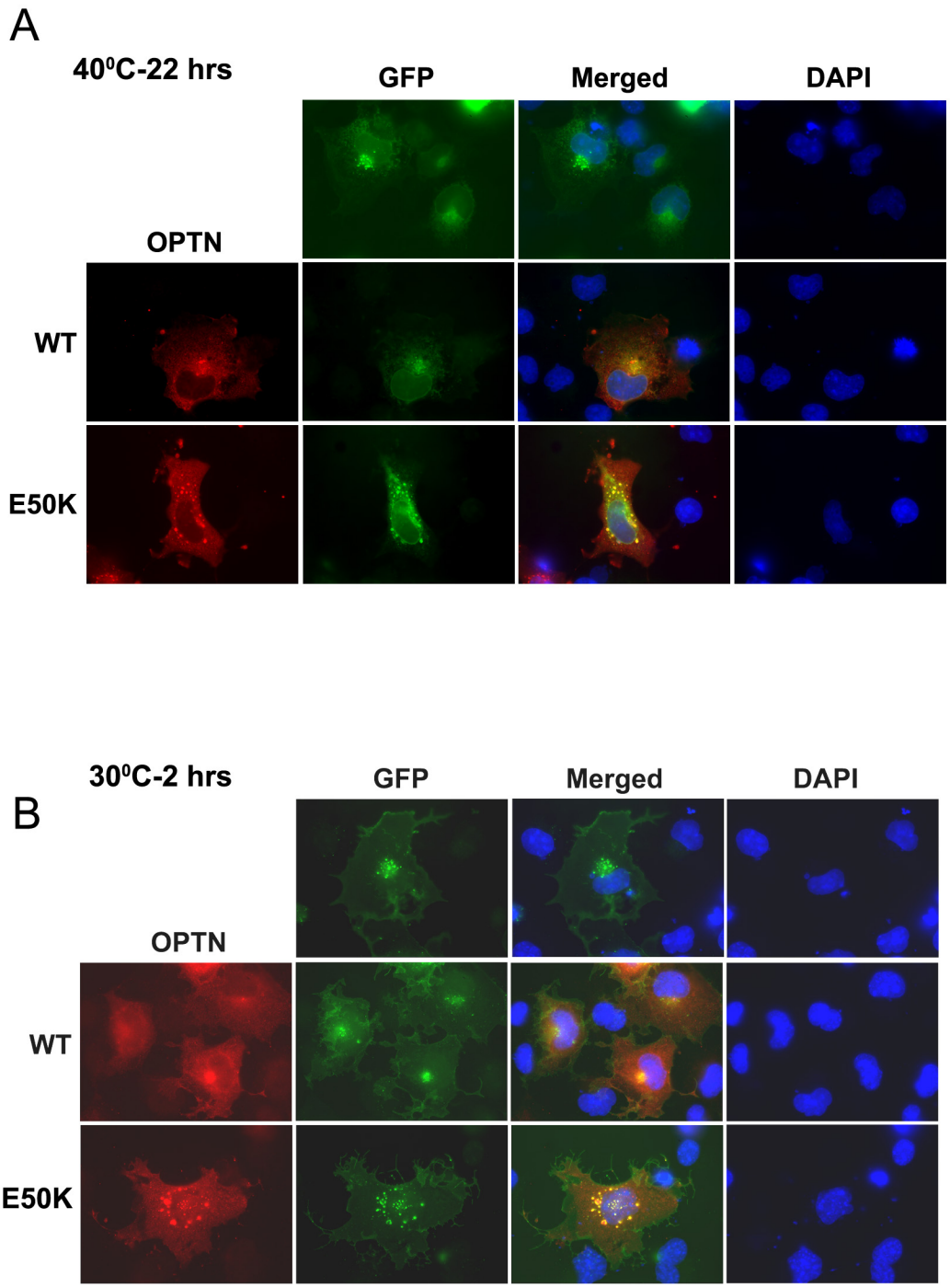

Figure 5.9: Effect of optineurin and E50K overexpression on VSVG-GFP transport to the plasma membrane.

VSVG-GFP alone or in combination with optineurin or E50K was transfected in Cos-1 cells. After 22 hours of incubation at 40°C (A), cells were shifted to 30°C for 2 hours (B) and the effect of OPTN/E50K expression upon transport of VSVG-GFP from ER to Golgi and membrane was observed. VSVG at 40°C showed ER localization and some amount in Golgi and upon shifting to 30°C it folded properly and transported to Golgi and membrane. Even in the presence of wild type OPTN it transported similarly as VSVG alone. But in the presence of E50K, some amount of protein got trapped in the E50K vesicular structures although major amount of protein still showed proper transport.

HO-1 is a phase-2 detoxification protein whose gene is commonly induced by agents and chemicals that cause oxidative stress (Ryter *et al*., 2006). H_2O_2, the most common ROS generator and TNF-α, IL-1 induce HO-1 mRNA levels. Note that TNF-α also induces optineurin mRNA levels. MnSOD is a mitochondrial superoxide dismutase which detoxifies superoxide anions. Our observation in chapter 3 that MnSOD reduces E50K induced cell death and ROS generation prompted us to investigate the impact of oxidative stress and E50K overexpression on mRNA levels of MnSOD. Our results suggest that the retinal ganglion cell line in general is not defective in responding to oxidative stress, because there was induction of mRNA levels of the antioxidant genes tested. While PGC1α and HO-1 mRNA showed marked induction on H_2O_2 and antioxidant treatment, MnSOD showed no significant induction on H_2O_2 treatment and no change with antioxidants. However, on E50K overexpression there is a slight decrease in PGC1α levels. In this case HO-1 and MnSOD levels remain unchanged. In our RT-PCR analysis, we did not observe any change in MnSOD mRNA levels on E50K overexpression. Hence, based on the basis of these results, it can be concluded that the RGC-5 cell line as such is not defective in responding to oxidative stress but E50K overexpression might cause defect in responding to oxidative stress because PGC1α mRNA level is decreased upon E50K overexpression. Thus, in addition to causing oxidative stress by generating ROS (see chapter 3), the E50K mutant might also cause a defect in response to oxidative stress. However this needs to be examined in detail by further experiments. Our results also indicate that in RGC-5 cells there may be a defect in the induction of MnSOD in response to oxidative stress.

Optineurin plays an important role in vesicular transport mediated by interaction with Rab8 (Hattula and Peranen, 2000) and MyosinVI (Sahlender *et al*., 2005). Our yeast two-hybrid interaction study shows that the most common mutant of optineurin, E50K shows subtle alteration in interaction with Rab8. The mutant interacts with activated Rab8 only, which is the constitutively active GTP-bound form and does not show interaction with wild type Rab8 and dominant negative Rab8 (dominant negative GDP-bound form). It means that E50K mutant specifically binds GTP bound form of Rab8. Wild type optineurin interacts with both wild type Rab8 and activated Rab8 but not with dominant negative form of Rab8. Other mutants of optineurin, viz., H26D, H486R and R545Q interact with wild type Rab8 and activated Rab8 just like WT optineurin. Since only E50K mutant induces death of RGC and also shows altered interaction with Rab8, it is likely that altered interaction with Rab8 might be contributing to induction of cell death by E50K. We observed that both WT and E50K mutant showed co-localization with WT Rab8 and activated Rab8. It is likely that in mammalian cell lines, a proportion of wild type Rab8 gets converted into active form and E50K mutant might be co-localizing with the active Rab8.

Rab8 partially colocalizes with Rab11 suggesting that it is connected to the endocytic recycling compartment (Hattula *et al.,* 2006). Rab11 is concentrated in the pericentrolar recycling endosomes and plays a key role in passage of the recycling transferrin receptor through that compartment (Ullrich *et al*., 1996). It was demonstrated that vesicular structures formed by E50K mutant actually co-localize with markers of recycling endosomes (A.Nagabhushana and G.Swarup, unpublished observation). Hence, we further checked whether

optineurin and E50K interact with Rab11, where we observed they did not interact, contrary to its interaction with Rab8. Hence, we suggest that optineurin specifically shows interaction with Rab8.

5.4 Summary and conclusion

The results described in this chapter suggest that

- **RGC-5 cell line in general is not defective in responding to oxidative stress although there might be a selective defect in the induction of MnSOD.**
- **PGC1α levels are decreased on E50K overexpression- indicating that this mutant might cause a defect in responsiveness of cells to oxidative stress.**
- **E50K mutant shows subtle alteration in interaction with Rab8, which might contribute to cell death induced by this mutant in RGC-5.**

Hence, to conclude, we suggest that a defect in responding to oxidative stress and defective interaction with Rab8 might be some of the contributing factors for the cell death induced by E50K mutant observed in retinal ganglion cell line.

Summary of Results and Conclusions

SUMMARY OF RESULTS AND CONCLUSIONS

- **E50K mutant of optineurin selectively induces death of retinal ganglion cells**

  - .E50K mutant induces cell death in the rat retinal ganglion cell line (RGC-5).
  - E50K- induced cell death is cell type specific and is not seen in Cos-1, HeLa, IMR- 32 (non-ocular) and D407 (ocular) cell lines.
  - E50K- induced cell death requires caspases-1 and -9 and is inhibited by Bcl-2.
  - E50K expression increases reactive oxygen species in RGC-5 cells.
  - Antioxidants (N-acetyl cysteine and Trolox) and Mn Superoxide dismutase inhibit E50K induced cell death in RGC- 5 cells.
  - Optineurin overexpression potentiates TNF-α induced cell death in RGC-5 cells.
  - Endogenous optineurin shows cytoplasmic distribution and also colocalizes with Golgi; on the other hand overexpressed optineurin shows cytoplasmic distribution and does not colocalize with Golgi.
  - E50K mutant shows vesicular structures scattered in the cytoplasm and most of them lie in the vicinity of Golgi.

- **Identification of optineurin interacting proteins by yeast two-hybrid assay**

  - The interacting partners fall under different categories based on their functions.
    a. Proteins involved in NF-κB signaling pathway (CYLD, A20 & UXT).
    b. Protein involved in vesicular trafficking (TBC1D17)
    c. Proteins that have a role in immunity (IK-cytokine, BAT4).

d. Other proteins- HIBADH & ZBTB33.

- E50K mutant showed altered interaction with IK-cytokine, HIBADH and UXT.
- H486R mutant showed altered interaction with UXT and IK-cytokine and did not interact with HIBADH and ZBTB33.
- Other mutants, R545Q and H26D did not show any alteration in interaction with the proteins studied compared to wild type optineurin.
- Two of the interacting partners, viz., TBC1D17 and IK-cytokine, lie in the region of glaucoma loci; hence there exists a possibility that these genes have an association with the disease.

➢ **Attempt to understand the mechanism of E50K induced cell death in RGC-5 cells**

- Hydrogen peroxide treatment increased PGC1α and HO-1 levels whereas MnSOD showed no significant increase.
- Both NAC and Trolox increased the PGC1α and HO-1 mRNA levels with increasing concentration whereas MnSOD levels remained unaltered.
- PGC1α levels are decreased on E50K overexpression- indicating that the mutant might cause a defect in responsiveness of cells to oxidative stress.
- E50K mutant shows subtle alteration in interaction with Rab8 which might contribute to cell death induced by this mutant in RGC-5.

In conclusion, our study shows that

✓ **E50K mutant of optineurin induces cell death selectively in RGC-5 cells which is mediated by oxidative stress.**

✓ **Other mutants (H26D & H486R) of optineurin do not show cell death**

in RGC-5, hence the disease status here may be by indirect mechanism or there might be need for other susceptibility factors.

- ✓ **E50K induced cell death is inhibited by antioxidants suggesting the potential of antioxidants in preventing or delaying some forms of glaucoma.**
- ✓ **Optineurin is a multifunctional protein which is likely to be involved in NF-κB regulation, vesicular trafficking, immune response and transcriptional regulation.**
- ✓ **Two of the optineurin interacting partners lie in the region of known glaucoma loci implying that these genes might be responsible for the disease.**
- ✓ **H486R and E50K mutants show altered interaction with some optineurin interacting proteins.**
- ✓ **A defect in responding to oxidative stress and defective interaction with Rab8 might be some of the contributing factors for the cell death induced by E50K mutant observed in retinal ganglion cell line.**

References

REFERENCES

Abu-Amero KK, Morales J, Bosley TM. Mitochondrial abnormalities in patients with primary open-angle glaucoma. *Invest Ophthalmol Vis Sci*. 2006; **47**: 2533-2541.

Akarsu AN, Turacli ME, Aktan SG, Barsoum-Homsy M, Chevrette L, Sayli BS, Sarfarazi M. A second locus (GLC3B) for primary congenital glaucoma (Buphthalmos) maps to the 1p36 region. *Hum Mol Genet*. 1996; **5**: 1199-1203.

Allingham RR, Wiggs JL, Hauser ER, Larocque-Abramson KR, Santiago-Turla C, Broomer B, Del Bono EA, Graham FL, Haines JL, Pericak-Vance MA, Hauser MA. Early adult-onset POAG linked to 15q11-13 using ordered subset analysis. *Invest Ophthalmol Vis Sci*. 2005; **46**: 2002-2005.

Alvarado JA, Murphy C, Juster R. Trabecular meshwork cellularity in primary open-angle glaucoma and nonglaucomatous normals. *Ophthalmology.* 1984; **91**: 564-579.

Alward WL, Kwon YH, Kawase K, Craig JE, Hayreh SS, Johnson AT, Khanna CL, Yamamoto T, Mackey DA, Roos BR, Affatigato LM, Sheffield VC, Stone EM. Evaluation of optineurin sequence variations in 1,048 patients with open-angle glaucoma. *Am J Ophthalmol.* 2003; **136**: 904-910.

Anborgh PH, Godin C, Pampillo M, Dhami GK, Dale LB, Cregan SP, Truant R, Ferguson SS. Inhibition of metabotropic glutamate receptor signaling by the huntingtin-binding protein optineurin*. J Biol Chem.* 2005; **280**: 34840-34848.

Arend O, Plange N, Sponsel WE, Remky A. Pathogenetic aspects of the glaucomatous optic neuropathy: fluorescein angiographic findings in patients with primary open angle glaucoma. *Brain Res Bull*. 2004; **62**: 517-524.

Assier E, Bouzinba-Segard H, Stolzenberg M.-C, Stephens R, Bardos J, Freemont P, Charron D, Trowsdale J, Rich T. Isolation, sequencing and expression of RED, a novel human gene encoding an acidic-basic dipeptide repeat. *Gene. 1999;* **230**: 145-154.

Aung T, Ebenezer ND, Brice G, Child AH, Prescott Q, Lehmann OJ, Hitchings RA, Bhattacharya SS. Prevalence of optineurin sequence variants in adult primary open angle glaucoma: implications for diagnostic testing. *J Med Genet*. 2003; **40**: e101.

Aung T, Rezaie T, Okada K, Viswanathan AC, Child AH, Brice G, Bhattacharya SS, Lehmann OJ, Sarfarazi M, Hitchings RA. Clinical features and course of patients with glaucoma with the E50K mutation in the optineurin gene. *Invest Ophthalmol Vis Sci*. 2005; **46**: 2816-2822.

Ayala-Lugo RM, Pawar H, Reed DM, Lichter PR, Moroi SE, Page M, Eadie J, Azocar V, Maul E, Ntim-Amponsah C, Bromley W, Obeng-Nyarkoh E, Johnson AT, Kijek TG, Downs CA, Johnson JM, Perez-Grossmann RA, Guevara-Fujita ML, Fujita R, Wallace MR, Richards JE. Variation in optineurin (OPTN) allele frequencies between and within populations. *Mol Vis.* 2007; **13**: 151-163.

Baird PN, Foote SJ, Mackey DA, Craig J, Speed TP, Bureau A. Evidence for a novel glaucoma locus at chromosome 3p21–22. *Hum Genet.* 2005; **117**: 249-257.

Banerjee R, Das PK, Srilakshmi GV, Choudhari A, Rao NM. Novel series of nonglycerol based cationic transfection lipids for use in liposomal gene delivery. *J Med Chem.* 1999; **42**: 4292-4300.

Bejjani BA, Lewis RA, Tomey KF, Anderson KL, Dueker DK, Jabak M, Astle WF, Otterud B, Leppert M, Lupski JR.Mutations in CYP1B1, the gene for cytochrome P4501B1, are the predominant cause of primary congenital glaucoma in Saudi Arabia. *Am J Hum Genet*. 1998; **62**: 325-333.

Bignell GR, Warren W, Seal S, Takahashi M, Rapley E, Barfoot R, Green H, Brown C, Biggs PJ, Lakhani SR, Jones C, Hansen J, Blair E, Hofmann B, Siebert R, Turner G, Evans DG, Schrander-Stumpel C, Beemer FA, van Den Ouweland A, Halley D, Delpech B, Cleveland MG, Leigh I, Leisti J, Rasmussen S. Identification of the familial cylindromatosis tumour-suppressor gene. *Nat Genet.* 2000; **25**: 160-165.

Blum R, Pfeiffer F, Feick P, Nastainczyk W, Kohler B, Schafer KH, Schulz I. Intracellular localization and in vivo trafficking of p24A and p23. *J. Cell. Sci.* 1999; **112**: 537-548.

Bonne C, Muller A, Villain M. Free radicals in retinal ischemia. *Gen Pharmacol* 1998; **30**: 275-280.

Boye K, Grotterød I, Aasheim HC, Hovig E, Maelandsmo GM. Activation of NF-kappaB by extracellular S100A4: analysis of signal transduction mechanisms and identification of target genes. *Int J Cancer.* 2008; **123**: 1301-1310.

Braissant O, Wahli W. Differential expression of peroxisome proliferator-activated receptor-alpha, -beta, and -gamma during rat embryonic development. *Endocrinology.* 1998; **139**: 2748-2754.

Brummelkamp TR, Nijman SM, Dirac AM, Bernards R. Loss of the cylindromatosis tumour suppressor inhibits apoptosis by activating NF-kappaB. *Nature*. 2003; **424**: 797-801.

Caballero M, Rowlette LL, Borras T. Altered secretion of a TIGR/MYOC mutant lacking the olfactomedin domain. *Biochim. Biophys. Acta.* 2000; **1502**: 447-460.

Casson RJ. Possible role of excitotoxicity in the pathogenesis of glaucoma. *Clin Exp Ophthalmol.* 2006; **34**: 54-63.

Chien CT, Bartel PL, Sternglanz R and Fields S. The two-hybrid system: a method to identify and clone genes for proteins that interact with a protein of interest. *Proc Natl Acad Sci USA*. 1991; **88**: 9578-9582.

Chung HS, Harris A, Evans DW, Kagemann L, Garzozi HJ, Martin B. Vascular aspects in the pathophysiology of glaucomatous optic neuropathy. *Surv Ophthalmol.* 1999; **43** Suppl 1: S43-50.

Cioffi GA. Ischemic model of optic nerve injury. *Trans American Ophthalmol Society,* 2005; **103**: 592-613.

Cotinet A, Goureau O, Hicks D, Thillaye-Goldenberg B, de Kozak Y. Tumor necrosis factor and nitric oxide production by retinal Müller glial cells from rats exhibiting inherited retinal dystrophy. *Glia*. 1997; **20**: 59-69.

Courtois G. Tumor suppressor CYLD: negative regulation of NF-kappaB signaling and more. *Cell Mol Life Sci*. 2008; **65**: 1123-1132.

Danias J, Lee KC, Zamora MF, Chen B, Shen F, Filippopoulos T, Su Y, Goldblum D, Podos SM, Mittag T. Quantitative analysis of retinal ganglion cell (RGC) loss in aging DBA/2NNia glaucomatous mice: comparison with RGC loss in aging C57/BL6 mice. *Invest Ophthalmol Vis Sci.* 2003; **44**: 5151-5162.

Daniel JM, Reynolds AB. The catenin p120(ctn) interacts with Kaiso, a novel BTB/POZ domain zinc finger transcription factor. *Mol Cell Biol.* 1999; **19**: 3614-3623.

Daniel JM, Spring CM, Crawford HC, Reynolds AB, Baig A. The p120(ctn)-binding partner Kaiso is a bi-modal DNA-binding protein that recognizes both a sequence-specific consensus and methylated CpG dinucleotides. *Nucleic Acids Res.* 2002; **30**: 2911-2919.

Davis AA, Bernstein PS, Bok D, Turner J, Nachtigal M, Hunt RC. A human retinal pigment epithelial cell line that retains epithelial characteristics after prolonged culture. *Invest. Ophthalmol. Vis. Sci*. 1995; **36**: 955-964.

De Flora S, Izzotti A, Randerath K, Randerath E, Bartsch H, Nair J, Balansky R, van Schooten F, Degan P, Fronza G, Walsh D, Lewtas J. DNA adducts and chronic degenerative disease. Pathogenetic relevance and implications in preventive medicine. *Mutat Res.* 1996; **366**: 197-238.

De Marco N, Buon M, Troise F, Diez-Roux G. Optineurin increases cell survival and translocates to the nucleus in a RAB8 dependent manner upon an apoptotic stimulus. *J Biol Chem*. 2006; **281**: 16147-16156.

Dixit V M, Green S, Sarma V, Holzman LB, Wolf FW, O'Rourke K, Ward P, Prochownik EV, Marks RM. Tumor necrosis factor-alpha induction of novel gene products in human endothelial cells including a macrophage-specific chemotaxin. *J. Biol. Chem.*1990; **265**: 2973-2978.

Dreyer EB, Zurakowski D, Schumer RA, Podos SM, Lipton SA. Elevated glutamate levels in the vitreous body of humans and monkeys with glaucoma. *Arch Ophthalmol.* 1996; **114**: 299-305.

Faber PW,Barnes GT, Srinidhi J, Chen J, Gusella JF, MacDonald ME. Huntingtin interacts with a family of WW domain proteins. *Hum Mol Genet.* 1998; **7**: 1463-1474.

Fan BJ, Wang DY, Fan DS, Tam PO, Lam DS, Tham CC, Lam CY, Lau TC, Pang CP. SNPs and interaction analyses of myocilin, optineurin, and apolipoprotein E in primary open angle glaucoma patients. *Mol Vis.* 2005; **11**: 625-631.

Fan BJ, Wang DY, Lam DS, Pang CP. Gene mapping for primary open angle glaucoma. *Clin Biochem.* 2006; **39**: 249-258.

Fan BJ, Ko WC, Wang DY, Canlas O, Ritch R, Lam DS, Pang CP. Fine mapping of new glaucoma locus GLC1M and exclusion of neuregulin 2 as the causative gene. *Mol Vis*. 2007; **13**: 779-784.

Farkas RH, Chowers I, Hackam AS, Kageyama M, Nickells RW, Otteson DC, Duh EJ, Wang C, Valenta DF, Gunatilaka TL, Pease ME, Quigley HA, Zack DJ. Increased expression of iron-regulating genes in monkey and human glaucoma. *Invest Ophthalmol Vis Sci* . 2004; **45**: 1410-1417.

Fields S and Song O. A novel genetic system to detect protein-protein interactions. *Nature*. 1989; **340**: 245-246.

Fingert JH, Alward WL, Kwon YH, Shankar SP, Andorf JL, Mackey DA, Sheffield VC, Stone EM. No association between variations in the WDR36 gene and primary open-angle glaucoma. *Arch Ophthalmol*. 2007; **125**: 434-436.

Flammer J, Haefliger IO, Orgül S, Resink T. Vascular dysregulation: a principal risk factor for glaucomatous damage? *J Glaucoma*. 1999; 8: 212-219.

Flammer J, Mozaffarieh M. What is the present pathogenetic concept of glaucomatous optic neuropathy? *Surv. Ophth.* 2007; **52**: S162-S173.

Flammer J, Orgul S, Costa VP, Orzalesi N, Krieglstein GK, Serra LM, Renard JP, Stefansson E. The impact of ocular blood flow in glaucoma. *Prog Retin Eye Res.* 2002; **21**: 359-393.

Flammer J. The vascular concept of glaucoma. Surv Ophthalmol. 1994; **38** Suppl: S3-6.

Franz GH, Stephanie JC, Esther HM, Pfeiffer Norbert. Complex autoantibody repertoires in patients with glaucoma. *Mol Vis.* 2004; **10**: 132-137.

Fuchs E, Haas AK, Spooner RA, Yoshimura S, Lord JM, Barr FA. Specific Rab GTPase-activating proteins define the Shiga toxin and epidermal growth factor uptake pathways. *J Cell Biol*. 2007; **177**: 1133-1143.

Funayama T, Ishikawa K, Ohtake Y, et al. Variants in optineurin gene and their association with tumor necrosis factor-α polymorphisms in Japanese patients with glaucoma. *Invest Ophthalmol Vis Sci*. 2004; **45**: 4359-4367.

Funayama T, Mashima Y, Ohtake Y, Ishikawa K, Fuse N, Yasuda N, Fukuchi T, Murakami A, Hotta Y, Shimada NSNPs and interaction analyses of noelin 2, myocilin, and optineurin genes in Japanese patients with open-angle glaucoma. *Invest Ophthalmol Vis Sci.* 2006; **47**: 5368-5375.

Fuse N, Takahashi K, Akiyama H, Nakazawa T, Seimiya M, Kuwahara S, Tamai M. Molecular genetic analysis of optineurin gene for primary open-angle and normal tension glaucoma in the Japanese population. *J Glaucoma*. 2004; **13**: 299-303.

Gao J, Huo L, Sun X, Liu M, Li D, Dong JT, Zhou J. The tumor suppressor CYLD regulates microtubule dynamics and plays a role in cell migration.*J Biol Chem*. 2008; **283**: 8802-8809.

Grus FH, Joachim SC, Bruns K, Lackner KJ, Pfeiffer N, Wax MB. Serum autoantibodies to alpha-fodrin are present in glaucoma patients from Germany and the United States. *Invest OphthalmolVis Sci.* 2006; **47**: 968-976.

Gstaiger M, Luke B, Hess D, Oakeley EJ, Wirbelauer C, Blondel M, Vigneron M, Peter M, Krek W. Control of nutrient-sensitive transcription programs by the unconventional prefoldin URI. *Science*. 2003; **302:** 1208-1212.

Gupta S, Radha V, Sudhakar Ch, Swarup G. A nuclear protein tyrosine phosphatase activates p53 and induces caspase-1 dependent apoptosis. *FEBS lett*. 2002; **532**: 61-66.

Harada T, Harada C, Nakamura K, Quah HM, Okumura A, Namekata K, Saeki T, Aihara M, Yoshida H, Mitani A, Tanaka K. The potential role of glutamate transporters in the pathogenesis of normal tension glaucoma. *J Clin Invest*. 2007; **117**: 1763-1770.

Hattula K, Peranen J. FIP-2, a coiled-coil protein, links Huntingtin to Rab8 and modulates cellular morphogenesis. *Curr Biol*. 2000; **10**: 1603-1606.

Hattula K, Furuhjelm J, Tikkanen J, Tanhuanpää K, Laakkonen P, Peränen J. Characterization of the Rab8-specific membrane traffic route linked to protrusion formation. *J Cell Sci*. 2006; **119**: 4866-4877.

Hauser MA, Sena DF, Flor J, Walter J, Auguste J, Larocque-Abramson K, Graham F, Delbono E, Haines JL, Pericak-Vance MA, Rand Allingham R, Wiggs JL. Distribution of optineurin sequence variations in an

ethnically diverse population of low-tension glaucoma patients from the United States. *J Glaucoma*. 2006; **15**: 358-363.

He Y, Leung KW, Zhang YH, Duan S, Zhong XF, Jiang RZ, Peng Z, Tombran-Tink J, Ge J. Mitochondrial complex I defect induces ROS release and degeneration in trabecular meshwork cells of POAG patients: protection by antioxidants. *Invest Ophthalmol Vis Sci.* 2008; **49**:1447-1458.

Heyninck K, Valck DD, Berghe WV, Criekinge WV, Contreras R, Fiers W, Haegeman G, Beyaert R. The Zinc Finger Protein A20 Inhibits TNF-induced NF-κB-dependent Gene Expression by Interfering with an RIP- or TRAF2-mediated Transactivation Signal and Directly Binds to a Novel NF-κB-inhibiting Protein ABIN. *J. Cell Biol.* 1999; **145**: 1471-1482.

Huffel VS, Delaei F, Heyninck K, De Valck D, Beyaert R. Identification of a novel A20-binding inhibitor of nuclear factor-kappa B activation termed ABIN-2. *J Biol Chem.* 2001; **276**: 30216-30223.

Inoue H, Nojima H, Okayama H. High efficiency transformation of Escherichia coli with plasmids. *Gene*. 1990; **96**: 23-28.

Itoh T, Satoh M, Kanno E, Fukuda M. Screening for target Rabs of TBC (Tre-2/Bub2/Cdc16) domain-containing proteins based on their Rab-binding activity. *Genes Cells*. 2006; **11**: 1023-1037.

Izzotti A, Sacca SC, Cartiglia C, De Flora S. Oxidative deoxyribonucleic acid damage in the eyes of glaucoma patients. *Am J Med.* 2003; **114**: 638-646.

Izzotti A, Bagnis A, Sacca SC. The role of oxidative stress in glaucoma. *Mut. Res*. 2006; **612**: 105-114.

James P, Halladay J, Craig EA. Genomic libraries and host strain designed for efficient two-hybrid selection in yeast. *Genetics*. 1996; **144**: 1425-1436.

Joe MK, Sohn S, Hur W, Moon Y, Choi YR, Kee C. Accumulation of mutant myocilins in ER leads to ER stress and potential cytotoxicity in human trabecular meshwork cells. *Biochem. Biophys. Res. Commun*. 2003; **312**: 592-600.

John SWM. Mechanistic insights into glaucoma provided by experimental genetics. *Invest Ophthalmol Vis Sci.* 2005; **46**: 2650-2661.

Kaiser HJ, Flammer J. Systemic hypotension: a risk factor for glaucomatous damage? *Ophthalmologica*. 1991; **203**: 15-18.

Kamata H, Hirata H. Redox regulation of cellular signalling. *Cell Signal*. 1999; **11**: 1-14.

Kamal D, Hitchings R. Normal tension glaucoma-a practical approach. *Br. J. Ophthalmol.* 1998; **82**: 835-840.

Kamatkar S, Radha V, Nambirajan S, Reddy RS, Swarup G. Two splice variants of a tyrosine phosphatase differ in substrate specificity. *J Biol Chem*. 1996; **271**: 26755-26761.

Kamphuis W, Schneemann A. Optineurin gene expression level in human trabecular meshwork does not change in response to pressure elevation. *Ophthalmic Res.* 2003; **35**: 93-96.

Ko ML, Peng PH, Ma MC, Ritch R, Chen CF. Dynamic changes in reactive oxygen species and antioxidant levels in retinas in experimental glaucoma. *Free Radic Biol Med*. 2005; **39**: 365-373.

Kortuem K, Geiger LK, Levin LA. Differential susceptibility of retinal ganglion cells to reactive oxygen species. *Invest Ophthalmol Vis Sci*. 2000; **41**: 3176-3182.

Kovalenko A, Chable-Bessia C, Cantarella G, Israel A, Wallach D, Courtois G. The tumor suppressor CYLD negatively regulates NF-kappaB signaling by deubiquitination. *Nature*. 2003; **424**: 801-805.

Kroeber M, Ohlmann A, Russell P, Tamm ER. Transgenic studies on the role of optineurin in the mouse eye. *Exp Eye Res.* 2006; **82**: 1075-1085.

Krief P, Augery-Bourget Y, Plaisance S, Merck MF, Assier E, Tanchou V, Billard M, Boucheix C, Jasmin C, Azzarone B. A new cytokine (IK) down-regulating HLA class II: monoclonal antibodies, cloning and chromosome localization. *Oncogene. 1994*; **9**: 3449-3456.

Krishnamoorthy RR, Agarwal P, Prasanna G, Vopat K, Lambert W, Sheedlo HJ, Pang IH, Shade D, Wordinger RJ, Yorio T, Clark AF, Agarwal N. Characterization of a transformed rat retinal ganglion cell line. *Brain Res.* 2001: **86**: 1-12.

Kuehn MH, Fingert JH, Kwon YH. Retinal ganglion cell death in glaucoma: mechanisms and neuroprotective strategies. *Ophthalmol Clin North Am*. 2005; **18**: 383-395.

Laegreid A, Thommesen L, Jahr TG, Sundan A, Espevik T. Tumor necrosis factor induces lipopolysaccharide tolerance in a human adenocarcinoma cell line mainly through the TNF p55 receptor. *J. Biol. Chem*. 1995; **270**: 25418-25425.

Lam TT, Siew E, Chu R, Tso MO. Ameliorative effect of MK-801 on retinal ischemia. *J Ocul Pharmacol Ther*. 1997; **13**: 129-137.

Leung YF, Fan BJ, Lam DS, Lee WS, Tam PO, Chua JK, Tham CC, Lai JS, Fan DS, Pang CP. Different optineurin mutation pattern in primary open-angle glaucoma*. Invest Ophthalmol Vis Sci.* 2003; **44**: 3880-3884.

Li Y, Kang J, Horwitz MS. Interaction of an adenovirus E3 14.7- kilodalton protein with a novel tumor necrosis factor alpha-inducible cellular protein containing leucine zipper domains. *Mol Cell Biol*. 1998; **18**: 1601-1610.

Libby RT, Gould DB, Anderson MG, John SWM. Complex genetics of glaucoma susceptibility. *Ann Rev Genomics Hum Genet*. 2005; **6**: 15-44.

Lin HJ, Tsai FJ, Chen WC, et al. Association of tumour necrosis factor alpha–308 gene polymorphism with primary open-angle glaucoma in Chinese. *Eye*. 2003; **17**: 31-34.

Lin Q, Weis S, Yang G, Weng YH, Helston R, Rish K, Smith A, Bordner J, Polte T, Gaunitz F, Dennery PA. Heme oxygenase-1 protein localizes to the nucleus and activates transcription factors important in oxidative stress. *J Biol Chem*. 2007; **282**: 20621-20633.

Lipton SA. Possible role for memantine in protecting retinal ganglion cells from glaucomatous damage. *Surv Ophthalmol.* 2003; **48**: S38-46 (Suppl. 1).

Maher P, Hanneken A. Flavonoids protect retinal ganglion cells from oxidative stress-induced death. *Invest Ophthalmol Vis Sci*. 2005a; **46**: 4796-4803.

Maher P, Hanneken A. The molecular basis of oxidative stress induced cell death in an immortalized retinal ganglion cell line. *Invest Ophthalmol Vis Sci*. 2005b; **46**: 749-757.

Maniatis T, Fritsch EF, Sambrook J. *Molecular Cloning, A Laboratory Manual*. Cold Spring Harbor Laboratory, Cold Spring Harbor, New York. 1982.

Markus SM, Taneja SS, Logan SK, Li W, Ha S, Hittelman AB, Rogatsky I, Garabedian MJ. Identification and characterization of ART-27, a novel coactivator for the androgen receptor N terminus. *Mol. Biol. Cell. 2002;* **13:** 670-682.

Martin SN, Sutherland J, Levin AV, Klose R, Priston M, Héon E. Molecular characterisation of congenital glaucoma in a consanguineous Canadian community: a step towards preventing glaucoma related blindness. *J Med Genet*. 2000; **37**: 422-427.

Martindale JL, Holbrook NJ. Cellular response to oxidative stress: signaling for suicide and survival. *J Cell Physiol*. 2002; **192**: 1-15.

Mashima Y, Suzuki Y, Sergeev Y, Ohtake Y, Tanino T, Kimura I, Miyata H, Aihara M, Tanihara H, Inatani M, Azuma N, Iwata T, Araie M.Novel cytochrome P4501B1 (CYP1B1) gene mutations in Japanese patients with primary congenital glaucoma. *Invest Ophthalmol Vis Sci*. 2001; **42**: 2211-2216.

Massoumi R, Chmielarska K, Hennecke K, Pfeifer A, Fassier R. Cyld inhibits tumor cells proliferation by blocking bcl-3 dependent NF-kB signaling. Cell. 2006; **125**: 665-677.

Mauro C ABIN-1 binds to NEMO/ IKKγ and co-operates with A20 in inhibiting NF-κB. *J.Biol.Chem*. 2006; **281**: 18482-18488.

McKinnon SJ, Goldberg LD, Peeples P, Walt JG and Bramley TJ. Current management of glaucoma and the need for complete therapy*. Am J Manag Care* 2008; **14**: S20-27.

McNabb DS and Guarente L. Genetic and biochemical probes for protein-protein interactions. *Curr Opin Biotechnol*. 1996; **7**: 554-559.

Mitchell P, Smith W, Attebo K, Healey PR. Prevalence of open-angle glaucoma in Australia: the Blue Mountains eye study. *Ophthalmology* 1996; **103:** 1661-1669.

Monemi S, Spaeth G, DaSilva A, Popinchalk S, Ilitchev E, Liebmann J, Ritch R, Héon E, Crick RP, Child A, Sarfarazi M.Identification of a novel adult-onset primary open-angle glaucoma (POAG) gene on 5q22.1.*Hum Mol Genet*. 2005; **14**: 725-733.

Moreland RJ, Dresser ME, Rodgers JS, Roe BA, Conaway JW, Conaway RC, Hanas JS. Identification of a transcription factor IIIA- interacting protein*. Nuc. Acids. Res*. 2000; **28**: 1986-1993.

Moreno MC, Campanelli J, Sande P, Sanez DA, Keller MI, Sarmiento MI, Rosenstein RE. Retinal oxidative stress induced by high intraocular pressure. *Free Radic. Biol. Med.* 2004; **37**: 803-812.

Morton S, Hesson L, Peggie M, Cohen P. Enhanced binding of TBK1 by an optineurin mutant that causes a familial form of primary open angle glaucoma. FEBS Lett. 2008; **582**: 997-1002.

Mozaffarieh M, Grieshaber MC, Flammer J. Oxygen and blood flow: players in the pathogenesis of glaucoma. *Mol Vis.* 2008; **14**: 224-233.

Mrowka R, Blüthgen N, Fähling M. Seed-based systematic discovery of specific transcription factor target genes. *FEBS J.* 2008; **275**: 3178-3192.

Mukhopadhyay A, Komatireddy S, Acharya M, Bhattacharjee A, Mandal AK, Thakur SK, Chandrasekhar G, Banarjee A, Thomas R, Chakrabarti S, Ray K. Evaluation of optineurin as a candidate gene in Indian patients with primary open angle glaucoma. *Mol. Vis*. 2005; **11**: 792-797.

Muraoka M, Hasegawa H, Kohno M, Inoue A, Miyazaki T, Terada M, Nose M, Yasukawa M. IK cytokine ameliorates the progression of lupus nephritis in MRL/*lpr* mice. *Arth. Rheum.* 2006; **54**: 3591-3600.

Murin R, Schaer A, Kowtharapu BS, Verleysdonk S, Hamprecht B. Expression of 3-hydroxyisobutyrate dehydrogenase in cultured neural cells. *J. Neurochem*. 2008; 105: 1176-1186.

Nakanishi S. Molecular diversity of glutamate receptors and implications for brain function. *Science*. 1992; **258**: 597-603.

Nie Z and Randazzo PA. Arf GAPs and membrane traffic. *J Cell Sci*. 2006; **119**: 1203-1211.

Ohia SE, Opere CA, LeDay AM. Pharmacological consequences of oxidative stress in ocular tissues. *Mutat. Res. Fund.Mol. Mech.*2005; **579**: 22-36.

Opipari AW, Boguski MS, Dixit VM. The A20 cDNA induced by tumor necrosis factor-alpha encodes a novel type of zinc finger protein. *J. Biol. Chem.* 1990; **265**: 14705-14708.

Park BC, Shen X, Samaraweera M, Yue BY. Studies of optineurin, a glaucoma gene: Golgi fragmentation and cell death from overexpression of wild-type and mutant optineurin in two ocular cell types. *Am J Pathol*. 2006; **169**: 1976-1989.

Park BC, Tibudan M, Samaraweera M, Shen X, Yue BY. Interaction between two glaucoma genes, optineurin and myocilin. *Genes Cells*. 2007; **12**: 969-979.

Peranen J, Auvinen P, Virta H, Wepf R, Simons K. Rab8 promotes polarized membrane transport through reorganization of actin and microtubules in fibroblasts. *J Cell Biol*. 1996; **135**: 153-167.

Pfeffer SR. Rab GTPase specifying and deciphering organelle identity and function. *Trends Cell Biol*. 2001; **11**: 487-491.

Radha V, Rajanna A, Swarup G. Induction of p53 dependent apoptosis upon overexpression of a nuclear protein tyrosine phosphatase. *FEBS Lett*. 1999; **453**: 308-312.

Radha V, Rajanna A, Swarup G. Phosphorylated guanine nucleotide exchange factor C3G, induced by pervanadate and Src family kinases localizes to the Golgi and subcortical actin cytoskeleton. *BMC Cell Biol.* 2004; **5**: 31.

Reddy AB, Kaur K, Mandal AK, Panicker SG, Thomas R, Hasnain SE, Balasubramanian D, Chakrabarti S.Mutation spectrum of the CYP1B1 gene in Indian primary congenital glaucoma patients. *Mol Vis*. 2004; **10**: 696-702.

Reiley W, Zhang M, Sun SC. Negative regulation of JNK signaling by the tumor suppressor CYLD. *J.Biol.Chem.* 2004; **279**: 55161-55167.

Resnikoff S, Pascolini D, Etya'ale D, Kocur I, Pararajasegaram R, Pokharel GP, Mariotti SP. Global data on visual impairment in the year 2002. *Bull World Health Organ.* 2004; **82**: 844-851.

Rezaie T, Child A, Hitchings R, Brice G, Miller L, Coca-Prados M, Héon E, Krupin T, Ritch R, Kreutzer D, Crick RP, Sarfarazi M. Adult-onset primary open-angle glaucoma caused by mutations in optineurin. *Science*. 2002; **295**: 1077-1079.

Rezaie T, Sarfarazi M. Molecular cloning, genomic structure, and protein characterization of mouse optineurin. *Genomics.* 2005; **85**: 131-138.

Rezaie T, Stoilov I, Sarfarazi M. Embryonic expression of the optineurin (glaucoma) gene in different stages of mouse development. *Mol Vis*. 2007; **13**: 1446-1450.

Romano C, Barrett DA, Li Z, Pestronk A, Wax MB. Antirhodopsin antibodies in sera from patients with normalpressure glaucoma. *Invest Ophthalmol Vis Sci* 1995; **36**: 1968-1975.

Rougraff PM, Paxton R, Kuntz MJ, Crabb DW Harris RA. Purification and characterization of 3-hydroxyisobutyrate dehydrogenase from rabbit liver. *J. Biol. Chem.* 1988; **263**: 327-331.

Rougraff PM, Zhang B, Kuntz MJ, Harris RA, Crabb DW. Cloning and sequence analysis of a cDNA for 3-hydroxyisobutyrate dehydrogenase. Evidence for its evolutionary relationship to other pyridine nucleotide-dependent dehydrogenases. *J. Biol. Chem*. 1989; **264:** 5899-5903.

Rudzinski M, Saragovi HU. Glaucoma: Validated and facile in vivo experimental models of a chronic neurodegenerative disease for drug development. *Curr Med Chem Central Nervous System Agents*, 2005; **5**: 43-49.

Ruzov A, Dunican DS, Prokhortchouk A, Pennings S, Stancheva I, Prokhortchouk E, Meehan RR. Kaiso is a genome-wide repressor of transcription that is essential for amphibian development. *Development*. 2004; **131**: 6185-6194.

Ryter SW, Alam J, Choi AM. Heme oxygenase-1/carbon monoxide: from basic science to therapeutic applications. *Physiol Rev*. 2006; **86**: 583-650.

Sahlender DA, Roberts RC, Arden SD, et al. Optineurin links myosin VI to the Golgi complex and is involved in Golgi organization and exocytosis. *J Cell Biol*. 2005; **169**: 285-295.

Sambrook J, Fritsch EF, Maniatis T. *Molecular cloning: a laboratory manual. 2nd edition.* Cold Spring Harbor Laboratory Press, Cold Spring Harbor, New York. 1989.

Sarfarazi M, Child A, Stoilova D, Brice G, Desai T, Trifan OC, Poinoosawmy D, Crick RP. Localization of the fourth locus (GLC1E) for adult-onset primary open-angle glaucoma to the 10p15-p14 region. *Am J Hum Genet*. 1998; **62**: 641-52.

Schori H, Kipnis J, Yoles E, WoldeMussie E, Ruiz G, Wheeler LA, Schwartz M. Vaccination for protection of retinal ganglion cells against death from glutamate cytotoxicity and ocular hypertension: Implications for glaucoma. *Proc Natl Acad Sci U S A*. 2001; **98**: 3398-3403.

Schroer A, Schneider S, Ropers HH, Nothwang HG. Cloning and characterization of UXT, a novel gene in human Xp11, which is widely and abundantly expressed in tumor tissue. *Genomics.* 1999; 56: 340-343.

Schwamborn K, Weil R, Courtois G, Whiteside ST, Israël A. Phorbol esters and cytokines regulate the expression of the NEMO-related protein, a molecule involved in a NF-kappa B-independent pathway. *J Biol Chem.* 2000; **275**: 22780-22789.

Seol DW, Billiar TR A caspase-9 variant missing the catalytic site is an endogenous inhibitor of apoptosis. *J Biol Chem.* 1999; **274**: 2072-2076.

Shen F, Chen B, Danias J, Lee KC, Lee H, Su Y, Podos SM, Mittag TW, Glutamate-induced glutamine synthetase expression in retinal Muller cells after short-term ocular hypertension in the rat. *Invest Ophthalmol Vis Sci*. 2004; **45**: 3107-3112.

Shields MB, Allingham RR, Damji K, Freedman S, Moroi S, Shafranov G. Textbook of glaucoma. 5th ed. Philadelphia, PA.Lippincott Williams & Wilkins; 2005.

Shivakrupa R, Radha V, Sudhakar C, Swarup G. Physical and functional interaction between Hck tyrosine kinase and guanine nucleotide exchange factor C3G results in apoptosis, which is independent of C3G catalytic domain. *J Biol Chem*. 2003; **278**: 52188-52194.

Sommer A, Tielsch JM, Katz J, et al. Relationship between intraocular pressure and primary open angle glaucoma among white and black Americans: the Baltimore eye survey. *Arch Ophthalmol.* 1991; **109:** 1090-1095.

Song HY, Rothe M, Goeddel DV. The tumor necrosis factor-inducible zinc finger protein A20 interacts with TRAF1/TRAF2 and inhibits NF-kappaB activation. *Proc Natl Acad Sci U S A.* 1996; **93**: 6721-6725.

Spies T, Blanck G, Bresnahan M, Sands J, Strominger J L. A new cluster of genes within the human major histocompatibility complex. *Science*. 1989; **243**: 214-217.

Sripriya S, Nirmaladevi J, George R, Hemamalini A, Baskaran M, Prema R, Ve Ramesh S, Karthiyayini T, Amali J, Job S, Vijaya L, Kumaramanickavel G. OPTN gene: profile of patients with glaucoma from India. *Mol Vis.* 2006; **12**: 816-820.

Stegmeier F, Sowa ME, Nalepa G, Gygi SP, Harper JW, Elledge SJ. The tumor suppressor CYLD regulates entry into mitosis. *Proc Natl Acad Sci U S A*. 2007; **104**: 8869-8874.

Stoilov I, Akarsu AN, Sarfarazi M. Identi.cation of three different truncating mutations in cytochrome P4501B1 (CYP1B1) as the principal cause of primary congenital glaucoma (Buphthalmos) in families linked to the GLC3A locus on chromosome 2p21. *Hum Mol Genet*. 1997; **6**: 641-647.

Stoilov IR, Sarfarazi M. The third genetic locus (GLC3C) for primary congenital glaucoma (PCG) maps to chromosome 14q24.3. ARVO Annual Meeting; 2002 May 5-10; Fort Lauderdale (FL).

Stoilova D, Child A, Trifan OC, Crick RP, Coakes RL, Sarfarazi M. Localization of a locus (GLC1B) for adult-onset primary open angle glaucoma to the 2cen–q13 region. *Genomics.* 1996; **36**: 142-150.

Stone EM, Fingert JH, Alward WLM, Nguyen TD, Polansky JR. Identification of a gene that causes primary open angle glaucoma. *Science*. 1997; **275** : 668-670.

St-Pierre J, Drori S, Uldry M, Silvaggi JM, Rhee J, Jäger S, Handschin C, Zheng K, Lin J, Yang W, Simon DK, Bachoo R, Spiegelman BM. Suppression of reactive oxygen species and neurodegeneration by the PGC-1 transcriptional coactivators. *Cell.* 2006; **127**: 397-408.

Stroissnigg H, Repitz M, Miloloza A, Linhartova I, Beug H, Wiche G, Propst F. FIP-2, an Iκ-Bkinase-γ-related protein, is associated with the Golgi apparatus and translocates to the marginal band during chicken erythroblast differentiation. *Exp. Cell. Res*. 2002; **278**: 133-145.

Sucher NJ, Lipton SA, Dreyer EB. Molecular basis of glutamate toxicity in retinal ganglion cells. *Vision Res. 1997;* **37:** 3483-3493.

Sun S, Tang Y, Lou X, Zhu L, Yang K, Zhang B, Shi H, Wang C. UXT is a novel and essential cofactor in the NF-kappaB transcriptional enhanceosome. *J Cell Biol.* 2007; **178**: 231-244.

Suriyapperuma SP, Child A, Desai T, Brice G, Kerr A, Crick RP, Sarfarazi M. A new locus (GLC1H) for adult-onset primary open-angle glaucoma maps to the 2p15-p16 region. *Arch Ophthalmol*. 2007; **125**: 86-92.

Suzuki Y, Iwase A, Araie M. Yamamoto T, Abe H, Shirato S, Kuwayama Y, Mishima HK, Shimizu H, Tomita G, Inoue Y, Kitazawa Y; Tajimi Study Group. Risk factors for open-angle glaucoma in a Japanese population: the Tajimi Study. *Ophthalmology*. 2006; **113**: 1613-1617.

Takahashi Y, Katai N, Murata T, Taniguchi S-I, Hayashi T. Development of spontaneous optic neuropathy in NF-κBp50-deficient mice: requirement for NF-κBp50 in ganglion cell survival. *Neuropath. App. Neuro*. 2007; **33:** 692-705.

Tamm ER. Myocilin and glaucoma: facts and ideas. *Prog. Retin. Eye Res.* 2002; **21**: 395-428.

Taneja SS, Ha S, Swenson NK, Torra IP, Rome S, Walden PD, Huang HY, Shapiro E, Garabedian MJ, Logan SK. ART-27, an androgen receptor coactivator regulated in prostate development and cancer. J Biol Chem. 2004; **279**: 13944-13952.

Tezel G, Li LY, Patil RV, Wax MB. TNF-α and TNF-α receptor-1 in the retina of normal and glaucomatous eyes. *Invest Ophthalmol Vis Sci*. 2001; **42**: 1787-1794.

Tezel G, Wax MB. Increased production of tumor necrosis factor-alpha by glial cells exposed to simulated ischemia or elevated hydrostatic pressure induces apoptosis in cocultured retinal ganglion cells. *J Neurosci.* 2000a; **20**: 8693-8700.

Tezel G, Wax MB. The mechanisms of hsp27 antibodymediated apoptosis in retinal neuronal cells. *J Neurosci* 2000b; **20**: 3552-3562.

Tezel G. Oxidative Stress in Glaucomatous Neurodegeneration: Mechanisms and Consequences. *Prog Retin Eye Res*. 2006; **25**: 490-513.

Tezel G, Yang X, Cai J. Proteomic identification of oxidatively modified retinal proteins in a chronic
pressure-induced rat model of glaucoma. *Invest Ophthalmol Vis Sci.* 2005; **46**: 3177-3187.

Tezel G, Kass MA, Kolker AE, Wax MB. Comparative optic disc analysis in normal pressure glaucoma, primary open-angle glaucoma, and ocular hypertension. *Ophthalmology.* 1996; **103**: 2105-2113.

Tielsch JM, Katz J, Sommer A, Quigley HA, Javitt JC. Family history and risk of primary open angle glaucoma: the Baltimore eye survey. *Arch Ophthalmol* 1994; **112:** 69-73.

Toda Y, Tang S, Kashiwagi K, Mabuchi F, Lijima H, Tsukahara S, Yamagata Z. Mutations in the optineurin gene in Japanese patients with primary open-angle glaucoma and normal tension glaucoma. *Am J Med Genet*. 2004; **125**: 1-4.

Trifan OC, Traboulsi EI, Stoilova D, Alozie I, Nguyen R, Raja S, Sarfarazi M.. A third locus (GLC1D) for adult-onset primary open-angle glaucoma maps to the 8q23 region. *Am J Ophthalmol.* 1998; **126**: 17-28.

Trompouki E, Hatzivassiliou E, Tsichritzis T, Farmer H, Ashworth A, Mosialos G. CYLD is a deubiquitinating enzyme that negatively regulates NF-kappaB activation by TNFR family members. *Nature*. 2003; **424**: 793-796.

Ullrich O, Reinsch S, Urbé S, Zerial M, Parton RG. Rab11 regulates recycling through the pericentriolar recycling endosome. *J Cell Biol*. 1996; **135**: 913-924.

Umeda T, Matsuo T, Nagayama M, Tamura N, Tanabe Y, Ohtsuki H. Clinical relevance of optineurin sequence alterations in Japanese glaucoma patients. *Ophthalmic Genet*. 2004; **25**: 91-99.

Vittitow J, Borrás T. Expression of optineurin, a glaucoma-linked gene, is influenced by elevated intraocular pressure. *Biochem Biophys Res Commun.* 2002; **298**: 67-74.

Vorwerk CK, Gorla MS, Dreyer EB. An experimental basis for implicating excitotoxicity in glaucomatous optic neuropathy. *Surv Ophthalmol.* 1999; **43**: S142-150.

Wagner S, Carpentier I, Rogov V, Kreike M, Ikeda F, Löhr F, Wu CJ, Ashwell JD, Dötsch V, Dikic I, Beyaert R. Ubiquitin binding mediates the NF-kappaB inhibitory potential of ABIN proteins. *Oncogene*. 2008; **27**: 3739-3745.

Wagner S, Carpentier I, Rogov V, Kreike M, Ikeda F, Löhr F, Wu CJ, Ashwell JD, Dötsch V, Dikic I, Beyaert R. Ubiquitin binding mediates the NF-kappaB inhibitory potential of ABIN proteins. Oncogene. 2008; **27**: 3739-3745.

Wang N, Chintala SK, Fini ME, Schuman JS. Activation of a tissue-specific stress response in the aqueous outflow pathway of the eye defines the glaucoma disease phenotype. *Nat. Med*. 2001; **7**: 304-309.

Wang JT, Kunzevitzky NJ, Dugas JC, Cameron M, Barres BA, Goldberg JL. Disease gene candidates revealed by expression profiling of retinal ganglion cell development. *J Neurosci.* 2007; **27**: 8593-8603.

Wang DY, Fan BJ, Chua JK, Tam PO, Leung CK, Lam DS, Pang CP. A genome-wide scan maps a novel juvenile-onset primary open-angle glaucoma locus to 15q. *Invest Ophthalmol Vis Sci*. 2006; **47**: 5315-5321.

Wax MB, Tezel G, Edward PD. Clinical and ocular histopathological findings in a patient with normalpressure glaucoma. *Arch Ophthalmol.* 1998; **116**: 993-1001.

Weinreb RN, Khaw PT. Primary open-angle glaucoma. *Lancet.* 2004; 363: 1711-1720.

Weisschuh N, Alavi MV, Bonin M, Wissinger B. Identification of genes that are linked with optineurin expression using a combined RNAi--microarray approach. *Exp Eye Res*. 2007; **85**: 450-461.

Weisschuh N, Neumann D, Wolf C, Wissinger B, Gramer E. Prevalence of myocilin and optineurin sequence variants in German normal tension glaucoma patients. *Mol. Vis.* 2005; **11**: 284-287.

Wertz IE, O'Rourke KM, Zhou H, Eby M, Aravind L, Seshagiri S, Wu P, Wiesmann C, Baker R, Boone DL, Ma A, Koonin EV, Dixit VM. De-ubiquitination and ubiquitin ligase domains of A20 downregulate NF-kappaB signalling. *Nature.* 2004; **430**: 694-699.

Wiggs JL, Allingham RR, Hossain A, et al. Genome-wide scan for adult onset primary open angle glaucoma. *Hum Mol Genet.* 2000; **9**: 1109-1117.

Wiggs JL, Lynch S, Ynagi G, et al. A genomewide scan identifies novel early-onset primary open-angle glaucoma loci on 9q22 and 20p12. *Am J Hum Genet.* 2004; **74**: 1314-1320.

Wirtz MK, Samples JR, Kramer PL, Rust K, Topinka JR, Yount J, Koler RD, Acott TS. Mapping a gene for adult-onset primary open-angle glaucoma to chromosome 3q. *Am J Hum Genet.* 1997; **60**: 296-304.

Wirtz MK, Samples JR, Rust K, Lie J, Nordling L, Schilling K, Acott TS, Kramer PL. GLC1F, a new primary open-angle glaucoma locus, maps to 7q35-q36.*Arch Ophthalmol*. 1999; **117**: 237-241.

Wertz IE, O'Rourke KM, Zhou H, Eby M, Aravind L, Seshagiri S, Wu P, Wiesmann C, Baker R, Boone DL, Ma A, Koonin EV, Dixit VM. De-ubiquitination and ubiquitin ligase domains of A20 downregulate NF-kappaB signalling. *Nature*. 2004; **430**: 694-699.

Willoughby CE, Chan LL, Herd S, Billingsley G, Noordeh N, Levin AV, Buys Y, Trope G, Sarfarazi M, Héon E. Defining the pathogenicity of optineurin in juvenile open-angle glaucoma. *Invest Ophthalmol Vis Sci*. 2004; **45**: 3122-3130.

Wolfs RC, Klaver CC, Ramrattan RS, van Duijn CM, Hofman A, de Jong PT. Genetic risk of primary open-angle glaucoma. Population-based familial aggregation study. *Arch Ophthalmol.* 1998; **116**:1640-1645.

Xu L, Wang Y, Wang S, Wang Y, Jonas JB. High myopia and glaucoma susceptibility the Beijing Eye Study. *Ophthalmology.* 2007; **114**: 216-20.

Yamamoto T, Kitazawa Y. Vascular pathogenesis of normal-tension glaucoma: a possible pathogenetic factor, other than intraocular pressure, of glaucomatous optic neuropathy. *Pro. Ret. Eye Res.* 1998; **17**: 127-143.

Yan X, Tezel G, Wax MB, Edward DP. Matrix metalloproteinases and tumor necrosis factor-α in glaucomatous optic nerve head.*Arch Ophthalmol*. 2000;**118**: 666-673.

Yang J, Tezel G, Patil RV, Romano C, Wax MB. Serum autoantibody against glutathione S-transferase in patients with glaucoma. *Invest Ophthalmol Vis Sci*. 2001; **42**: 1273-1276.

Yoon HG, Chan DW, Reynolds AB, Qin J, Wong JM. NCoR mediates DNA methylation-dependent repression through a methyl CpG binding protein Kaiso. *Mol Cell*. 2003; **12**: 723-734.

Yuan L, Neufeld AH. Tumor necrosis factor-α: a potentially neurodestructive cytokine produced by glia in the human glaucomatous optic nerve head. *Glia*. 2000; **32**: 42-50.

Zhang SQ, Kovalenko A, Cantarella G, Wallach D. Recruitment of the IKK signalosome to the p55 TNF receptor: RIP and A20 bind to NEMO (IKKgamma) upon receptor stimulation. *Immunity.* 2000; **12**: 301-311.

Zhao H, Wang Q, Zhang H, Liu Q, Du X, Richter M, Greene MI. UXT is a novel centrosomal protein essential for cell viability. *Mol Biol Cell*. 2005; **16**: 5857-5865.

Zhu G, Wu CJ, Zhao Y, Ashwell JD. Optineurin negatively regulates TNFalpha- induced NF-kappaB activation by competing with NEMO for ubiquitinated RIP. *Curr Biol.* 2007; **17**: 1438-1443.

Publications

PUBLICATIONS

- **Chalasani ML,** Radha V, Gupta V, Agarwal N, Balasubramanian D and Swarup G. A glaucoma-associated mutant of optineurin selectively induces death of retinal ganglion cells which is inhibited by antioxidants. *Invest Ophthalmol Vis Sci.* 2007 Apr; **48**(4): 1607-14.

- **Chalasani ML,** Balasubramanian D and Swarup G. Focus on Molecules: Optineurin. *Exp Eye Res*, 2008 Jul; **87**(1): 1-2.